PHILOSOPHICAL TRANSACTIONS OF THE ROYAL SOCIETY A MATHEMATICAL, PHYSICAL & ENGINEERING SCIENCES

Free Surface Oscillations and Tides of Lakes Michigan and Superior

C. H. Mortimer and E. J. Fee

Phil. Trans. R. Soc. Lond. A 1976 **281**, 1-61
doi: 10.1098/rsta.1976.0020

Phil. Trans. R. Soc. Lond. A. **281**, 1–61 (1976) [1]
Printed in Great Britain

FREE SURFACE OSCILLATIONS AND TIDES OF LAKES MICHIGAN AND SUPERIOR

By C. H. MORTIMER, F.R.S. and E. J. FEE†
Center for Great Lakes Studies,
The University of Wisconsin–Milwaukee, U.S.A.‡

WITH A SUPPLEMENTARY NOTE AND FIGURE BY
C. H. Mortimer, D. B. Rao and D. J. Schwab

(*Received* 17 *September* 1973 – *Revised* 14 *March* 1975)

CONTENTS

† Present address: Freshwater Institute, Fisheries Research Board of Canada, 501 University Crescent, Winnipeg, Manitoba, Canada.
‡ Contribution no. 99.

From records of water levels at nineteen shoreline stations on Lakes Michigan, Huron and Superior (figure 1), we have prepared power spectra from 95 station-data sets and 128 spectra of interstation coherence and phase difference. Those spectra have been used to

(1) identify the first five free gravitational, barotropic modes (surface seiches) of the three basins;

(ii) estimate the corresponding seiche frequencies, Lake Huron table 2, Lake Michigan tables 3 and 4, Lake Superior table 7;

(iii) determine, for some modes, the phase progression around the basin imposed by the Earth's rotation; and

(iv) speculate on the structure of other oscillations, including diurnal and semi-diurnal tides.

Because the number of recording stations was limited, the phase progression of individual modes could only be determined with confidence for the first and second in Lake Michigan (figure 13), for the first, second, third, and eighth mode in Lake Superior (figures 22 and 32*b*) and for the semidiurnal tide in both basins (figure 31). Except for the Superior semidiurnal tide, which progresses *clockwise*, all the modes illustrated in figures 13 and 22 and the Lake Michigan semidiurnal tide conform to a positive amphidromic pattern – *counterclockwise* progression. Possible reasons for the difference in tidal behaviour in the two basins are discussed in §4 and by Hamblin (1976). There is very close agreement between the observed frequency and the phase progression of the first three and eighth Superior modes and results from the two dimensional computations of Platzman (1972) and Rao & Schwab (1976).

Because some of the level recorders were not protected from local harbour oscillations in the period range below 2 h, and because some of the data sets listed in tables 1 and 6 were available only in the form of hourly readings, spectra from some stations exhibited contamination by aliasing. Section 2(*b*) is devoted to a discussion of: (i) the nature of this spectral contamination (see figure 4); (ii) its extent in our examples; and (iii) attempts to minimize its influence through identification of the principal aliases and exploitation of the discovery that useful information can still be extracted from interstation coherence and phase spectra, even if the power spectra from one or both stations of the pair are badly aliased.

With aliases identified or absent, the remaining spectral and interstation coherence peaks correspond to free modes (and tides). In Lake Michigan the first three modes are the most strongly excited and are clearly identified as longitudinal seiches (§§2(*c*–*f*), 2(*i*)). A transverse (E–W) seiche is also strongly excited, probably in the form of a negative amphidrome, in the south-central reach of the basin (for example T1 in figure 6), but the structure and identity of oscillations corresponding to spectral peaks at higher frequencies cannot yet be resolved.

For Green Bay, a 192 km (120 mile) long gulf opening into Lake Michigan, a remarkable double resonance is described in §2(*g*). The Bay responds as a viscously damped system driven by two forcing oscillations – the semidiurnal tide and the first mode of the main Michigan basin – at respective frequencies 1.93 and 2.67 cycles per day (c/d), one on each side of the natural frequency of the Bay-Lake system, 2.2 c/d (figures 9 and 10).

In the Superior basin, topographically more complex than Michigan, the first three longitudinal modes are also the most conspicuous, but some modes above the third are also strongly excited. Of these, the fourth, fifth, and eighth modes can be identified through comparison with Rao & Schwab's (1976) numerical determinations. The most striking feature of the eighth mode, often strongly excited, is a transverse (N–S) oscillation of the eastern half of the basin as a negative amphidrome (figure 32*b*).

In spite of prior removal of a linear trend from the input data, the spectra exhibit a steep rise in power as the low-frequency end is approached, where interpretation is therefore difficult. However, examination of the frequency range below 4 c/d, in §§2(*h*) and 3(*e*) and in figure 11, establishes the following points:

(i) for reasons discussed in the text, the semidiurnal tidal peak covers a narrower frequency range than peaks corresponding to the seiche modes;

(ii) there is minor but persistent evidence of a co-oscillation of the main Michigan basin and Green Bay;

(iii) diurnal oscillations arising from tidal and meterorological forcing, §4, are generated more strongly in the Superior than in the Michigan basin;

(iv) no spectral peaks are unambiguously identified as surface manifestations of internal waves known to be present, for example in the near-inertial frequency range 1.3–1.4 c/d; and

(v) there is a small but significant rise in power near 0.35 c/d in spectra from both basins. Possible but not yet verified explanations of this rise are: meteorological forcing; excitation of a rotational mode (Rao & Schwab 1976); or both. For Lake Michigan a possible further explanation is provided by excitation of the lowest gravitational mode of the combined Michigan–Huron basin, seen in the currents of the connecting straits (figure 12).

1. Introduction

Oscillations of water level in the Laurentian Great Lakes, in the form of tides and seiches (free standing waves), have attracted interest and speculaton for more than a century (see references in Young (1929) and Mortimer (1965)). By using computational procedures based on the equations of one-dimensional motion in channels, several authors have estimated the periods of the free surface modes in particular basins (Defant 1953; Platzman & Rao 1964*a*; Simpson & Anderson 1964; Rockwell 1966; Yuen 1969). Taking a notable step forward, Platzman (1972) used resonance iteration to determine the period and *two dimensional* structure of the first free gravitational mode in Lake Superior, taking real basin dimensions and rotation into account. Platzman's results show remarkably close agreement with the observed period and phase progression which we illustrate in figure 22*a*, in spite of the complex form of the basin. Application of Platzman's method to the higher modes is difficult in practice; and Rao & Schwab (1976) have developed a simpler, but equally precise method which yields results for any desired set of modes in one operation. In the paper which follows, Rao & Schwab apply their method to Lakes Ontario and Superior and compare the results for the first five Superior modes with the observed periods and phase distributions, presented here. A further comparison, for the eighth mode, is made in the supplementary note, §5, figure 32*b*.

Verifications of calculated periods and structures of free modes by direct observations of a lake's responses to meteorological perturbations are rarely possible by inspection of water level records alone. An exception is the remarkably persistent transverse seiche in Lake Michigan (Mortimer 1965). The first accurate comparisons were therefore based on power spectra of water level fluctuations: Lake Erie (Platzman & Rao 1964*b*); Lake Michigan (Mortimer 1965). The latter spectra were formed from 15 min average water levels, derived from two months of continuous record at nine stations, and were therefore relatively free of aliasing, as shown later. But that analysis did not yield estimates of interstation coherence or phase progression, a deficiency which we have removed in the present study.

Our analysis was prompted initially by an expectation, based on previous findings in Lac Léman (Mortimer 1963), that small-amplitude oscillations in surface level produced by long internal waves would yield spectral peaks from which the internal wave frequencies could be identified. That expectation was not fulfilled for either Lake Michigan or Superior. For each station, we compared spectra based on data from December to May (lake unstratified) with spectra for June to November (lake stratified); and we looked in vain for identifiable peaks in

PHILOSOPHICAL TRANSACTIONS OF THE ROYAL SOCIETY A MATHEMATICAL, PHYSICAL & ENGINEERING SCIENCES

the near-inertial frequency range, 1.4–1.5 c/d, as surface evidence of the Poincaré waves, so prominent in the internal wave patterns of the Great Lakes (Mortimer 1971, 1974).

In order to combine satisfactory frequency resolution with adequate statistical confidence over the frequency range of interest, most of our spectra are based on long series of hourly values (details in tables 1 and 6) conveniently available as tabulated unaveraged readings from water level charts. The penalty for that convenience is contamination of the spectra by aliasing at some stations. Although such contamination should, as a rule, be carefully avoided by appropiate instrumental or numerical filtering, useful spectral information can still be extracted in the presence of unavoidable aliasing; and our preoccupation with this matter in 2(*b*) and the substantial volume of computational work – power spectra from 95 data sets and 128 coherence and phase spectra for station pairs – are justified by the capability of alias recognition and rejection and by the discovery that signals from real oscillations can still be extracted from interstation coherence and phase spectra, even if the power spectra from one station or from both are strongly aliased.

The locations of all recording stations are shown in figure 1; ten on Lake Superior, seven on Michigan, and one on Huron, all at the shoreline. For brevity, we shall refer to the stations by

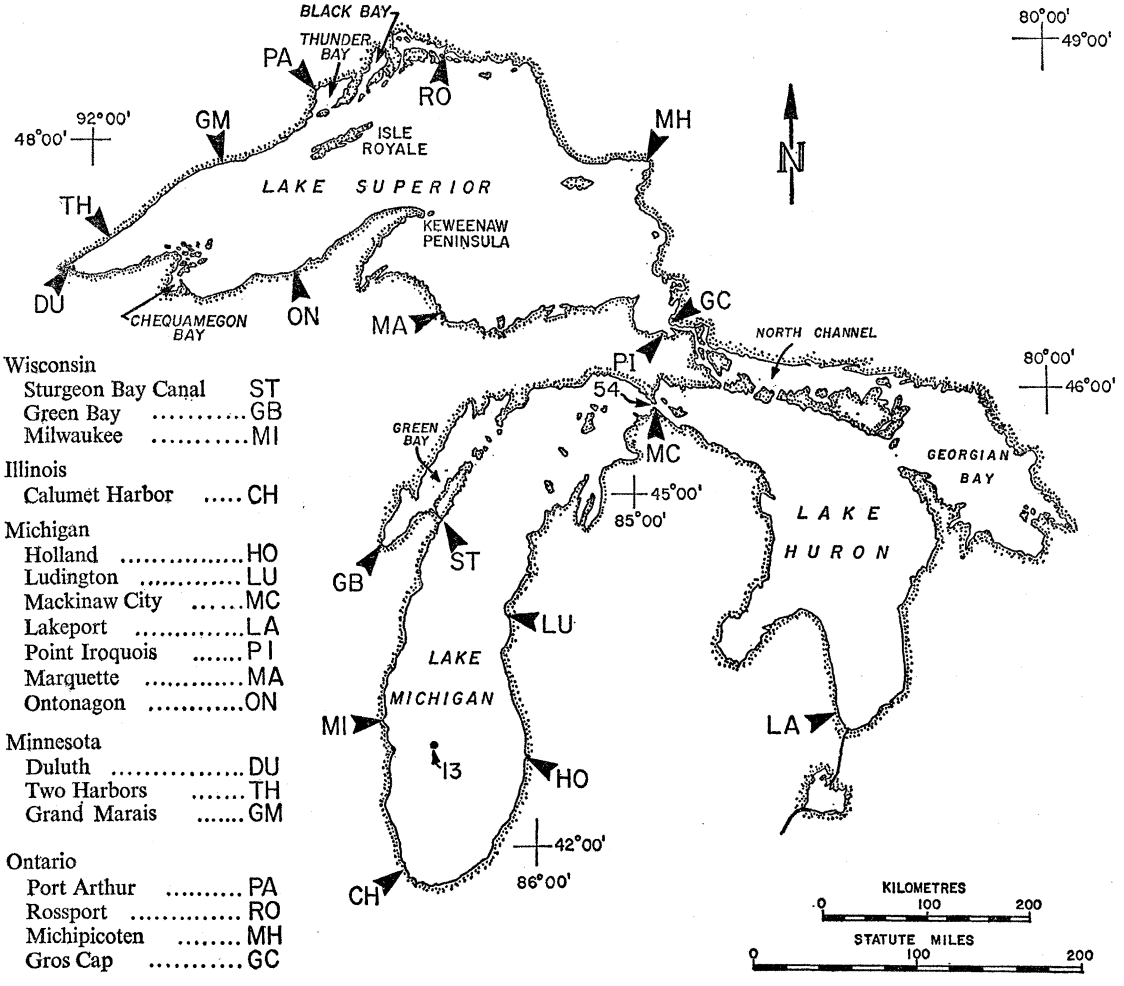

FIGURE 1. Water level recording stations on the Upper Great Lakes: locations with code letters used in the text. Stations 13 and 54 were the respective sources of wind and current information illustrated in figure 12.

their code letters in figure 1. The Straits of Mackinac connect Lakes Michigan and Huron to form a double-basin lake. Lake Superior is a single basin. Power spectra for each station and interstation coherence and phase spectra for station pairs are used to identify the free, gravitational modes and tides in the two lakes and, in particular, to describe the two dimensional (amphidromic) patterns imposed on those oscillations by the Earth's rotation.

2. The Lake Michigan–Huron spectra

(*a*) *Data sources and computational procedures*

Water levels were recorded by the U.S. Army Engineers, Lake Survey, at shore stations (figure 1) in stilling wells connected by narrow pipes to the outside water, usually in a harbour or protected channel. The high frequency cut-off point, not precisely determined in this study, varied from well to well. All wells suppressed short, surface storm waves, and some suppressed local harbour or channel oscillations; others did not. The original records were mainly in the form of continuous traces (Leupold Stevens, type A, float gauge); but in a few cases Fisher–Porter gauges provided 5 min readings on punched tape.

Table 1. Particulars of spectra of fluctuations in Lake Michigan–Huron water levels

			particulars of the spectra				
data sets	subsets, see text and figure 5	intervals covered by record, month (year)	no. of input readings, N	no. of bands, m†	Δt min	frequency range c/d	no. of station pairs analysed
1961–62	F	7–8 (1961) and 11–12 (1962)	5952	500	15‡	0–48	0
	G	artificially aliased, cf. figure 4 and text				0–12	0
1962–63	A	6–11 (1962)	4384§	300	60	0–12	10
	B	12(62)–5(63)	4384	300	60	0–12	10
	C	6–11 (1963)	4384	300	60	0–12	10
	D	6(62)–11(63)	13 152	300	60	0–12	10
	E	6(62)–11(63)	13 152‖	300	60	0–12	23
1969	H	5–11 (1969)	61 620	3600	5	0–144	3¶
			15 405	500	15††	0–48	3
			5135	300	60††	0–12	3

† Equivalent to the commonly used term 'lag' (Blackman & Tukey) and used here as an abbreviation of 'number of spectral bands, subdivisions, or estimates'.

‡ 15 min averages estimated from Leupold Stevens recorder charts; otherwise, non-averaged readings were used, except for††.

§ The 18-month data set was divided into three 6-month sections for analysis, to accommodate I.B.M. Share Program 574; spectra of sub-set D are the combined spectra of A, B, and C (see figure 5).

‖ The same 18-month records were analysed undivided by Fee's (1969) procedure.

¶ ST, LU, GB.

†† Averaged from 5 min readings, obtained from the punched paper tape of a Fisher–Porter recorder.

Inputs for our analysis were sets of N data points, either as spot readings or as averages from the original charts or tapes, digitized at equally spaced intervals, Δt. The input data sets are listed, with particulars, in table 1. For Lakes Michigan–Huron the 1961–2 sets comprised 15 min averages estimated by eye from the recorder chart. The 1962–3 sets were hourly, unaveraged readings, tabulated from the charts and kindly placed at our disposal by the U.S.

Lake Survey for the following stations: Michigan basin, CH, HO, LU, ST, GB, MI; Huron basin, LA; and MC common to both basins. The 1969 sets were 5 min readings (tape supplied by U.S. Lake Survey) or averages of these for ST, LU, and GB.

The outputs of the analysis were power spectra for each station and cross-spectra for selected pairs of stations, yielding interstation coherence and phase estimates. Power spectra alone were prepared from the 1961–2 set (Mortimer 1965, using the method of Blackman & Tukey 1958). Power spectra and cross-spectra were prepared from the 1962–3 sets by using I.B.M. Share Program no. 574 (described in Munk, Snodgrass & Tucker 1959) and later by Fee's (1969) procedure. Employing the Cooley & Tukey (1965) fast Fourier transform, Fee's procedure gave very similar results, but required much less computer time than program no. 574 and placed less restriction on the size of the input set. Fee's method was used exclusively for the 1969 Michigan set and for the Superior analyses. The assumptions, definitions, and statistical confidence which apply to the two methods are set out in the publications cited.

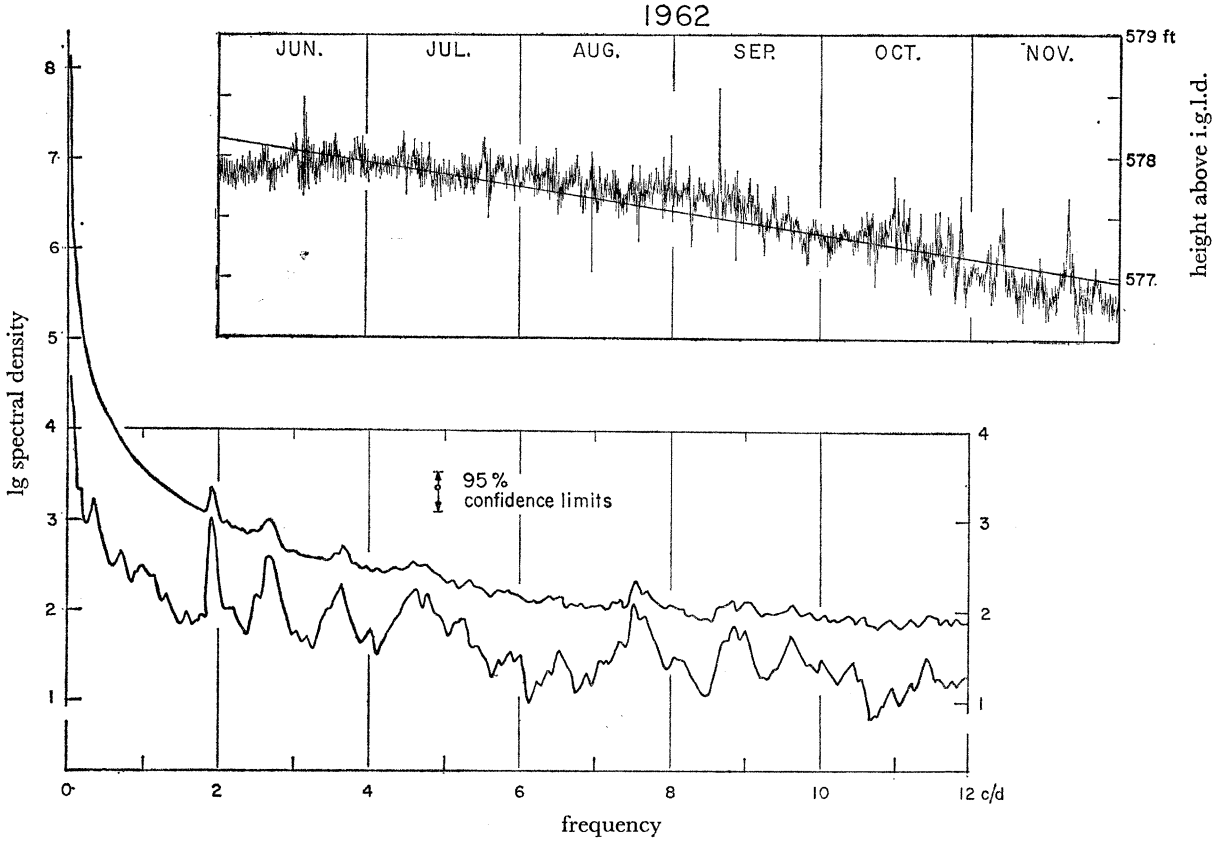

FIGURE 2. *Upper portion:* a linear trend fitted to an MC data set (hourly readings, June–November 1962). *Lower portion:* power spectra prepared from the data set, with prior removal (lower spectrum) and without prior removal (upper spectrum) of the linear trend.

A concise summary of the spectral method is also given by Munk & Macdonald (1960); and Godin's treatment (1972, particularly chapter 3) provides further insight.

The characteristics and the information content of the spectra are strongly influenced by three choices: the number, N, of input data points; the sampling interval, Δt; and the number, m, of spectral sub-divisions (frequency bands) in which the spectral or cross-spectral estimates

are to be displayed. Choice of Δt fixes the frequency range of the spectrum between zero and $1/(2\Delta t)$; and the choice of m determines (with N) the frequency resolution of the spectrum. If the amplitudes of oscillations contributing to the original record are large enough in comparison with non-periodic 'noise', corresponding peaks appear above the noise level in the spectrum. But even for a sharply tuned signal, the peak appears spread across several frequency bands (see figure 11, for example) because N is finite and because the procedure includes some smoothing of spectral estimates to improve statistical reliability. If the spectrum is fairly flat over its frequency range, the limits of confidence to be placed on an estimate in a given frequency band can be determined from tables of the χ^2 distribution (Godin 1972, pp. 185–7) with the degrees of freedom given approximately by $2N/m$ (Blackman & Tukey 1958). Although this conclusion may require some modification for our 'peaky' spectra and in the light of later discussion, we have inserted the 95% confidence limits derived from $2\ N/m$ on all spectral diagrams. Our choices of m (table 1) therefore represent compromises which balance frequency resolution of the estimates against their statistical reliability.

To remove some of the very low frequency power from the spectra, we subtracted a best-fitting linear trend, as well as the mean, from each set of input data before analysis. Trend removal reduces the 'leakage' of power from lower to higher frequency regions of the spectrum and improves display and identification of the peaks. For example, failure to remove the trend from the input data for figure 2 obscures all but the summits of the principal spectral peaks. But because the best-fitting linear trend is not the same for all data sets, trend removal complicates the scaling of spectral power density in absolute units. Also, in any given spectrum, the amplitudes of individual peaks are made up of unidentified contributions from separate storms. There can therefore be no absolute amplitude comparison between one peak and another or between one spectrum and another. Because of this and because our principal objective was to estimate the period and phase structure of the free modes – an estimate not influenced by trend removal – we chose to leave (relative) spectral density unscaled.

For Lake Michigan we examined and compared three sets (8 subsets) of spectra, particulars of which are given in table 1. The results are presented mainly in the form of diagrams, one for each station pair, of which only a selection is illustrated here. We plan to assemble the remainder (for Lake Superior also) in a Special Report of the Center for Great Lakes Studies, The University of Wisconsin, Milwaukee. Each diagram presents a power spectrum for each station of the pair, with no. 1 at the top, and also interstation coherence and phase spectra, as defined on p. 289 of Munk *et al.* (1959). Coherence is scaled from 0 to 1 and phase from $+180°$ to $-180°$; a positive phase angle denotes a lead of station 2 over station 1. Frequency is scaled in cycles per day. (This unit is used throughout, abbreviated to c/d, except where the use of period (h) is more convenient.)

The statistical confidence limits to be placed on the phase estimate in any given spectral band are determined by the number of degrees of freedom, given approximately by $2N/m$, and on the interstation coherence for that band, as illustrated on page 292 of Munk *et al.* (1959). An alternative formula is given by Godin (1972, p. 187). Calculation of the confidence limits for the coherence estimate is more complicated (see appendix B in Munk & Cartwright 1966), but it suffices for our purpose to follow Munk & Macdonald's (1960, p. 294) approximate rule that a coherence value greater than $(2m/N)^{\frac{1}{2}}$ 'indicates a meaningful phase relation between the two records'. So defined, the lower limit of 'meaningful' interstation coherence for the spectral series listed in table 1 (and for Lake Superior in the later table 6) ranges between 0.21 and 0.37

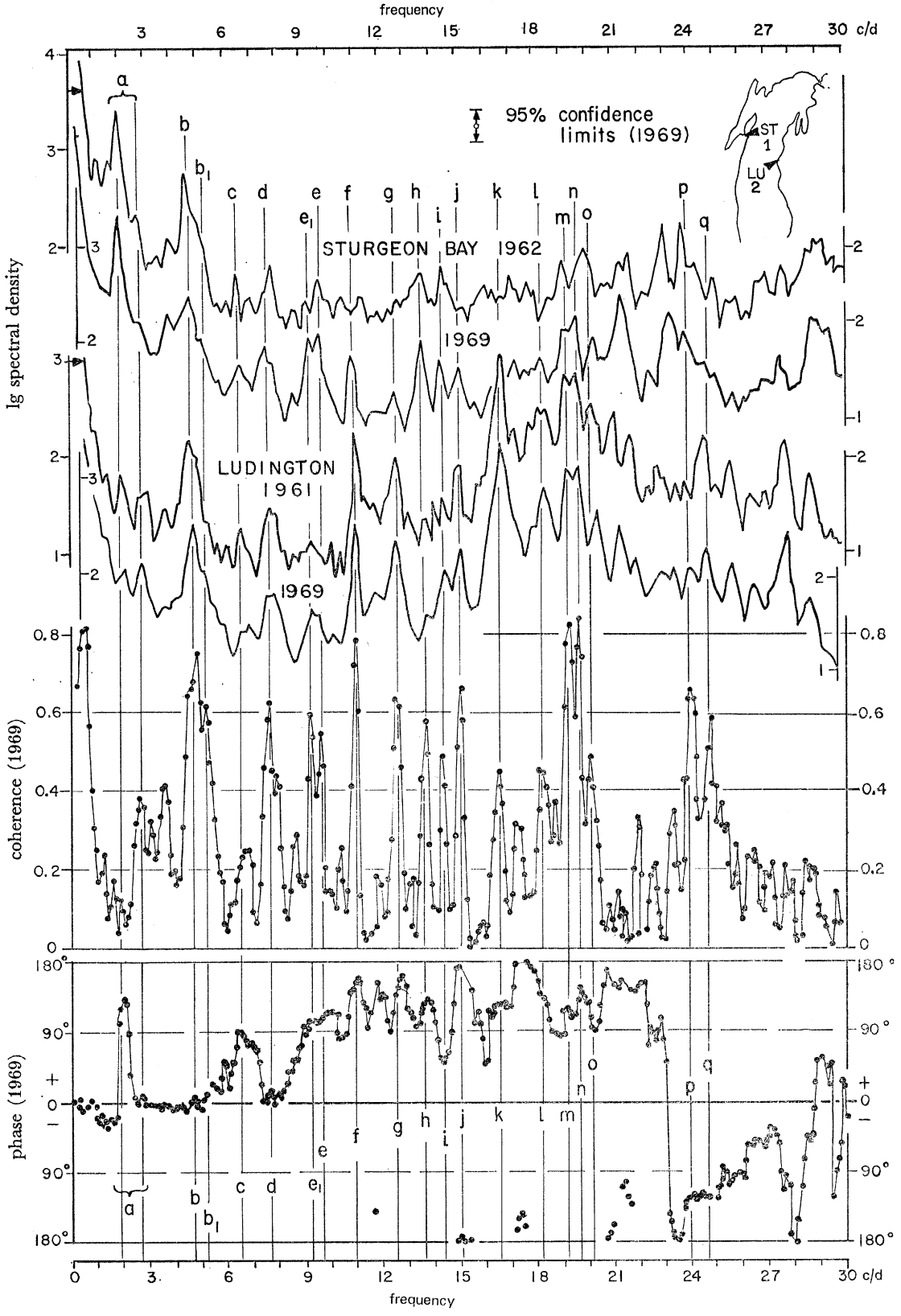

FIGURE 3. Lake Michigan: power spectra of water level fluctuations at stations ST and LU (from subsets E 1961–2 and H 1969, table 1) and spectra of interstation coherence and phase difference (subset H only). Peaks corresponding to coherence greater than 0.3 are lettered for later identification.

and is 0.34 for the diagrams discussed in the next paragraph. In later discussion we shall refer to coherence above 0.6 as 'high' and to coherence between 0.3 and 0.6 as 'moderate'.

Useful starting points for the analysis are figures 3 and 4 (and later figures 16 and 17 for Lake Superior), because they cover the entire frequency range within which significant spectral power and interstation coherence is found. In figure 3, two spectra are presented for each station, ST and LU, one from the 1969 series and one from the 1961–2 series (0–30 c/d portions, Mortimer 1965). ST/LU coherence and phase are shown for the 1969 series only. Comparison between the 1961–2 and 1969 spectra discloses differences in detail but close similarity in main features. Most of the conspicuous spectral peaks coincide in frequency with peaks in interstation coherence; and the highest coherences (greater than 0.6) coincide with peaks in the 1969 spectra from both ST and LU. Vertical lines are drawn to mark all coherence peaks greater than 0.3, and these are lettered for future reference.

(*b*) *The aliasing phenomenon*

The convenience of using the 1962–3 tabulated data ($\Delta t = 1$ h), rather than averages prepared from continuous records, brought with it an aliasing penalty (Blackman & Tukey 1958) in those cases in which the stilling well admitted oscillations of large amplitude at frequencies above the Nyquist frequency, $1/(2\Delta t)$, i.e. 12 c/d in this case. By analogy with a stroboscope, for which a flashing (sampling) rate has been determined by the choice of Δt, all oscillations of frequency greater than $1/(2\Delta t)$ manifest themselves as low-frequency aliases in the 0 to $1/(2\Delta t)$ spectrum. Stated more explicitly, an oscillation at frequency f within that spectral range cannot be distinguished from oscillations of higher frequencies defined by the series $(n/\Delta t) \pm f$, in which n is a positive integer. Wherever possible, aliasing should be eliminated by appropriate instrumental or numerical filtration to remove all power at frequencies greater than $1/(2\Delta t)$. But when this counsel of perfection cannot be followed, the difficulty can be circumvented, at least partially, if the principal aliases in the 0 to $1/(2\Delta t)$ spectrum can be identified. Although the underlying principles are well known, their brief illustration here will considerably shorten later discussion.

It is convenient to take station LU for the illustration, because the 0–12 c/d spectra for that station (based on sampling at $\Delta t = 60$ min) showed exceptionally severe contamination by aliasing. In figure 4, which demonstrates why this is so, the upper portion presents the 0–48 c/d part of a 0–144 c/d LU spectrum prepared from 5 min readings. The power content above 30 c/d is small enough to be neglected. Below that frequency, spectral peaks are lettered as in figure 3; and the highest spectral density in this example is found in two regions – 0–1 and 17–20 c/d – separated by a broad valley. Because of this power distribution, and because the production of a 0–12 c/d LU spectrum from hourly readings is equivalent to folding and combining the four panels of the 0–48 c/d spectrum in the manner shown in figure 4, the conspicuous peaks k to m are transferred to the 5–8 c/d valley region in the folded 0–12 c/d spectrum (bottom right of figure 4) where they appear as very prominent aliases. As already noted, the general result of the folding operation is that the power content (spectral density) of any spectral band – centred on frequency f in the folded 0 to $1/(2\Delta t)$ spectrum – is the sum of all power contributions, including the true content of band f as well as contributions from bands centred on the higher frequencies defined by the series $(n/\Delta t) \pm f$.

This folding or 'artificial aliasing' technique, illustrated in figure 4, permits us to identify the principal aliases in the folded 0–12 c/d spectrum and probably therefore also in any

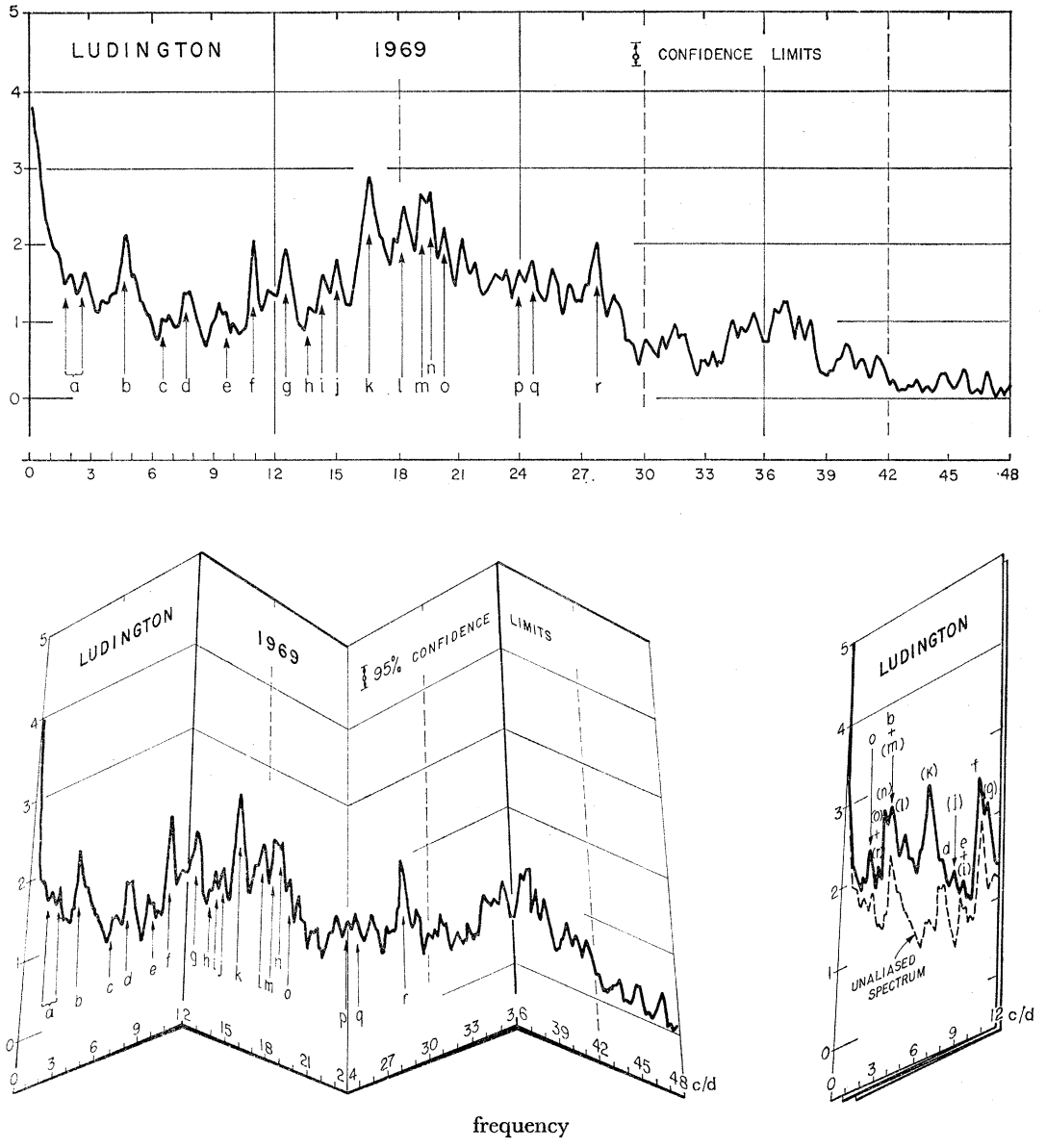

FIGURE 4. *Upper portion:* the 0–48 c/d portion of an unaliased power spectrum of water level fluctuations at station LU, Lake Michigan (subset H, table 1) with peaks labelled as in figure 3. *Lower portion:* the above spectrum folded to produce the equivalent of an aliased 0–12 c/d spectrum (see text). Alias peaks are denoted by bracketed letters, which indicate their probable origin (cf. figure 3).

spectrum prepared for the same station from other data sets sampled at intervals of $\Delta t = 1$ h. The principal alias peaks are labelled with *bracketed* letters, which indicate their origins in the unaliased spectra of figure 3 or 4. The same technique is applied in later examples (figures 5 and 6), for which unaliased 0- 48 c/d spectra (1961–2, series F, table 1) were available for folding and comparison with the 1962–3, 0–12 c/d, spectra for the same stations. In the extreme example illustrated in figure 4, the folded 0–12 c/d LU spectrum (bottom right) shows true spectral peaks at *a*, *d* and *f*; alias peaks at (*n*), (*l*), (*k*) and (*g*); combinations of true peaks and aliases at $b + (m)$ and $e + (i)$; and a peak combining two aliases at $(o) + (r)$. Comparison with

the 0–12 c/d portion of the unaliased spectrum, before folding, shows that aliasing not only introduces spurious peaks, but also fills up spectral valleys.

In no other example was a 0–12 c/d station spectrum as severely aliased as the folded spectrum in figure 4; but also in cases of less severe contamination, the main features of the true spectrum could be reconstructed by combining the above method of alias identification with an examination of the coherence and phase relations between station pairs. This result, which emerges from later analyses, is based on the fact that the whole-basin free modes generally exhibited consistently high or moderate coherence between many stations, whereas aliases generally did not. For example, the coincidences of presumed aliases (*s*) and (*j*) with moderate interstation coherence in later figures 24 and 25, respectively, are exceptions to the general rule. Such exceptions presumably arise when aliases originate from strong, high-frequency oscillations common to both stations, so that interstation coherence existing at the original frequency is carried over to the alias frequency. The fact that such cases appear to be exceptional in our material allows valid conclusions to be drawn from interstation coherence and phase relations, even when one or both of the station power spectra are badly contaminated by aliasing.

(*c*) *The principal spectral features and their reproducibility*

The degree of reproducibility of the main features in power spectra, prepared from different sets of data from one station, is illustrated for a representative example in figure 5, station CH near the southern end of the basin. Spectrum F, shown in histogram form, is the 0–12 c/d portion of the (unfolded and unaliased) 0–48 c/d 1961 CH spectrum (Mortimer 1965). Plotted above spectrum F is spectrum G, prepared by folding the 0–48 c/d 1961 spectrum in the manner illustrated in figure 4, to produce an artificially aliased 0–12 c/d spectrum with filled-in valleys and spurious alias peaks. These are probably aliases of peaks *h* to *m* in figures 3 and 4, a correct interpretation if those peaks represent oscillations which affect CH as well as ST and LU.

Spectra A, B, and C, prepared from the three consecutive six-month data sets (1962–3, table 1) are averaged in spectrum D. Spectrum E, based on the same 1962–3 eighteen-month set of hourly readings, was prepared by Fee's (1969) method. Allowing for the difference in scale, spectra D and E are identical in all significant features. Spectra A, B and C, with their wider confidence limits, show greater variance; but no obvious seasonal trend can be seen.

The numbered and lettered vertical lines in this and following figures represent later best estimates of the frequencies of the first five free modes and the semidiurnal and diurnal tidal responses. Peaks corresponding to these lines and to the transverse mode T1 are generally recognizable in all figure 5 spectra, most clearly in D and E, although some peaks may be modified and broadened by aliases, e.g. mode $2+(m)$, mode $4+(k)$, and mode $5+(i)+(j)$. Alias (*l*) also appears as an isolated peak in spectra D, E and G.

Spectra sets, similar to those assembled for CH in figure 5, were prepared for other stations, but the results for only two are shown here (spectra E, F and G for HO and MC in later figure 6). The degree of aliasing varied from severe for LU (figure 4) through moderate for HO and MC to negligible for GB. As we intend to discuss strongly aliased cases elsewhere, the present analysis is confined to moderately or weakly aliased examples.

All the power spectra prepared from the data sets listed in table 1 show principal peaks corresponding to the free modes and tide. But these peaks differ in relative height in a manner characteristic for the particular station and related to its location in the amphidromic oscillation pattern for each mode (see §2(*i*)). In every spectrum the semidiurnal tidal peak (SD) is

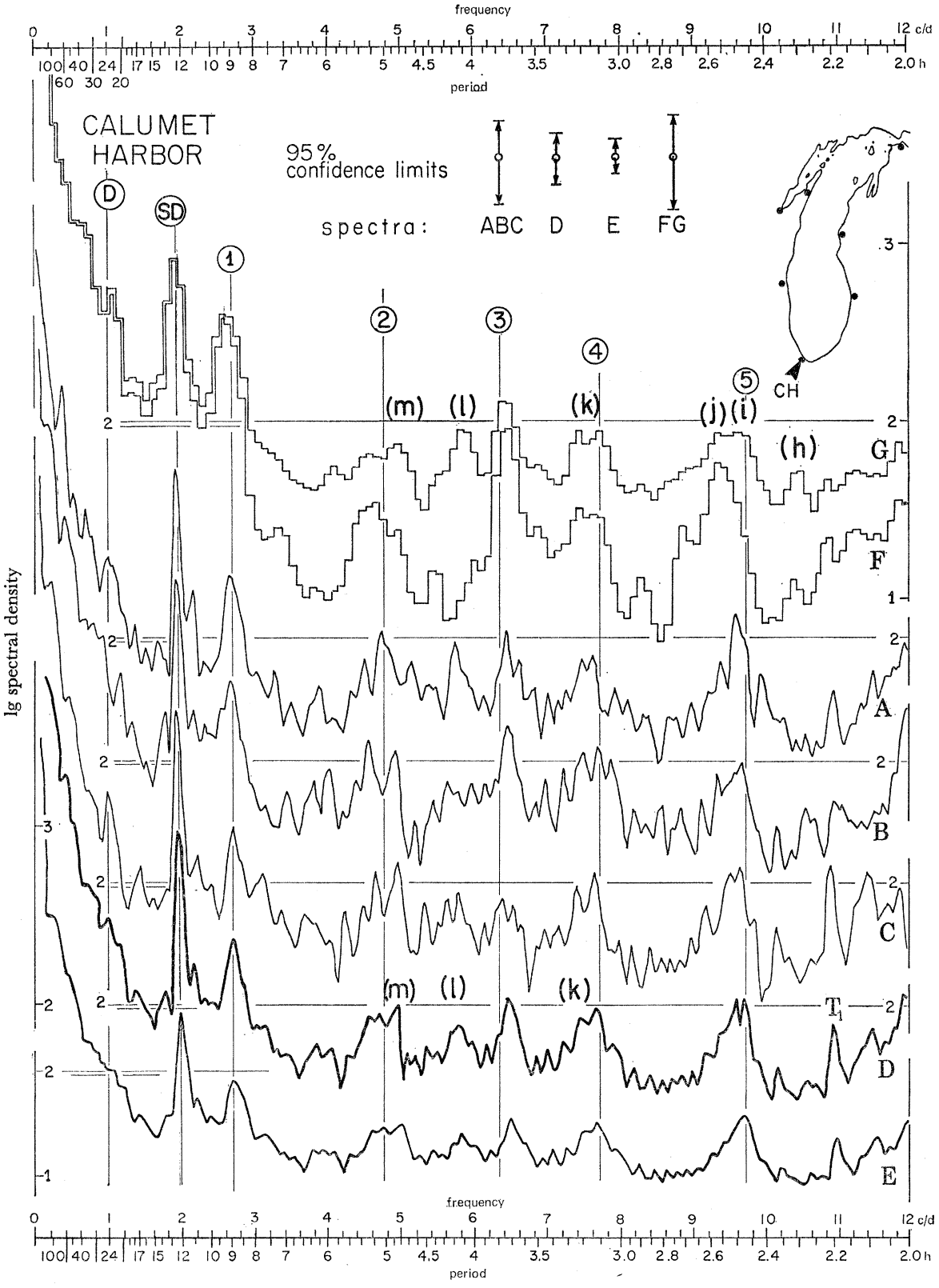

FIGURE 5. Lake Michigan: power spectra of water level fluctuations at station CH, prepared from different data subsets (table 1) and by different methods, as explained in the text. Spectrum G is an 'artificially aliased' version of spectrum F, and the bracketed letters denote aliases identified according to their presumed origin as whole-basin, high-frequency oscillations labelled in figures 3 and 4.

PHILOSOPHICAL TRANSACTIONS OF THE ROYAL SOCIETY A MATHEMATICAL, PHYSICAL & ENGINEERING SCIENCES

narrow compared with the usually much broader peaks of the free modes. The tide-generating force is applied over a very narrow frequency range close to 1.9% c/d, falling within one spectral frequency band. However, the method of analysis spreads the tidal peak over a base five bands wide (see later figure 11). While some peaks representing free modes are also relatively narrow (for example the 'sharply tuned' T1 peak at 11.0 c/d at HO in figure 6), others are much broader (for example H1 at 3.6 c/d at LA in figure 7). This greater breadth may reflect merging of neighbouring co-oscillations, or aliases, or variations in seiche amplitude (see Godin 1972, §1.10); but we suspect that some of the broadening must be attributed to interactions of basin irregularities with differences in the direction of applied wind stress. For example, in the early forcing stages of an oscillation, winds from different directions may act along oscillation axes of lengths differing slightly from that of the axis of the ensuing free oscillation. Also, adjustments of particular basin or multi-basin resonances to fluctuating or non-uniform wind stresses may produce small frequency shifts.

(*d*) *Interstation comparisons*

Power spectra from single stations are not alone sufficient to identify and describe the forced and free oscillations in basins of complex shape: information on coherence and phase differences between pairs of stations is also required. The procedures described in §2(*a*) were applied to the 1962–3 data (after removal of the mean and linear trend) to produce coherence and phase diagrams, as well as power spectra, for the following station pairs: MC/GB; ST/GB; and for all possible station pair and data set combinations among CH, HO, LU, MC, ST, MI, and LA, 63 interstation spectra in all. We here discuss the results from six pairs only, with some results from series H (1969) for comparison; but the results from all available pairs were used to explore the phase progressions of the tides and of the free modes, summarized in later figures 13 and 31.

For the pair HO/MC illustrated in figure 6, the highest coherence maxima (near 0.8) correspond to the semidiurnal tide and the first longitudinal mode, represented by high, narrow peaks in both the HO and MC power spectra, and with interstation phase differences of about 160° (HO leading MC). The smaller (0.2) coherence peaks are identified with the free modes 2, 3 and 4. The numbered vertical lines are placed at the frequencies later determined (table 3) as the best fits for modes 1–5, averaged for all spectra. In individual cases the fit is not always exact. For example, lines 3 and 4 in figure 6 do not exactly fit the corresponding coherence peaks. Mode 2 is relatively weakly excited because, as we later show in figure 13, HO lies near the southern amphidromic point for that mode. The small second modal peak visible in the unaliased HO spectrum (F) is obscured by aliasing in the other HO spectra. Nevertheless, that mode is represented by a distinct, though small, coherence peak and by an anticipated in-phase HO/MC relation, again illustrating the point that moderate aliasing does not entirely obscure the information contained in coherence and phase diagrams.

The HO/MC phase diagram shows other general features, also reproduced in later figures. For example, in those frequency regions in which interstation coherence is low, the phase points are relatively scattered. Near particular tidal or free modal frequencies, the phase points exhibit more compact groupings, particularly if high spectral peaks and high coherence show that particular mode to be strongly excited. Such groupings, evident in other examples (see figures 9 and 16), presumably reflect the influence of coherence on the statistical confidence of the phase estimate, as discussed in §2(*a*).

PHILOSOPHICAL TRANSACTIONS OF THE ROYAL SOCIETY A MATHEMATICAL, PHYSICAL & ENGINEERING SCIENCES

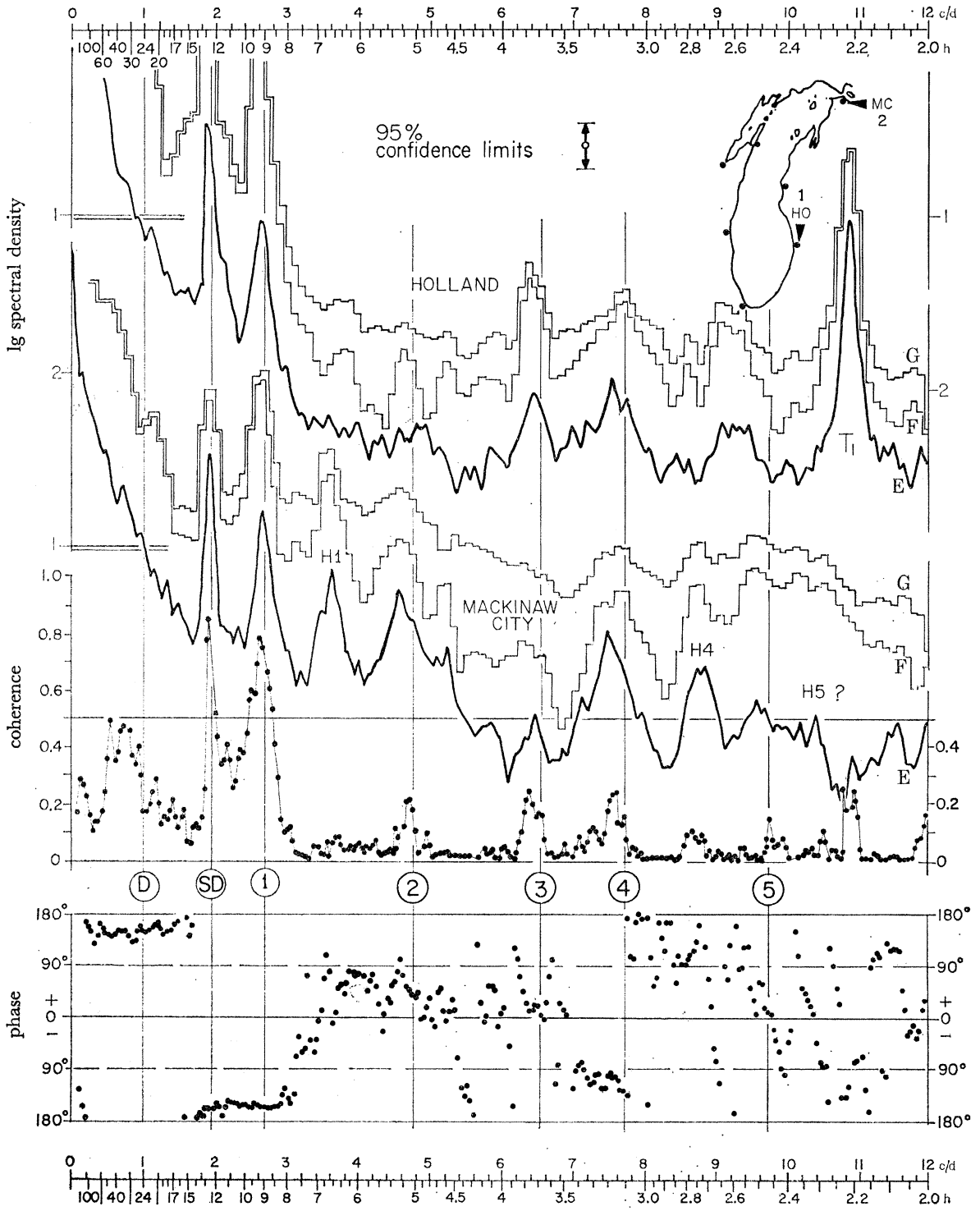

FIGURE 6. Lake Michigan: power spectra of water level fluctuations at stations HO and MC (subsets E and F, table 1) and spectra of interstation coherence and phase difference (subset E only). In this and later figures, peaks D, SD, 1 to 5, and T1 represent the tidal and free mode responses of the Michigan basin as later determined; and H1, H4, and H5 represent Huron responses seen at MC. For further details see the last sentence in the legend of figure 5.

The HO/MC phase differences for modes 2, 3 and 4 are $+30°$, $+10°$, and $-120°$, respectively. Mode 5 is only weakly represented if at all. The highest HO peak at 11.0 c/d represents a higher mode strongly excited as a transverse oscillation (TI, demonstrated by Mortimer 1965) in the southern half of the basin and not seen in the MC spectrum. However, the small HO/MC coherence peak at the same frequency may indicate a weak HO/MC co-oscillation. The alternative explanation – an effect of the computational method arising when a very strong oscillation is represented in one spectrum of a pair, but not in the other – seems unlikely because neither the large MC peak at 3.6 c/d nor the broad HO peak centred on 9.2 c/d are associated with significant HO/MC coherence values.

The prominent peaks H1 and H4 in the MC spectrum represent Huron basin oscillations, to be discussed in §2(*e*). Also noted, for later discussion, is a moderately high coherence band and a $+140°$ phase difference in the low frequency range 0.4–0.8 c/d.

The main features of the figure 6 spectra are thus accounted for, except for the rather broad but significant peak in the HO energy spectrum centred at 9.2 c/d and not identifiable as an alias of any peak in figure 3. We have not yet identified the origin of this peak, but it may be significant that HO and LU, unlike other stations, are situated on small lakes, separated from the main Michigan basin by narrow channels. There exists, therefore, the possibility that these lakes resonate with particular whole-basin or local Lake Michigan oscillations and behave as Helmholtz resonators with nodes and oscillatory flows in the connecting channel. A similar explanation has been given (Mortimer 1965) for the large peaks *k* to *n* in the LU spectrum (figure 4).

The extremities of the Michigan and Huron basins are respectively represented in figure 7 by the station pairs CH/MC and LA/MC, the latter station being common to both basins. It is convenient to assemble the station power spectra and the interstation coherence and phase diagrams for both station pairs in one figure. Coherence values below 0.1 are omitted. The LA and MC spectra are not badly contaminated by aliasing (confirmed for MC in figure 6); and the moderate extent of CH aliasing and the positions of the principal aliases were illustrated in figure 5. The Michigan modes 1–4 and the Huron modes H1–H4 are clearly identified in figure 7 by the combined evidence of spectral peaks, coherence maxima, and corresponding phase indications. With the exception of H4 (phase at $-90°$), the free modes of both basins follow the anticipated rule that the odd-numbered modes and the semidiurnal tide are approximately out-of-phase at the basin extremities, while the even-numbered modes are approximately in phase. The fifth mode in each basin is only weakly excited (low coherence); a diurnal tide cannot be detected; and moderate interstation coherence again appears in the frequency range 0.3–0.8 c/d, with a phase difference near $-150°$ for LA/MC and 180° for MC/CH.

Similar analyses of interstation coherence and phase for other station pairs confirm this identification of the Michigan and Huron modes and also define the phase progression of the modes (and tides) around the Michigan basin, as later described in §§2(*i*) and 4.

(*e*) *The free modes of the Huron basin*

For a tentative identification of the Huron modes we have examined only the station pair LA/MC. Nevertheless, coincidences of coherence maxima in the upper part of figure 7 with peaks in the LA and MC power spectra, and the LA/MC phase relations already noted, serve to identify the semidirunal tide and the first three (and fourth and fifth?) Huron modes. Estimates of their frequencies and periods are presented in table 2, corresponding to those

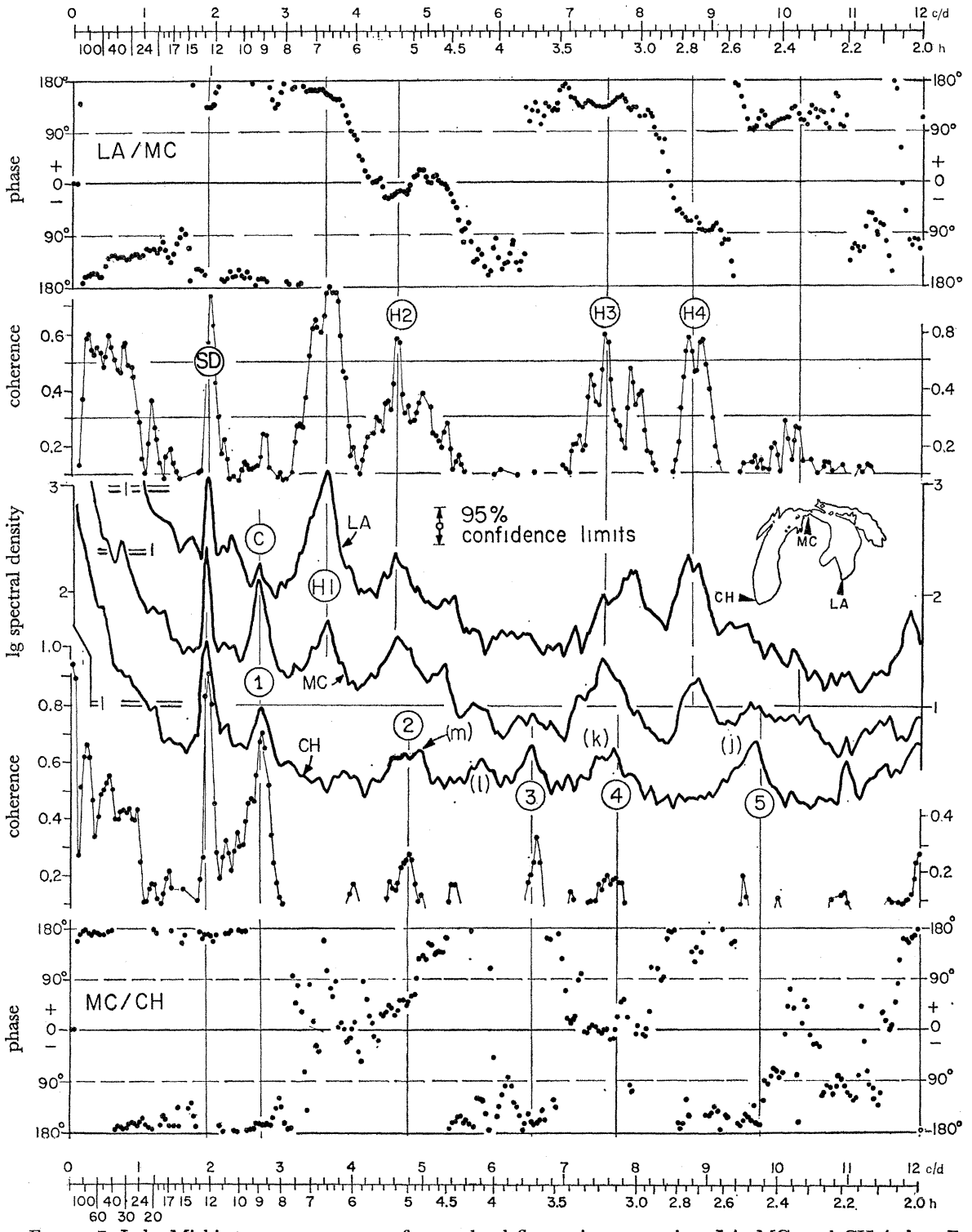

FIGURE 7. Lake Michigan: power spectra of water level fluctuations at stations LA, MC, and CH (subset E, table 1) and spectra of coherence and phase difference for station pairs LA/MC (upper portion) and MC/CH (lower portion). As in figure 6 and later figures, peaks 1 to 5 represent Michigan modes. Peaks H1 to H5 represent Huron modes; and peaks labelled with bracketed letters represent aliases identified in figure 5.

PHILOSOPHICAL TRANSACTIONS OF THE ROYAL SOCIETY A MATHEMATICAL, PHYSICAL & ENGINEERING SCIENCES

'spectral band numbers' (defined in a table 2 footnote) which lie closest to the LA/MC coherence maxima in figure 7. These 'observed' free modal periods are compared with those computed for the first five longitudinal modes by Mortimer (1965, using Defant's 1918 method), by Rockwell (1966, using Platzman & Rao's 1964*a* method), and by Yuen (1969). Except for H2, Rockwell's computed periods for the Huron basin, with Georgian Bay and North Channel omitted and with the Straits of Mackinac assumed closed, fit the observed periods closely. The fit is not quite as good with the Huron periods he computed for the co-oscillating Michigan–Huron basin (Straits open).

TABLE 2. LAKE HURON: PERIODS OF THE FIRST FIVE SEICHE MODES TENTATIVELY IDENTIFIED IN FIGURE 7 AND COMPARED WITH COMPUTED ESTIMATES

mode no.	spectral band no.†	angle by which MC leads LA/deg	coherence MC/LA	frequency c/d	period h	computed periods/h‡ Mortimer§ (1965)	Rockwell‖ (1966)	Yuen¶ (1969)
H 1	90	156	0.77	3.60	6.67	6.9	6.71	6.98
H 2	114	−14	0.59	4.56	5.26	5.0	4.80	4.96
H 3	188	132	0.61	7.52	3.19	3.6	3.18	3.52
H 4	218	−69	0.60	8.72	2.75	3.0	2.66	2.74
	222††	−84	0.58	8.87	2.70	—	—	—
H 5	256	117	0.26	10.23	2.34	2.4	2.26	2.46

† The spectrum presents a power density estimate in each of m subdivisions or frequency bands, of which there are 300 of width 0.04 c/d in these examples. The particular spectral band number chosen here is that which lies closest to the peaks of LA/MC coherence in figure 7. The tabulated frequencies (and equivalent periods) are the central frequencies of the selected spectral bands.

‡ For main basin, excluding North Channel and Georgian Bay.

§ Based on 23 sections using Defant's (1918) method, Straits of Mackinac assumed closed.

‖ Based on 65 sections using Platzman & Rao's (1964*b*) method, Straits of Mackinac assumed closed. With the Straits open, Rockwell's period estimates for modes 1–5 are reduced by: 4, 5, 2, 2 and 1 %, respectively.

¶ Based on 71 sections.

†† Second coherence peak of equal height to that at band number 218.

The spectral density and coherence peaks for H4 each show two distinct 'summits' of approximately equal height. Entries for both are made in table 2.

The broad coherence peaks associated with H2 and H3 contain one or more subsidiary peaks, sometimes coinciding and sometims not with minor peaks in the MC and LA spectra. Aliasing or co-oscillations with the Michigan basin do not provide obvious explanations for these subsidiary coherence peaks or for the twin peaks at H4. Co-oscillations with Georgian Bay or the North Channel are possibilities; and there is also a possibility that a mode involving a transverse seiche of the main Huron basin accounts for the high coherence at 7.9 c/d. Power spectra of water levels at Point Edward and Goderich, Ontario ($N = 2280$, $m = 120$, $\Delta t = 1$ h) were presented by Yuen (1969). The three highest peaks in each case corresponded to the semidiurnal tide and to the first and fourth (?) longitudinal modes near 3.6 and 8.9 c/d, respectively. Freeman & Murty's (1972) study of a storm surge on Lake Huron also includes incidental spectral evidence of a first and third mode oscillation near 3.8 (or 3.6) and 7.7 c/d, respectively.

The small peak marked C at 2.7 c/d in the LA (Huron) spectrum, figure 7, may represent co-oscillation with Michigan mode 1; but no counterpart co-oscillation with H1 (3.6 c/d) can be seen in the CH or in any other Lake Michigan spectra, except perhaps that of GB (see later figures 9 and 10). Because of high damping in the GB stilling well, aliasing is virtually absent

there; and this may permit the small signal from a weak Michigan–Huron co-oscillation to become visible.

The frequency of Huron mode 3 lies close to that of Michigan mode 4 (compare tables 2 and 3). A strong co-oscillation of the two basins is therefore to be expected at that frequency. The broad peak centred on 7.6 c/d in the MC spectrum may represent such a co-oscillation. The second modes of both basins also lie at closely neighbouring frequencies; and in the presumed co-oscillation there is evidence, although weak, of double maxima in interstation coherence or spectral density, or both. This is illustrated by figure 8, in which spectral density (not scaled) and interstation coherence (scaled and shaded) for LA/MC and various Michigan station pairs are plotted for each spectral band in the range 4.3–5.0 c/d. The fact that the LA/MC coherence is higher at band numbers 114–115 than at 119–120, while the opposite is true of CH/MC coherence, suggests that 114 and 119 (4.56 and 4.76 c/d) most nearly correspond to the respective Huron and Michigan second modes. But the appearance of a minor coherence

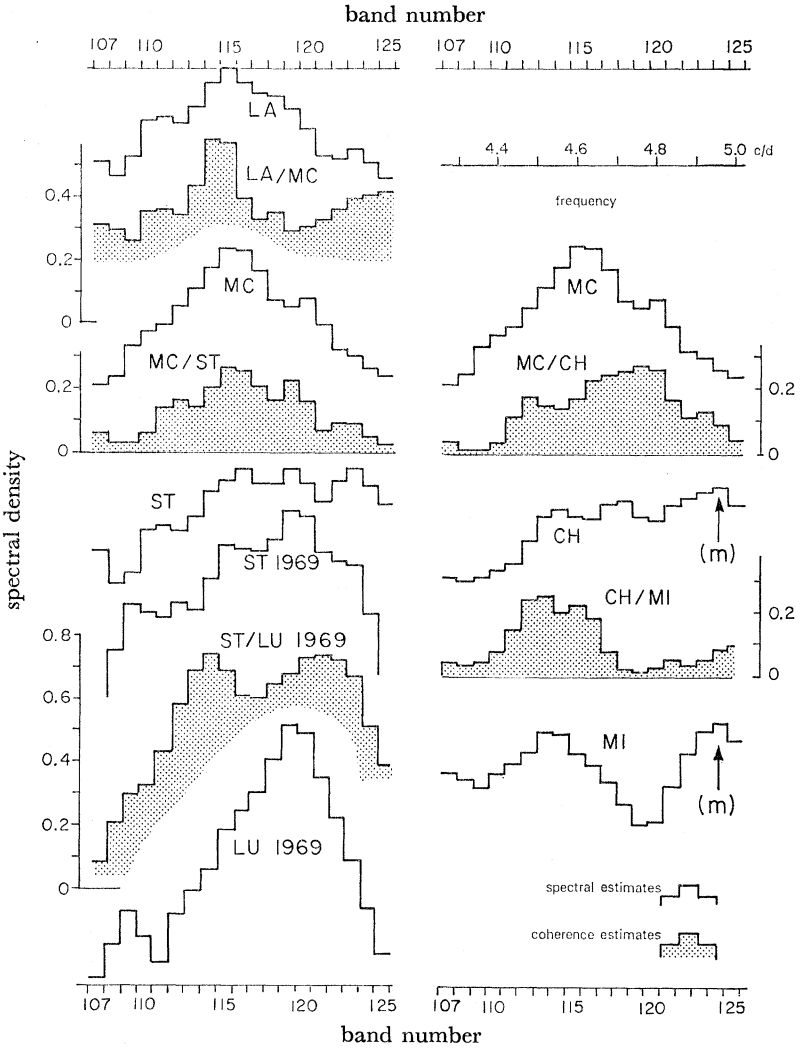

FIGURE 8. Lake Michigan: extracts from power spectra and interstation coherence of water level fluctuations over the frequency range 4.3 to 5.1 c/d: spectral density (unscaled) for LA, MC, ST, CH, and MI (subset E, table 1) and for ST and LU (subset H); and interstation coherence (scaled and shaded) for LA/MC, MC/ST, MC/CH, and CH/MI (subset E) and for ST/LU (subset H).

maximum near 114 for several Michigan station pairs, clearly seen in the unaliased 1969 ST/LU spectrum in figure 8, may be the signature of a Michigan–Huron co-oscillation, with two amphidromes in both basins.

We tentatively identify the CH and MI peaks at band number 124 as an alias of *m* (figure 3).

(*f*) *The free modes of the Michigan basin*

Interstation comparisons, similar to those described for the LA/MC pair and based on data series E and H (table 1), were made for all Lake Michigan station pairs. For each mode, most of the station pairs showed maxima in spectral density and interstation coherence coinciding with a particular spectral band. For the remaining station pairs the maximum was found in an adjacent spectral band or was divided equally between two bands. Therefore, with a band width of 0.04 c/d, the precision of the frequency estimates is about ±0.04 c/d. The estimates, as 'central' periods of the selected spectral bands, are compared in table 3 with those computed by Mortimer (1965) and Rockwell (1966); and the coherence and phase relations are also tabulated for the station pair (CH/MC) which occupies the extremities of the basin.

TABLE 3. LAKE MICHIGAN: PERIODS OF THE FIRST FIVE SEICHE MODES IDENTIFIED FROM INTERSTATION COHERENCES AND COMPARED WITH COMPUTED ESTIMATES

mode no.	spectral band no.†	angle by which CH leads MC (deg)	coherence CH/MC	frequency‡ (c/d)	period‡ (h)	computed periods/h: Mortimer§ (1965) *a*	Mortimer§ (1965) *b*	Rockwell‖ (1966) *c*	Rockwell‖ (1966) *d*
1	67	−169	0.71	2.69	8.96	9.2	9.1	9.09	8.83
2	119¶	50	0.27	4.76	5.04	5.5	4.9	4.92	4.87
3	165	−160	0.25	6.60	3.64	4.1	3.6	3.58	3.54
4	192	1	0.19	7.68	3.13	3.2	2.9	2.91	2.86
5	242	−168	0.05	9.68	2.48	2.5	2.4	2.42	2.39

† See first footnote to table 2. The band number selected is the one which scored the largest number of peak spectral densities and interstation coherence maxima (see table 4).

‡ The central frequency (and corresponding period) of the selected spectral band; see table 4 for weighted estimates of period.

§ By A. Defant's (1918) method with (*a*) 23 sections and (*b*) the 56 sections of F. Defant (1953).

‖ By Platzman & Rao's (1964*b*) method with 85 sections assuming that the Straits of Mackinac are (*c*) closed and (*d*) open.

¶ The choice of this band number is discussed in the text.

Among the free responses of the Michigan basin, the first (longitudinal) mode is the most strongly excited at most stations. Exceptions are (i) the stations in the southern central region where a higher mode (T1) with a transverse oscillation is dominant (for example HO, figure 6) and (ii) Stations ST and LU, which lie near the amphidromic nodal point for the first longitudinal mode (note the smallness of the 2.7 c/d peak at LU and ST in figures 3, 4 and 11). At ST and LU, as expected, the strongest response is that of the second longitudinal mode covering spectral band numbers 114–119. Among the 23 station pairs which make up spectral series E (table 1), the frequency distributions of coherence maxima corresponding to the first and third longitudinal modes and to the higher mode transverse oscillation (T1) are presented in table 4, with correspondingly weighted estimates of period. The agreement between these observed periods and those calculated by Rockwell's (1966) one dimensional method (assuming basin

closure at the Straits) is within 2% for the first mode. For the higher modes, his calculated period is always shorter by percentages not exceeding 9.4.

Except at ST and LU, the second Michigan longitudinal mode is not a dominant oscillation. In figure 8 we have already illustrated its co-oscillation with the Huron second mode and have distinguished between a Huron component at 4.56 c/d and a Michigan component at 4.76 c/d. At most stations in the Michigan basin, the third longitudinal mode is more strongly excited than the second, while the fourth is only weakly represented. Again ST and LU are exceptions. We have already noted the possibility of confusion of the fourth Michigan and the third Huron mode. The fifth mode response can be seen in the spectra of several Michigan stations, although interstation coherence is usually low (table 3).

The identity and structure of the presumed higher modes, represented by peaks T1 in figure 6 and *g* to *q* in figure 3, cannot be determined from our records.

TABLE 4. FREQUENCY DISTRIBUTION OF MODERATE TO HIGH COHERENCE MAXIMA FOR THE THREE MOST STRONGLY EXCITED FREE MODES IN THE MICHIGAN BASIN

mode	spectral band no.	frequency c/d	period h	number of station pairs†	period/h (weighted estimate)‡
1	66	2.64	9.09	3	
	66–67§			5	
	67	2.68	8.96	14	8.98 ± 0.02
	67–68§			1	
3	163	6.52	3.68	1	
	163–4§			3	
	164	6.56	3.66	3	
	165	6.60	3.64	6	3.65 ± 0.02
	165–6§				
T1‖	273–274§			4	
	274	10.96	2.19	5	2.19 ± 0.01
	274–5§			3	
	275	11.00	2.18	1	

† From the series E set of 23 (table 1); only station pairs with moderate or high interstation coherence are included.

‡ Weighted according to the distribution displayed in the previous column.

§ Cases in which two adjacent band numbers show high and nearly equal coherences.

‖ Higher mode characterized by a strong transverse oscillation in the southern half of the basin.

Mortimer (1965) speculated that the high peaks *k*, *m* and *n* in the LU spectrum might be oscillations of Lake Père Marquette – on which the LU recorder is situated – in resonance with free Michigan modes. The very high ST/LU coherence shown in figure 3 at the frequency of peaks *m* and *n* supports that hypothesis. The highest LU peak at *k* corresponds to a smaller but still significant ST/LU coherence.

(*g*) *The Green Bay resonances*

Attention to the remarkable double resonance at GB – a response of the Bay to the semi-diurnal tide and to the first mode of the main Michigan basin – was drawn by Mortimer (1965). This is illustrated by the 1962–3 MC/GB and the 1969 ST/GB interstation comparisons in figures 9 and 10. Because of exceptionally high damping of the recorder stilling well at GB, its spectrum is the least affected by aliasing of all the Michigan stations. Almost all of the power

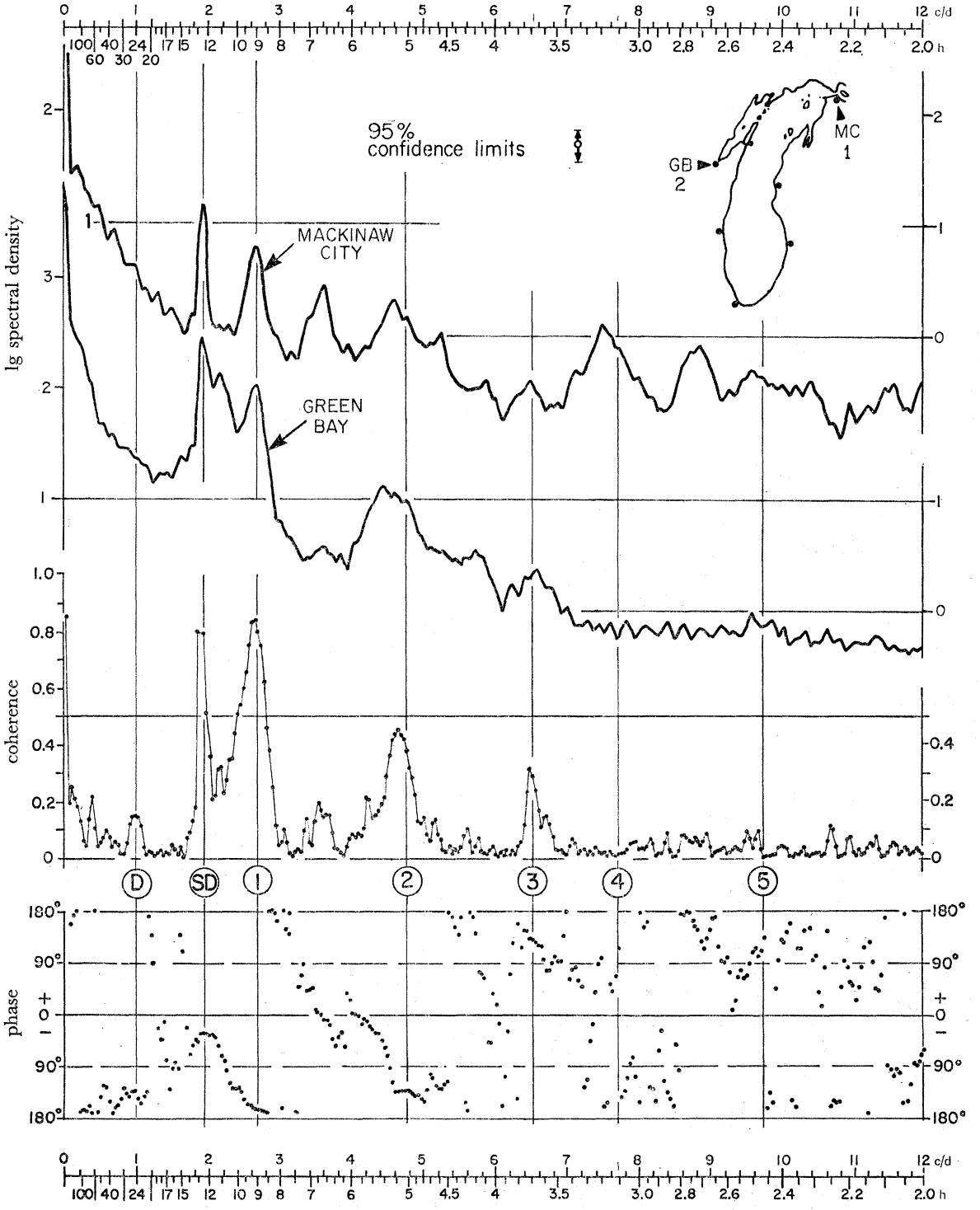

FIGURE 9. Lake Michigan: power spectra of water level fluctuations at stations MC and GB (subset E, table 1) and spectra of interstation coherence and phase difference.

PHILOSOPHICAL TRANSACTIONS OF THE ROYAL SOCIETY A MATHEMATICAL, PHYSICAL & ENGINEERING SCIENCES

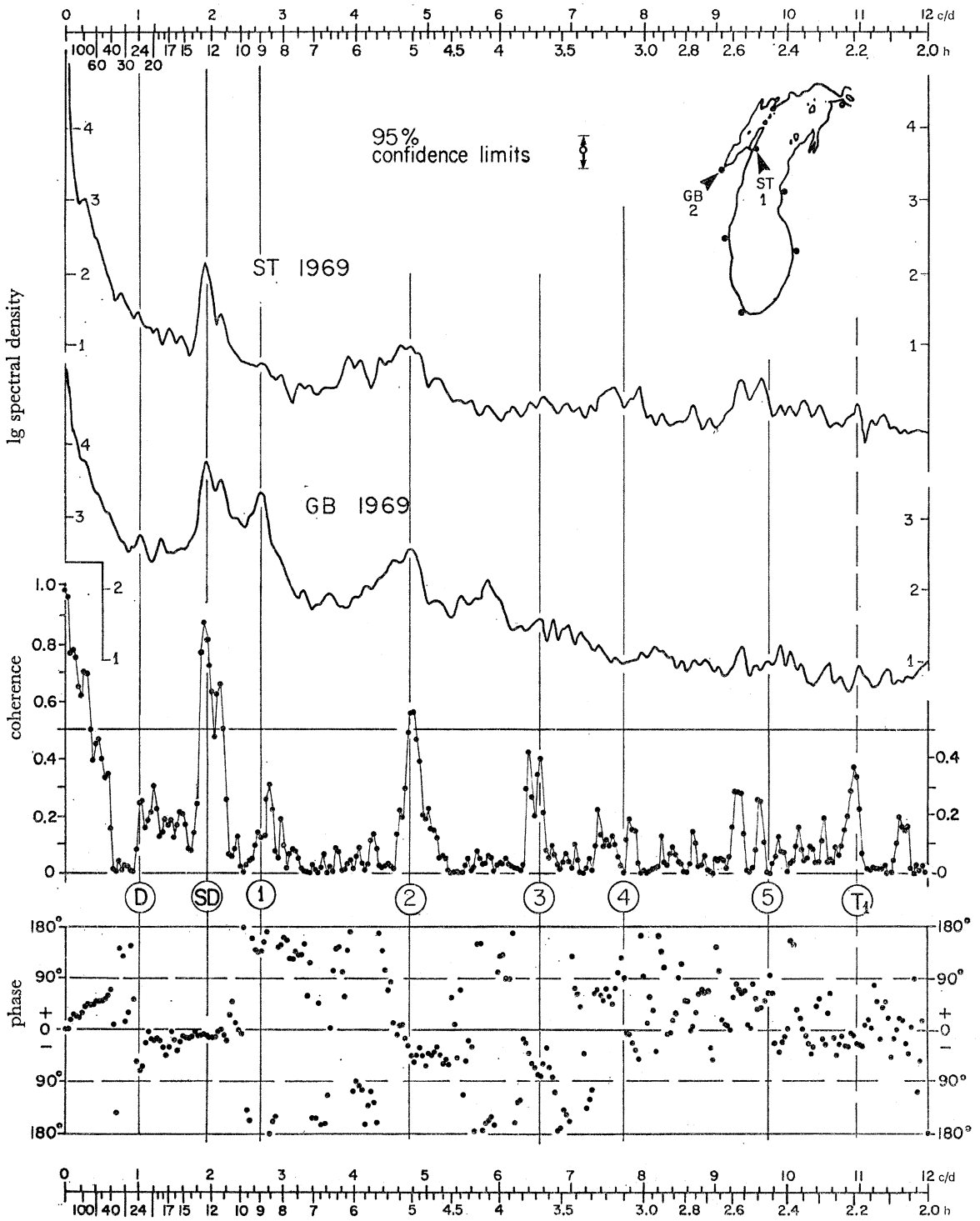

FIGURE 10. Lake Michigan: power spectra of water level fluctuations at stations ST and GB (subset H, table 1) and spectra of interstation coherence and phase difference.

is concentrated in a large broad peak with three summits at 1.95, 2.2 and 2.7 c/d. High MC/GB coherence identifies the first and third summits as resonances with the tide and the first Michigan mode, respectively; and we suggest that the middle summit at 2.2 c/d is a signature of the free response of the Bay or of the combined Bay–Lake system to wind stresses localized over the Bay. The response at this frequency, and the corresponding interstation coherence, varies between spectra prepared from different data sets, for example, figures 9 and 10. The result may depend on differences in the corresponding wind regimes. However, the small ST peak at 2.2 c/d and the high ST/GB coherence at that frequency in figure 10 must be interpreted with care. These features may be influenced by coupling between the Bay and the canal in which the ST recorder is placed. This matter will be discussed in §2(*i*).

The phase relations shown in figures 9 and 10 over the range 1.8–3.9 c/d are those of a viscously damped resonant system driven by forcing oscillations at two frequencies, one on either side of the resonant frequency. This conclusion is based on the observation that MC leads GB by 35° and 175° at 1.95 and 2.7 c/d respectively. The fact that interstation coherence at 2.7 c/d is much lower for ST/GB than for MC/GB reflects the already noted weakness of the first mode signal at ST. There is also, as suggested by the MC/GB and ST/GB interstation coherences, a distinct but smaller interaction between the Bay and the second and third modes of the main basin. The smaller coherence peak at 3.6 c/d in figure 9, but absent in figure 10, may represent a Michigan–Huron co-oscillation near the H1 frequency, as already noted.

(*h*) *Spectral features in the frequency range below* 4 c/d

Although the spectra we present are based on data from which the mean and a linear trend have been removed, there still remains a steep rise in power as zero frequency is approached. In all cases, interpretation is difficult below about 2 c/d. In an exploratory attempt to display the low frequency portions in expanded form, we superimposed the spectra for all eight stations (series D, table 1) and sketched the lower envelope of that family of curves, in the frequency range 0–4 c/d. Substraction of the ordinates of that envelope from each individual spectrum produced plots of power in each spectral band (figure 11). As noted earlier, contamination by aliasing is small (except in the case of LU and, to a lesser extent, in ST and MI) in that spectral region.

The central feature of the figure 11 spectra is a relatively narrow peak spread over not more than five spectral bands and corresponding to the semidiurnal tide. That peak cannot be detected at LU which, as figure 31 later demonstrates, lies very near the tidal amphidromic point. Prominent also are the much broader peaks, corresponding to the first longitudinal seiche modes, at 2.7 c/d in the Michigan spectra (although small or buried by aliasing in LU and ST) and at 3.6 c/d in the Huron spectra (MC and LA). The latter station also shows a minor peak near 2.7 c/d, which may represent a co-oscillation of the two basins. However, no comparable peak near 3.6 c/d is to be seen in the Michigan spectra, except for a questionable elevation in the ST spectrum and the small interstation coherence peak between *a* and *b* in figure 3 and at the same frequency in figure 9.

In comparison with the semidiurnal tidal peak, the seiche peaks are much broader. This breadth may be produced by a combination of (i) single basin oscillations, excited on some occasions, and (ii) Michigan–Huron co-oscillations at a slightly different frequency, excited on other occasions. Also differences in timing and direction of the winds, which initially set the seiches in motion, may involve slightly different forced periods and wavelengths before the

free response is established. The relative large breadth of the H1 peak at LA may be the consequence of the greater complexity in Huron topography.

The minor peaks at 2.15 c/d labelled G in the CH and MI spectra – also appearing as 'shoulders' in the tidal peak at G in spectra HO and ST, but not seen in the MC and LA spectra – probably represent a co-oscillation of the main Michigan basin with Green Bay. We

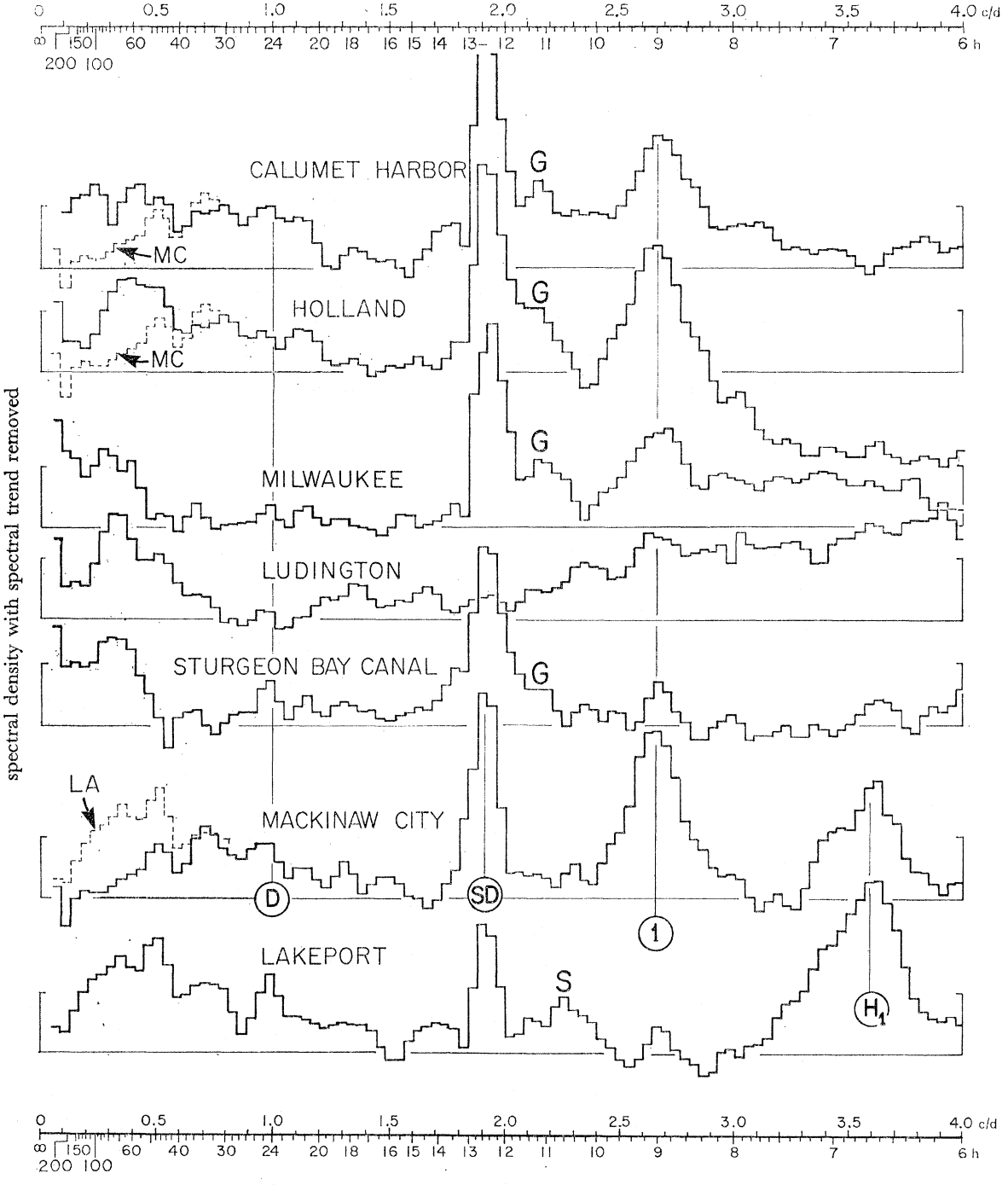

FIGURE 11. Lake Michigan–Huron: extracts of power spectra of water level fluctuations (unscaled and with spectral trends removed, see text) for CH, HO, MI, LU, ST, MC and LA over the frequency range 0–4 c/d.

speculated earlier that the minor spectral and coherence peak at 2.2 c/d in figures 9 and 10 may represent such an oscillation, perhaps set in motion by winds localized over the Bay, so that the Bay oscillation would force the Lake.

The repeated appearance of minor spectral features, of which G is an example, raises the general question of their statistical validity. Taken individually and compared with the 95 % confidence limits in other figures, such minor spectral features would have to be ruled statistically insignificant; but their appearance at the same frequency at a number of stations, or their persistence in all spectra from one station, suggests physical reality with a statistical confidence much greater than that indicated for a single spectrum. For example, the peak at S in the LA spectrum may represent a Lake Huron co-oscillation with the North Channel or the Georgian Bay basin or both. Forrester (1961) produced evidence for a conspicuous seiche of 10 hr period in the North Channel; and one of us (CHM, unpublished) used Defant's (1918) method to compute a fundamental period of 10.5 h for the North Channel, oscillating as a bay. The question of the applicability, to the type of spectrum presented here, of the Blackman & Tukey (1958) assumptions concerning statistical confidence needs re-examination.

Preparation of figure 11 was prompted by the discovery – in a smaller lake (Mortimer 1963; Lac Léman) – of the surface manifestation of an amphidromic internal seiche of 82 h period, also identified from temperature records. In stratified Lake Michigan, internal Poincaré waves of near-inertial frequency are conspicuous (Mortimer 1971, 1974); but this spectral region (1.3–1.4 c/d) in figure 11 coincides with an energy *minimum* (except at LU, which as figure 4 shows is subject to severe aliasing). This negative result may be the consequence of a much lower ratio of potential to kinetic energy in the internal Poincaré waves of near-inertial frequency than in the shore-trapped waves of the Kelvin type, of which the Léman internal seiche was an example. Also, the Michigan thermocline is rarely encountered close to shore, because littoral slopes are small and because up- or downwelling events are frequent.

In all spectra except MC, there is a rise in power as the frequency falls below 0.6 c/d, and a small maximum appears within the range 0.3–0.5 c/d (50–70 h period). This maximum could be attributed entirely to meteorological forcing or to rotational modes (see §3(*e*)); but a contribution is also possible from a low-frequency fundamental co-oscillation between the Michigan and Huron basins, first predicted by Endrös (1908) and for which Rockwell (1966) computed a period of 48 h. The single node of such a double-basin mode must lie in the Straits of Mackinac, which connect the two basins. Figure 12 (redrawn from U.S. Department of the Interior 1967) presents spectra of (*a*) wind speed at an offshore station 13 and (*b*) current at station 54 (station positions in figure 1). In addition to a strong diurnal periodicity, the wind spectrum shows an energy plateau in the 50–60 h period range. The physical reason for this is not clear. The currents in the Straits are characterized by a conspicuous broad spectral peak, centred on 60 h period, with a subsidiary tidal peak near 12.5 h. One month's record (figure 12*c*) of E–W flow through the Straits, shows dominance of a peridodic component in the period range 60–72 h. Oscillatory flow between the basins is very much greater than the net outflow from Michigan to Huron; and it is in the currents, rather than in level fluctuations, that evidence of this co-oscillation should be sought.

We therefore believe that Rockwell's computed period of 48 h may be an underestimate and that a Michigan–Huron co-oscillation of about 70 h period may contribute to the observed broad rise of spectral density in the region 0.3–0.5 c/d (50–80 h period) in figure 11. The absence of this rise in the MC spectrum may be significant (see the contrast between MC and

LA over this frequency range in figure 11) because MC is at the presumed node of the double-basin oscillation.

The coherence and out-of-phase relationships between the Lake Huron station LA and four other Lake Michigan stations over the frequency range 0.3–0.4 c/d, set out in table 5, lend some support to the hypothesis of a Michigan–Huron oscillation. An entry for LA/CH is omitted, because the coherence was very low (0.08).

If the basins co-oscillate in a fundamental mode with a 70 h period, it may be difficult to identify this oscillation unambiguously in the presence of meterorological forcing. The possibility of rotational modes (Rao & Schwab 1976) are considered in §3 (*e*). With an accompanying brief review of possible theoretical explanations for low-frequency oscillations, Hamblin (1968) describes a 0.7 c/d level fluctuation at the western end of Lake Ontario. His figure 2 spectra also show a rise near 0.33 c/d.

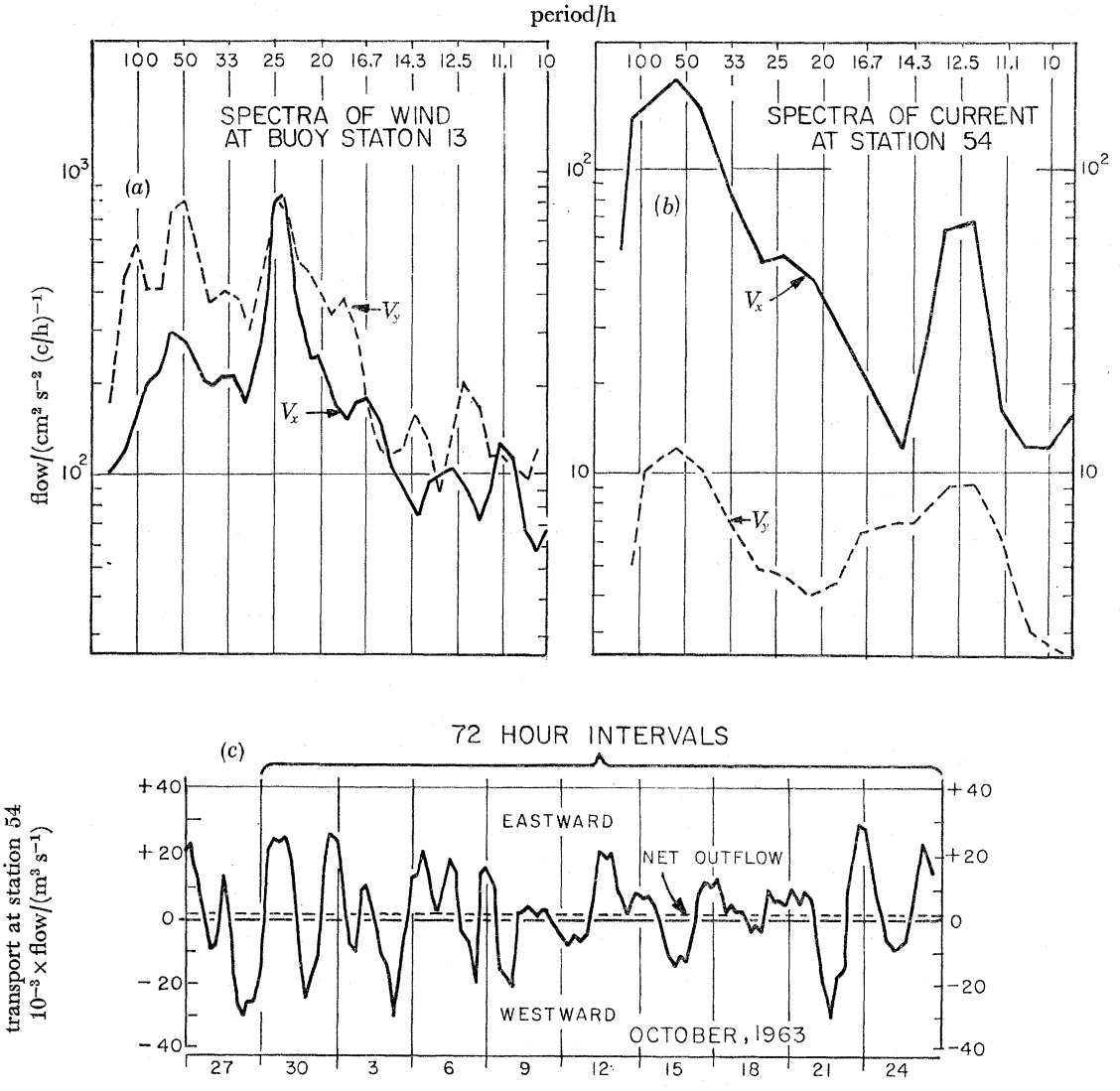

FIGURE 12. Lake Michigan: power spectra of (*a*) E–W (V_x) and N–S components of wind at station 13; (*b*) E–W (V_x) and N–S components of water current at station 54, 30 m depth; and (*c*) flow volumes through the Straits of Mackinac (station 54) – redrawn from U.S. Department of the Interior Report, 1967.

Although wind spectra from the offshore station (figure 12*a*) show a main peak at 1 c/d – at which frequency there is also forcing by diurnal tidal components – recognizable diurnal peaks are absent in the figure 11 spectra, except for doubtful LA, MC and ST indications. Diurnal peaks are more conspicuous in the Lake Superior spectra (see discussion in §4).

TABLE 5. COHERENCE AND PHASE DIFFERENCES BETWEEN A LAKE HURON STATION LA AND LAKE MICHIGAN STATIONS HO, MI, LU AND ST OVER THE FREQUENCY RANGE 0.3–0.4 c/d

station	coherence with LA†	angle by which LA leads/deg†
HO	0.23	−131
MI	0.13	150
LU	0.50	180
ST	0.45	150

† Average of spectral bands 8–10.

(*i*) *Phase progressions of the first and second Michigan modes*

As a consequence of basin dimensions, the set of seiches which the foregoing spectra have defined are strongly influenced by the Earth's rotation. The nodal lines, characteristic of seiches in basins for which rotation can be neglected, are here replaced by amphidromic points, at which elevation change is always zero, and around which the wave progresses in a counterclockwise (positive) or clockwise (negative) direction.

To reproduce the effect of rotation on Michigan seiches, F. Defant (1953) developed a simple, but unverified, one dimensional model, in which the seiche-induced flow (computed by A. Defant's 1918 method) was assumed to be always in geostrophic equilibrium (Kelvin wave dynamics). That model, illustrated for the first and second modes in figure 13, exhibits positive amphidromy. Adopting the conventions of tidal diagrams, cotidal lines radiate from the amphidromic point(s) and progress in a counterclockwise direction at a rate indicated by the phase angle, θ, relative to 0° at station MC. Therefore, if T is the period of the mode concerned, high water occurs along a given cotidal line (phase angle θ) at time interval $\theta T/360$ after high water at MC. The progression of high water is relatively rapid around the basin ends and slow past the amphidromic point.

Co-range lines in Defant's model predict the distribution of seiche amplitude relative to 100 at the southern end of the basin. Along the shoreline, that amplitude falls to a minimum (not zero) where the shoreline comes closest to the amphidromic points. For the first and second modes, that minimum is respectively 17% and 12% of the amplitude at the southern end of the basin, a prediction consistent with the relative heights of the first and second mode peaks at LU, ST, and HO, as seen in figures 3, 6, 10 and 11.

To compare the observed phase progressions with those predicted in figure 13, we examined the phase diagrams for all available (56) station pairs and estimated, for those spectral band numbers which correspond to the first and second mode (tables 3 and 4), a best fitting phase angle for each station, relative to 0° at MC. The fit was such that the deviations from the estimate shown by individual station pairs were reduced to a minimum. For example in the case of the first mode (spectral band number 67, 2.68 c/d), interstation coherence values for all pairs (except pairs including ST, omitted for reasons given later) ranged between 0.36 and 0.82;

and the individual station-pair phase differences did not deviate more than 3° from the square-bracketed values entered in large type in figure 13. That result confirms the positive amphidromy and fits Defant's predictions concerning the rate of phase progression quite well. A double Kelvin wave model is therefore appropriate (Mortimer 1975).

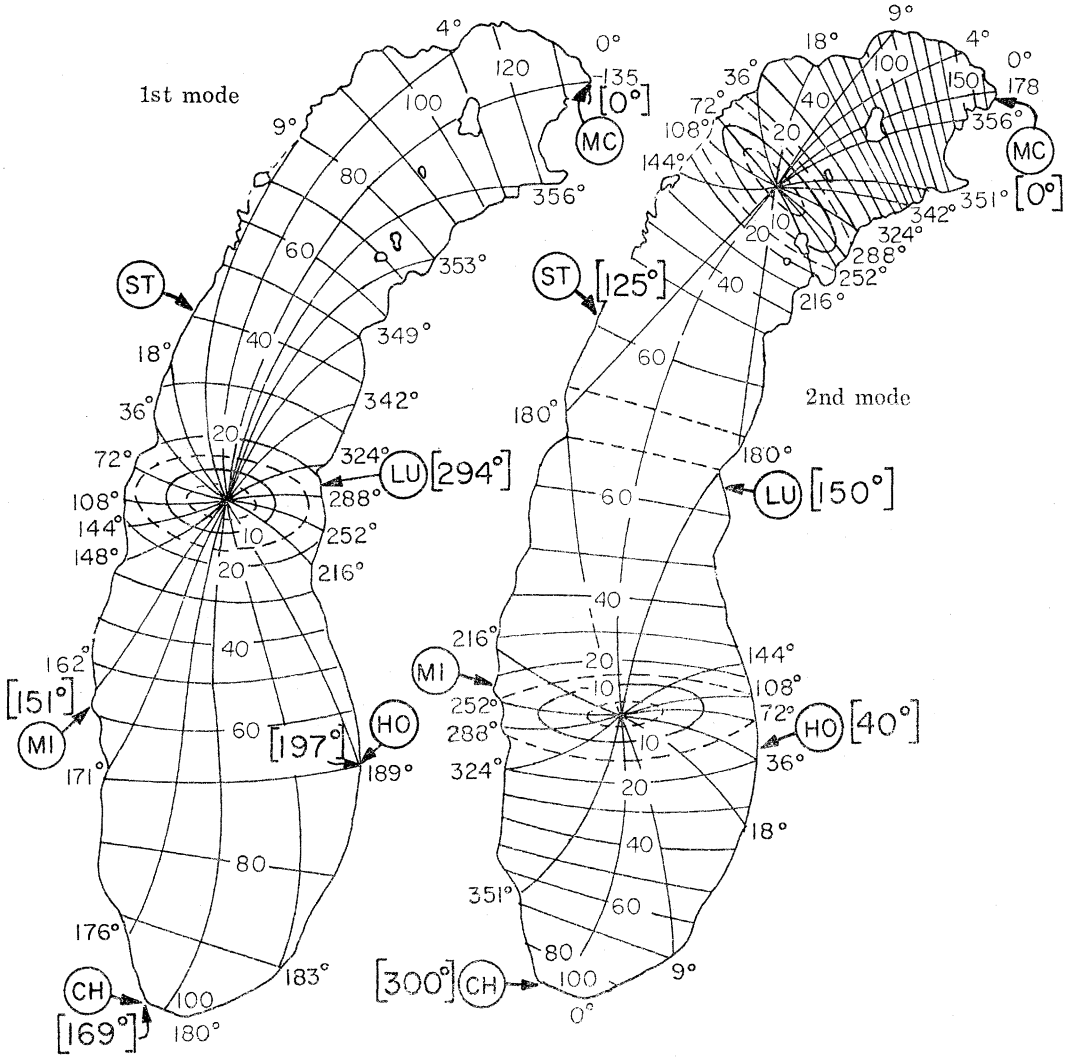

FIGURE 13. Defant's (1953) model of the phase progressions (co-tidal lines with phase angles relative to 0° at MC) and elevation distributions (co-range lines relative to 100 at CH) of the first and second free longitudinal surface modes of oscillation of Lake Michigan. Compared with the model are observed station phase angles [in square brackets] also relative to 0° at MC, derived from 56 interstation comparisons (see text).

Results obtained in the same way for the second mode (band number 119, 4.76 c/d) are also shown in figure 13, here including stations paired with ST. In this case, the mode was less strongly excited than the first; interstation coherences were much lower (0.1–0.6); and the deviations of individual phase estimates, from those given in the figure, ranged over ± 20°. The pattern is one of two positive amphidromes. The fit to Defant's model is good along the eastern shore, but less good on the west side. Coherences for station pairs including MI were very low because that station is close to the southern amphidromic point; no second mode phase angle is therefore estimated for that station in figure 13. It is significant that we found no regular phase progression around the Michigan basin for the presumed H2 portion of the double peak

in figure 8 (band number 114). This supports the identification of band number 119 as that corresponding to the Michigan second mode.

The third mode also fitted a pattern of positive amphidromy; but with only six stations available for the main basin, the results for this and higher modes are too fragmentary to illustrate here. Furthermore, any definitive study of the higher modes must take into account the phase changes which occur between the open lake shore and the recorder float, arising from stilling well design (see Noye 1968, 1970, 1972) and from the practical necessity of placing the recorders in the shelter of harbours or breakwaters.

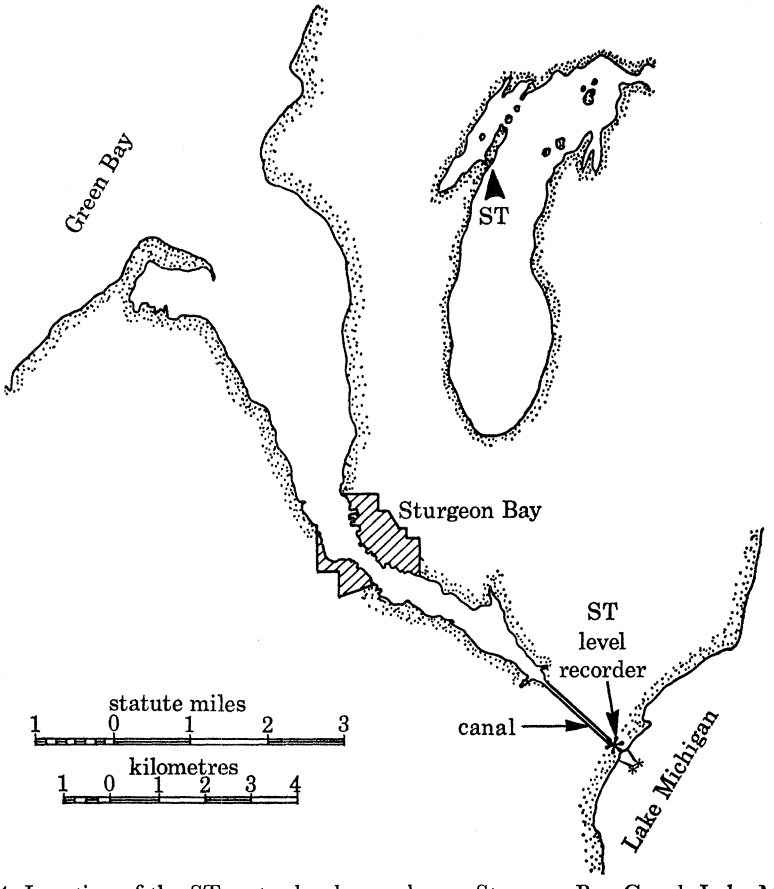

FIGURE 14. Location of the ST water level recorder on Sturgeon Bay Canal, Lake Michigan.

A striking example of the influence of local hydrographic factors is afforded by ST, which is the only Michigan recorder installed on a canal (figure 14) connecting the main basin with a separate arm, Green Bay. For ST we consistently found that the phase angle of the first mode was 50° in advance of that predicted for the main basin shoreline at that point in figure 13, whereas no such large difference was found for the second mode. The explanation may be found in the situation of the ST recorder – on the Sturgeon Bay canal, about 500 m from the Lake Michigan entrance – and in the ST/GB phase relations illustrated in figure 10. The Michigan first mode is nearly out of phase between GB and ST, whereas the second mode and the semi-diurnal tide are almost in phase. Therefore the first mode, but not the second, will give rise to large level and phase differences between one end of the canal and the other. We therefore expect the phase 'error' at ST, relative to the nearby Lake shoreline, to be large for the first

mode, but small for the second mode and the tide. Currents induced in the canal by particular modes or tide will be related not only to phase differences, but also to amplitude differences between the canal ends. For example, the amplitude of the semidiurnal tide is magnified by resonance in the Bay, but is small at ST. Therefore, although the GB/ST phase difference is small for the tide, the Bay/Lake amplitude difference and the GB/ST coherence (figure 10) are large. This is the probable explanation of Saylor's (1964 and personal communication) observed semidiurnal 'tidal' current in the canal (range ± 30 cm s^{-1}) persisting for ten days (11–20 October 1963) and lagging approximately one hour behind a semidiurnal oscillation (± 5 cm) of water level at the Bay end of the canal. On other occasions, when the first Lake mode is strongly excited at 2.7 c/d, its magnified amplitude in the Bay and the 180° GB/ST phase difference (figure 10) will probably combine to produce oscillating currents in the canal at that frequency also.

Because of stilling well design, no oscillations appear in the GB spectrum at frequencies greater than 6 c/d (figures 9, 10); but this does not prove the absence of higher GB modes or that they would not influence the phase difference between ST recorder and the Lake shore. Speculations on the behaviour of the higher modes must be deferred until data from more stations are available.

The analysis of Lake Superior spectra, which follows and for which results from more stations are at hand, carries speculations on the nature of the higher modes somewhat further in §3(*d*).

3. The Lake Superior spectra

(*a*) *Data sources*

The positions of the Lake Superior water level recording stations, all located in harbours or behind breakwaters, are shown in figure 1. Again for brevity, the stations will be referred to

Table 6. Particulars of spectra of fluctuations in Lake Superior water levels

series: station pairs (no. analysed)†	intervals covered by record, month (year)	particulars of the spectra‡			
		input data points, N	$\frac{\Delta t}{\text{min}}$	frequency range / c d^{-1}	significant coherence limit§
A: Canadian only (6)	1 (1967) to 6 (1968)	13872	60	0–12	0.21
B: U.S. & Canadian (18)	10 (1966) to 3 (1967)	4272	60	0–12	0.38
C: U.S. only (14)	10 (1966) to 3 (1967)	8545	30‖	0–24	0.27
D: U.S., Canadian, & U.S./Canadian (9)	5 to 10 (1969)	4416	60	0–12	0.37
TH/MA (1)¶	5 to 10 (1969)	53980 (m = 3000)	5	0–144	0.33
DU/GM, DU/TH	7 to 9 (1967)	26496 (m = 930)	5	0–144	0.27

† The number of station pairs analysed is shown bracketed.
‡ Number of spectral bands, $m = 300$, unless otherwise stated.
§ Interstation coherence limit above which a 'meaningful phase' estimate can be obtained, as defined by Munk & Macdonald (1960, p. 294).
‖ 30 min averages estimated by eye from record charts; non-averaged spot readings in the other series.
¶ Figures 15 and 16.

by the code letters in figure 1. For the identification of the free modes, tides, and interstation phase relations, six sets of spectra are available. Particulars of these and of the data sets from which they were derived are listed in table 6. Stations DU and TH are separated by only 40 km (25 miles); therefore the spectra from these two stations are very similar, and the DU/TH phase difference remains close to zero over the frequency range of principal interest, 0–12 c/d. (Compare later figures 18 and 19.) Therefore, to avoid duplication and possible interferences from the large Duluth–Superior harbour in which the DU recorder is situated, we concentrated mainly on TH for interstation comparisons. Records from only two stations, ON and MA, were available for the southern shore. It is particularly unfortunate that there was no recorder

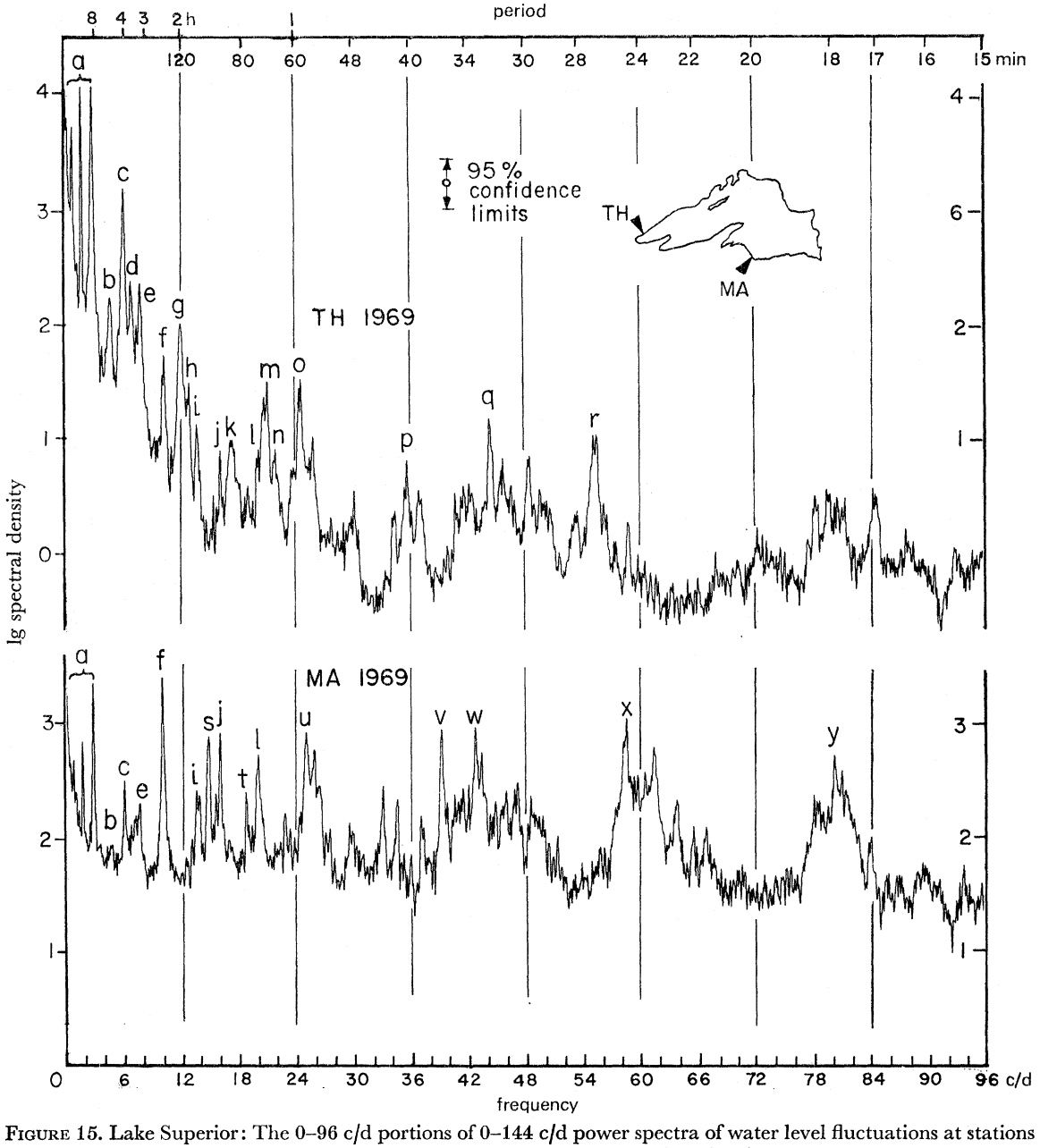

FIGURE 15. Lake Superior: The 0–96 c/d portions of 0–144 c/d power spectra of water level fluctuations at stations TH and MA (1969, table 6). Lettered peaks are referred to in the text.

on the Keweenaw Peninsula. Analysis of data from such a recorder would have removed some uncertainty in later diagrams of phase progression, particularly of the higher modes and postulated transverse oscillations.

By using Fee's (1969) method, power spectra and interstation coherence and phase spectra were prepared for 51 station pairs (table 6) according to the procedure (including trend removal) and with the statistical confidence limits described in §2(*a*). Fourteen of these station-pair diagrams illustrate this paper.

(*b*) *Correlations of spectral peaks with interstation coherence maxima; identification of the principal modes*

To illustrate general features of the spectra, we present the 0–96 c/d portions of the 0–144 c/d 1969 spectra for TH and MA in figure 15. As in the Lake Michigan examples, the principal peaks are distinguished by letters. The group of three peaks marked *a* and the peaks *c*, *e*, *f*, *i*, *j* and *l*, occur at the same frequencies in both spectra, whereas other spectral peaks – *b*, *d*, *g*, *h*, *k* and *m* to *r* in TH and *s* to *y* in MA – are found only in one spectrum.

The TH spectrum illustrates the feature common to most of the spectra considered here, i.e. a rapid decrease in power with increasing frequency over the range 0–24 c/d. An exception to this general rule, the MA spectrum shows no such rate of decrease. As a consequence, and for the reasons given in §2(*b*), MA spectra based on hourly readings (series A, B and D) exhibit strong contamination by aliasing, while TH spectra do not.

The expanded 0–24 c/d portions of the TH and MA spectra in figure 15 are reproduced as pair (i) in figure 16. The corresponding interstation coherence and phase relations disclose that those TH and MA peaks which coincided in frequency in figure 15(*a*, *c*, *e*, *f*, *i*, *j*, *l*) are associated with large maxima (0.5 or greater) in interstation coherence, whereas the other spectral peaks are not. However, some of the peaks not common to TH and MA (*b*, *h* and *t*) are associated with lower but distinct coherence maxima in figure 16. Whether these maxima are a consequence of the method of analysis or whether they represent weak co-oscillations is not clear. There are also minor coherence peaks at 15.7 and 20.6 c/d, with no obvious counterparts in the power spectra. The former peak may represent an alias of *y* (figure 15), but there is no obvious explanation for the latter. Another feature of figure 16, as of other figures and already noted Michigan examples, is that high coherence peaks usually correspond in frequency with relatively compact groupings of points in the phase diagram.

Less obvious in figure 16 is the indication, in the spectral and coherence diagrams, that several of the larger, broader peaks are made up of a principal summit flanked by one or more separate but lower summits at nearby frequencies, for example, *f*, *i*, *j* and the right-hand member of the *a* trio. In contrast to this, as we pointed out earlier for Michigan spectra, the middle peak of the *a* trio – at a frequency which identifies it as the semidiurnal tide – is single and relatively narrow. Possible reasons for the relative broadness of some non-tidal peaks were discussed in §§2(*c*) and 2(*h*); and Godin points out (1972, §1.10 and p. 201) that *amplitude* variation of a pure harmonic oscillation yields a spectral peak with two satellites. For our present purposes we shall assume that the major summit of each multiple peak represents a free mode of oscillation of the basin, after the initial forcing has ceased. The phase results illustrated in figure 16 will be discussed later with other interstation comparisons.

Also presented in figure 16 is a second pair of 1969 TH/MA spectra, marked (ii) and derived from hourly readings (series D, table 6), therefore yielding a frequency coverage of 0–12 c/d.

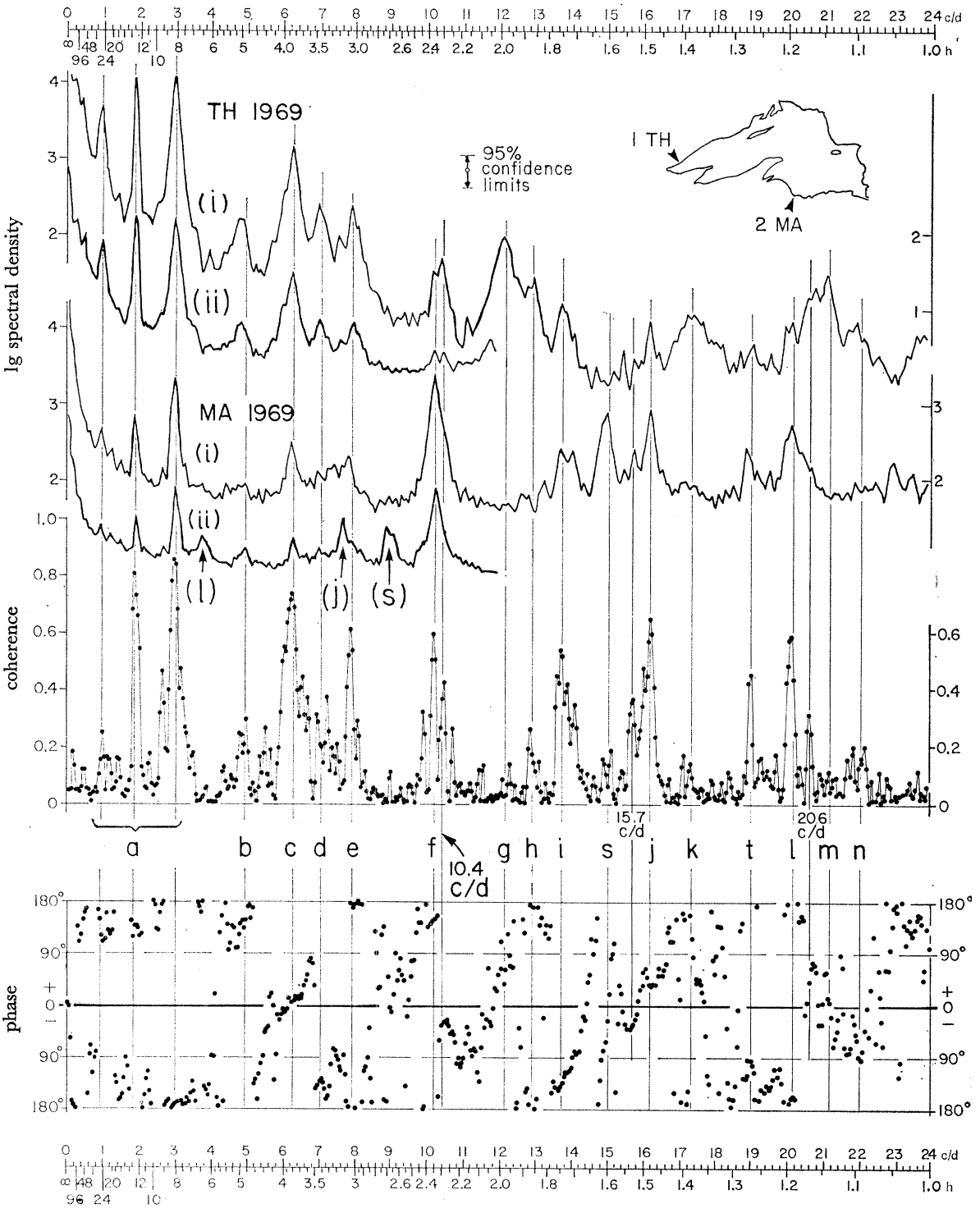

FIGURE 16. Lake Superior: power spectra of water level fluctuations at stations TH and MA, (i) $\Delta t = 5$ min and (ii) $\Delta t = 60$ min (1969, table 6), and spectra of interstation coherence and phase difference ($\Delta t = 5$ min).

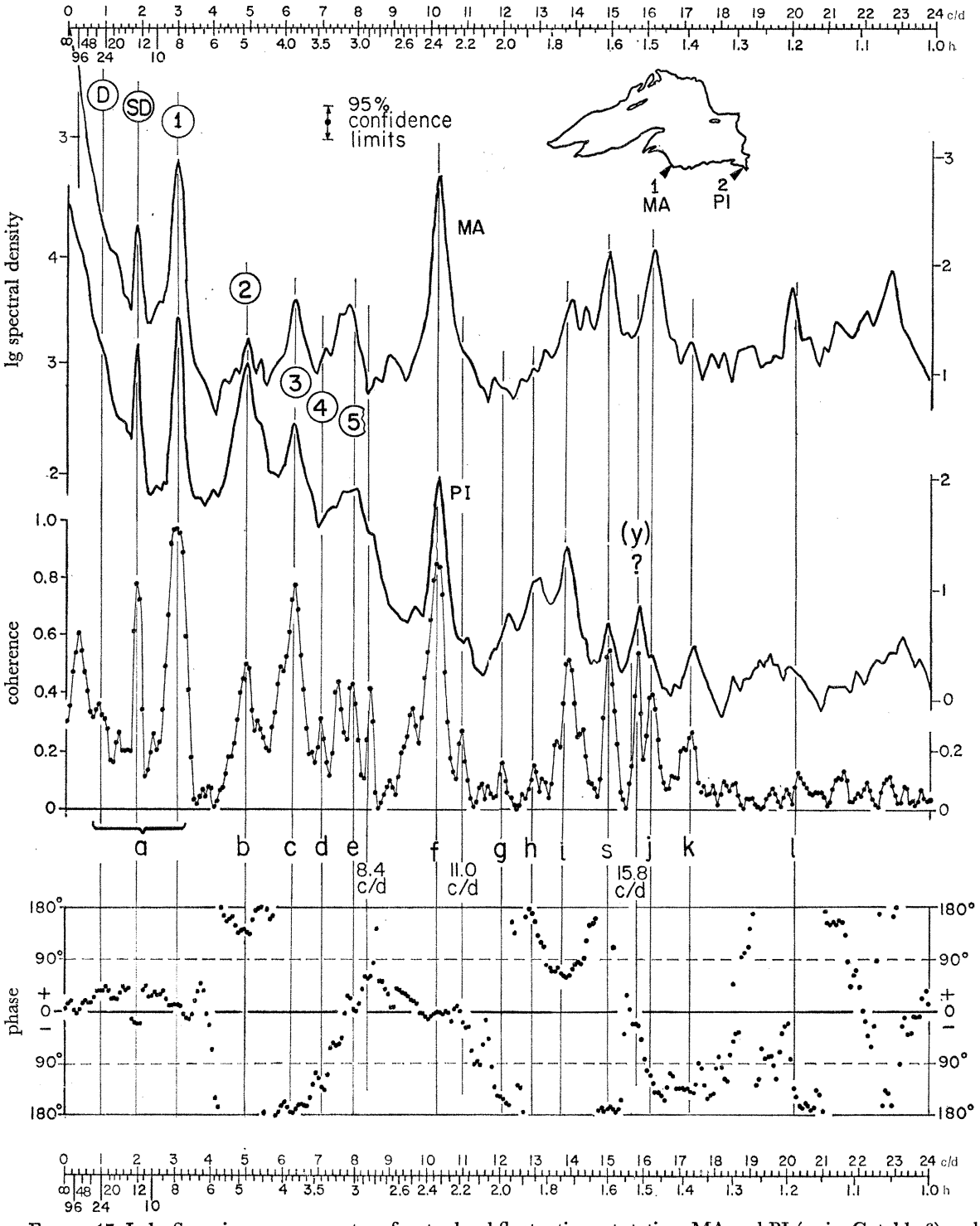

FIGURE 17. Lake Superior: power spectra of water level fluctuations at stations MA and PI (series C, table 6) and spectra of interstation coherence and phase difference. In this and later figures, vertical lines labelled D, S, and 1 to 5 represent best frequency estimates of the diurnal and semidiurnal tides and of the first five free modes of oscillation; lower case letters refer to peaks identified in figure 15.

Although the spectral density scales differ, comparison of spectra (i) and (ii) discloses the presence in both of the same principal peaks *a–f* and the appearance, in MA (ii), of three additional conspicuous peaks labelled (*l*), (*j*) and (*s*). These are clearly aliases of the large peaks *l*, *j* and *s* in MA (i), as can be seen by folding the MA (i) spectrum in the figure 4 manner. No such aliasing is visible in the TH (ii) spectrum, because the peaks in the 12–24 c/d range in TH (i) are much lower than those in the 0–12 c/d range. The aliases of *i* and *t*, at 10.3 and 4.9 c/d respectively in MA (ii), are obscured by the nearby 'true' peaks *f* and *b*.

TH/MA (and DU/MA) diagrams, prepared from different data sets from different years, are similar to figure 16 in their principal features and are therefore not reproduced here. For example, in the TH/MA diagram prepared from data series C, the same main peaks are present, but interstation coherence maxima are lower in the frequency range above 7 c/d. Also coherence maxima corresponding to spectral peaks *f* and *l* are inexplicably absent. (Small coherence peaks are, however, present at these frequencies in the DU/MA diagram.)

Figure 16 (MA paired with a western station, TH) may be compared with figure 17 (MA paired with an eastern station, PI) in this case prepared from the data series C, based on 30 min averages and presumably therefore protected against aliasing. Similarities between the two figures include the presence of the same conspicuous peaks, in the TH and PI spectra, at *a*, *b* (this peak more strongly excited at PI), *c*, *e*, *f*, *i* and *j*. Figure 17 differs from figure 16 in the following particulars: absence of a distinct diurnal peak; a lower response for *d*; flanking of *e* by coherence peaks at 7.4 and 8.4 c/d; flanking of *f* (considerably higher at PI than at TH and with a higher MA/PI coherence) by coherence peaks at 9.6 and 11.0 c/d; a reversal, for PI, of the TH height order of spectral peaks *g*, *h* and *i*; MA/PI coherence higher for *i* and lower for *j*; a large coherence peak for *f* and a small but distinct one for *k*; appearance of a high coherence peak near *j* at 15.8 c/d (possibly an alias of *y*, figure 15); and no coherence peak at *l*, *t* or at 20.6 c/d.

We conclude from this detailed comparison that most of the lettered peaks represent whole-basin oscillations, but that *s* and *k* are confined to the eastern part, in spite of the appearance of a broad peak covering the *k* frequency in the TH spectrum. If the large MA/PI coherence peak at 15.8 c/d in fact represents alias (*y*), the averaging procedure employed to prepare the data input for series C did not provide complete protection against aliasing. A similar result is noted by Hamblin (1968, p. 387).

Identification of the lowest longitudinal modes follows most simply from examination of coherence and phase differences between stations situated near the basin extremities, i.e. between station pairs TH/PI (figure 18) and DU/PI (figure 19) both prepared from data series C. The latter figure also illustrates the coherence and phase relations between the neighbouring stations DU and TH, which are nearly in phase in the range 0–14 c/d. Therefore, over that range, the TH/PI (not illustrated) and DU/PI coherence and phase diagrams are very similar. In both diagrams, the group of peaks *a*, *c*, *f*, *i*, and the group *b*, *d*, *h* correspond to oscillations which are approximately out of phase and in phase, respectively. At the frequency corresponding to peak *e*, PI leads TH by about 120°; and at *g*, PI lags TH also by about 120°. As the first two peaks of the *a* trio are identifiable from their frequencies as diurnal and semi-diurnal tides respectively, we conclude (i) that the third peak of the *a* trio corresponds to the first free longitudinal seiche mode, (ii) that peaks *b* and *c* and *d* correspond to the second, third and fourth modes, respectively, and (iii) that peak *e* may correspond to the fifth mode. The sixth mode, for which TH and PI would have been nearly in phase, is not represented.

PHILOSOPHICAL TRANSACTIONS OF THE ROYAL SOCIETY A MATHEMATICAL, PHYSICAL & ENGINEERING SCIENCES

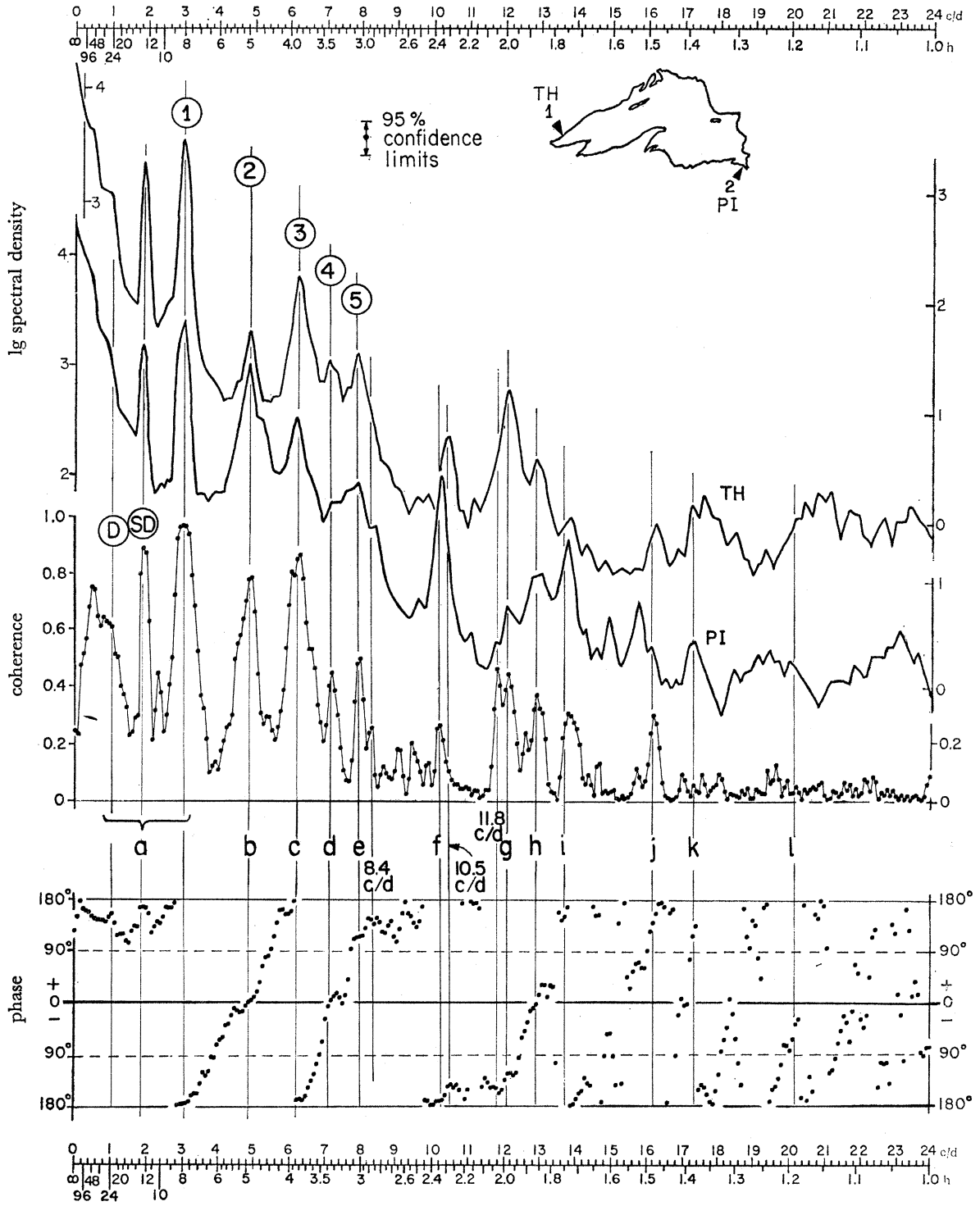

FIGURE 18. Lake Superior: power spectra of water level fluctuations at stations TH and PI (series C, table 6) and spectra of interstation coherence and phase difference. For further details see the last sentence of figure legend 17.

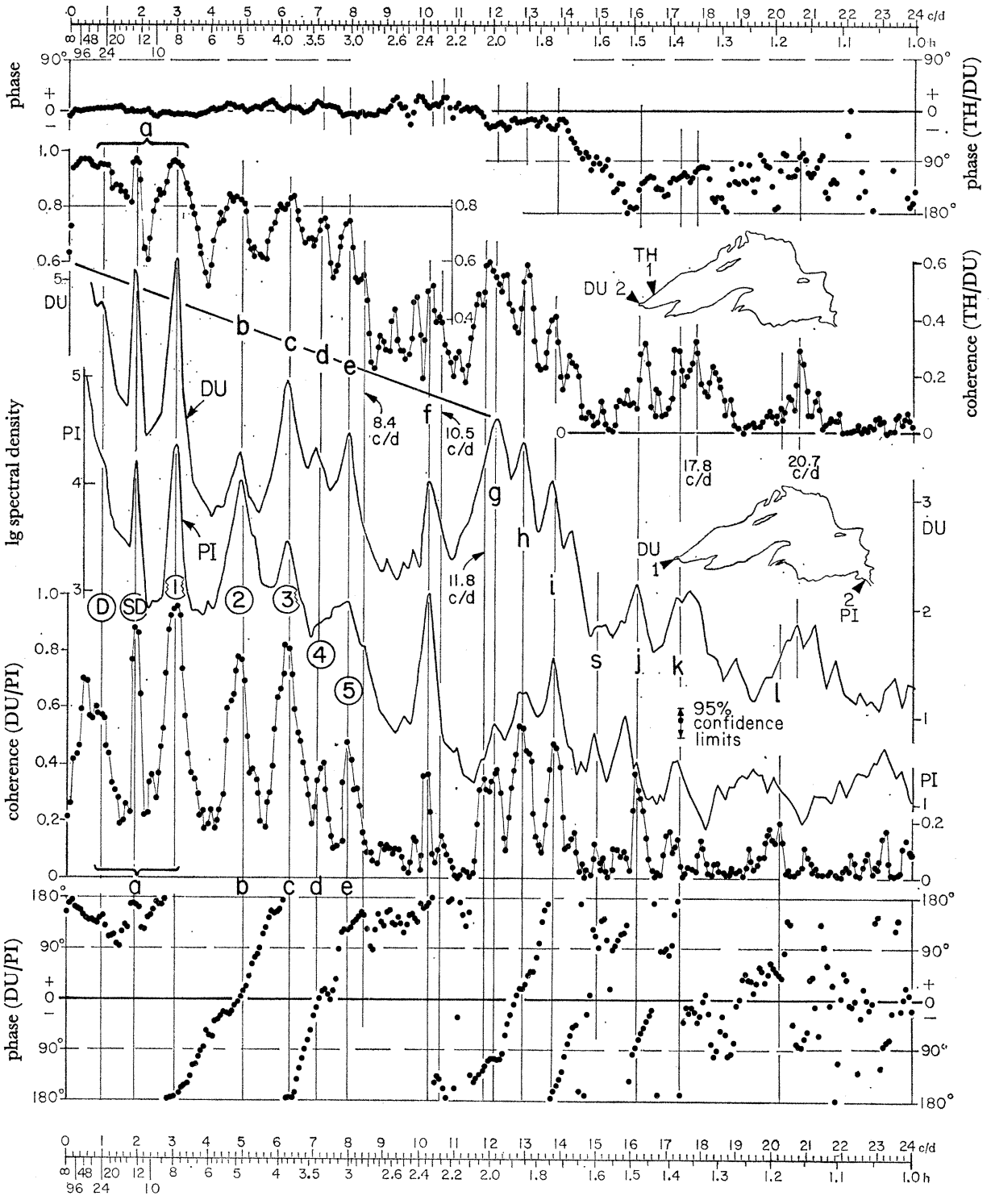

FIGURE 19. Lake Superior: upper portion, TH/DU interstation phase difference and coherence; lower portion, power spectra of water level fluctuations at stations DU and PI (series C, table 6) and spectra of interstation coherence and phase difference. For further details see the last sentence of figure legend 17.

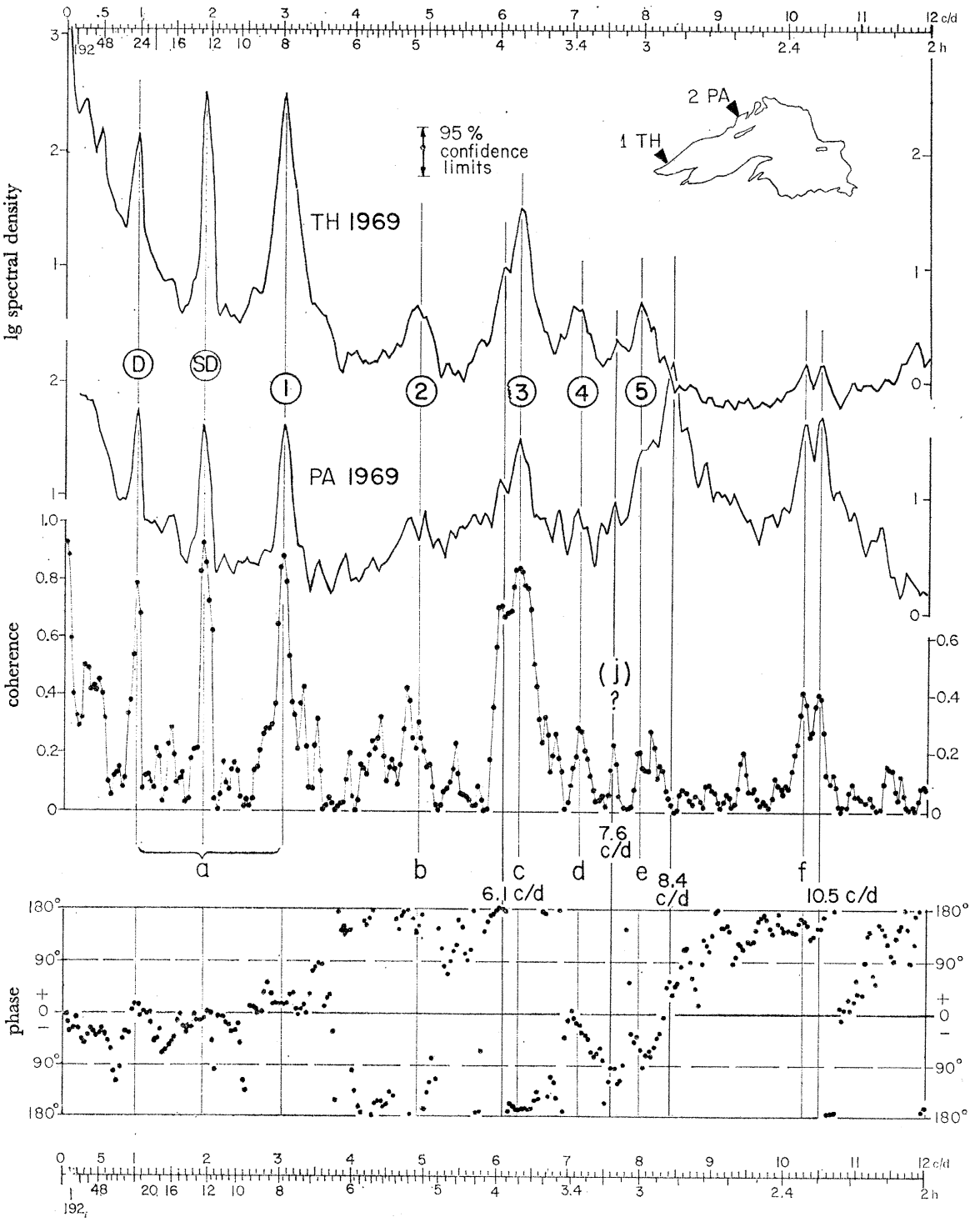

FIGURE 20. Lake Superior: power spectra of water level fluctuations at stations TH and PA (series D, table 6) and spectra of interstation coherence and phase difference. For further details see the last sentence of the description of figure 17.

PHILOSOPHICAL TRANSACTIONS OF THE ROYAL SOCIETY A MATHEMATICAL, PHYSICAL & ENGINEERING SCIENCES

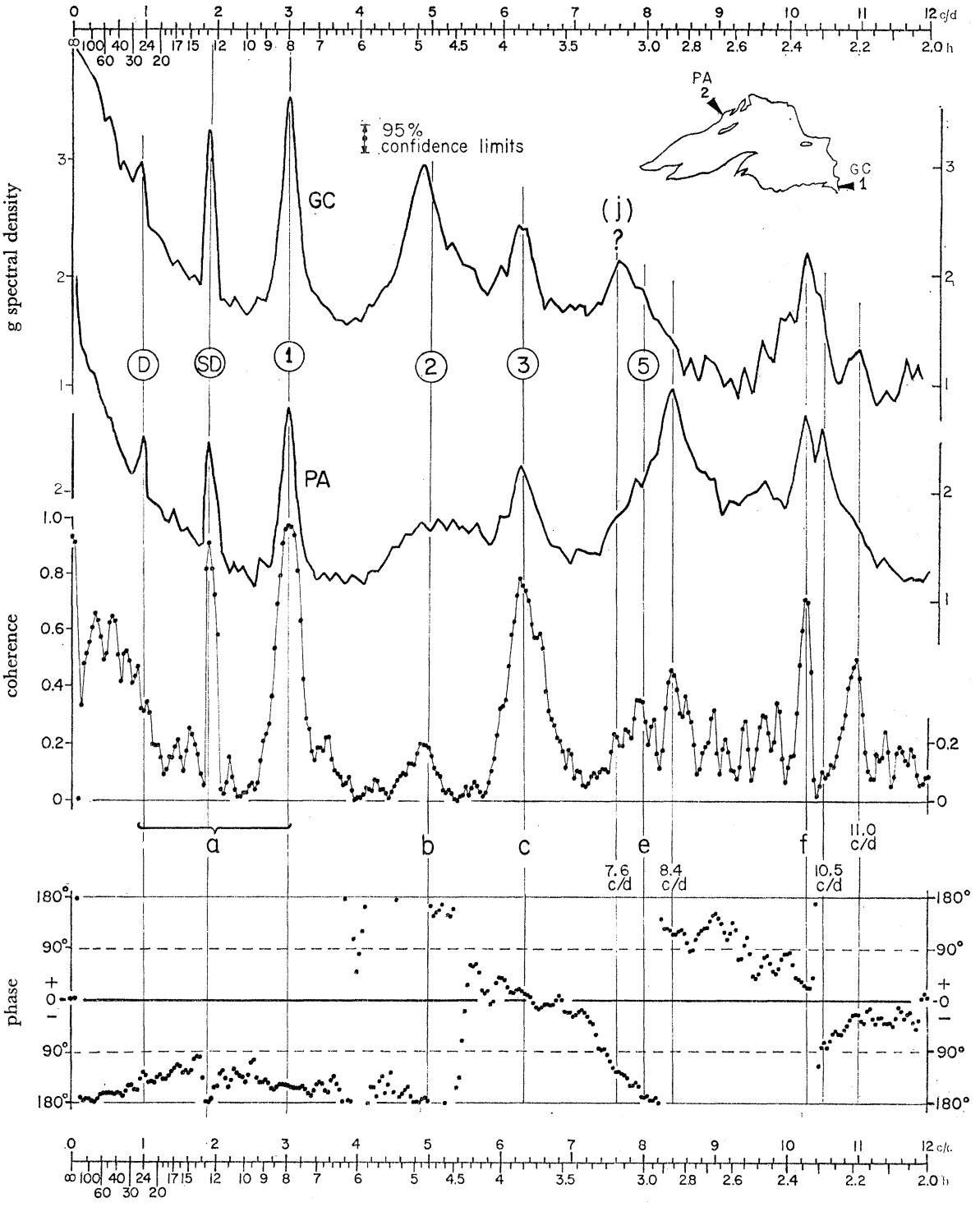

FIGURE 21. Lake Superior: power spectra of water level fluctuations at stations GC and PA (series A, table 6) and spectra of interstation coherence and phase difference. For further details see the last sentence of the description of figure 17.

PHILOSOPHICAL TRANSACTIONS OF THE ROYAL SOCIETY A MATHEMATICAL, PHYSICAL & ENGINEERING SCIENCES

Figure 19 also displays DU/TH coherence maxima for all the peaks *a–i*. Also stations PI and GC, separated by about 6 km (4 miles) at the eastern end of the basin, show a (not illustrated) high interstation coherence and remain nearly in phase over the frequency range 0–12 c/d, beyond which our exploration did not extend.

Later analysis, using all available interstation comparisons, suggests that the longitudinal modes above the third are not simple oscillations. However, as we shall need to refer to figures 17–19 in later discussion, it is convenient in these and in the following figures to identify the first five modes by number and the diurnal and semidiurnal peaks by the letters D and SD.

Station MA represented the southern shore in figures 16 and 17. Taking PA as representative of the northern shore, we now present a comparable pair of figures: figure 20 (PA paired with a western station, TH) and figure 21 (PA paired with an eastern station, GC), both covering the frequency range 0–12 c/d, but derived from different data sets, respectively D and A in table 6. Because the data set A was over three times as long as D, the spectra in figure 21 (GC/PA) have a smoother appearance than those in figure 20 (TH/PA). We did not investigate the degree of contamination by aliasing or 'noise' in either case, but the filling-in of the valleys between the main peaks of the PA spectrum suggest that it was subject to moderate contamination. Nevertheless, peaks *a*, *c* and *f* can be clearly recognized; the signatures of *b* and *e* are less strong, but clear. In addition, the GC/PA coherence diagram in figure 21 discloses the presence of two peaks not yet mentioned; the first at 8.4 c/d corresponds with the largest peak in the PA spectrum, the second at 11.0 c/d corresponds to small but distinct peak in the GC spectrum and a significant peak in GC/PA coherence. Coherence maxima at 8.4 and 11.0 c/d are not visible in figure 20, which suggests that the oscillations they represent, and which will be discussed later, are principally confined to the eastern part of the basin. Figure 20 shows a large interstation coherence peak at 6.1 c/d and a smaller coherence peak at 10.5 c/d, neither of which appear in figure 21.

(*c*) *Phase progressions and amplitude distributions of the first three modes*

For the determination of phase progressions, the spectral series listed in table 6 yielded 51 interstation comparisons. As for Lake Michigan, those spectral peaks which were identified by high interstation coherence and high spectral power as tides or free modes, were found at or close to particular frequency bands in the spectra of all station pairs. Except for the weakest oscillations, frequency estimates were within ± 1 bandwith, i.e. ± 0.04 c/d in the 0–12 c/d ($m = 300$) spectra. For example, in 33 interstation comparisons (series A, B and D) we found that mode 1 coherence was highest for band number 76 (7.90 h period) in 23 cases, highest for band number 77 (7.79 h) in 4 cases, and at the same level at bands 76 and 77 in 6 cases. This yields a weighted period estimate of 7.88 ± 0.02 h (3.05 c/d). For the higher modes, and particularly for those associated with low interstation coherence, the frequency estimates were less precise. Again, some modes appeared to be more sharply 'tuned' than others.

The method of estimating interstation phase differences must now be described in some detail. For each mode, the spectral band which corresponded to the greatest number of interstation coherence maxima was selected. For that band *all* individual interstation coherences and phase differences were plotted on a set of lake charts, one for each of the spectral series listed in table 6. From each chart, a 'best-fitted' set of station phase angles relative to 0° at GC was arrived at by inspection, giving greater weight to station pairs showing high interstation coherence. For the first three modes it was relatively easy to arrive at a self-consistent set of

station phase angles (figure 22) which minimized the deviations of individual station phase differences from the weighted mean. With increasing mode number, the process became more difficult with decreasing interstation coherences and greater angular deviations. These findings are summarized in tables 7 and 8. We intend to publish more detailed tables of weighted station angles, individual station deviations, and ranges of interstation coherence for each of the spectral sets A, B, C and D as a Special Report of the Center for Great Lakes Studies, The University of Wisconsin–Milwaukee.

TABLE 7. LAKE SUPERIOR: DEVIATIONS OF INDIVIDUAL ESTIMATES OF STATION PHASE ANGLE FROM THE WEIGHTED VALUES, GIVEN IN TABLE 8 AND BASED ON ALL SPECTRA IN SERIES A, B, C AND D (TABLE 6). The ranges of interstation coherence, corresponding to the data considered in the weighting, are also tabulated

mode no.	spectral band no.†	equivalent† frequency c/d	equivalent† period h	maximum deviation of individual station angles from those given in figure 22 and table 8 deg +	maximum deviation of individual station angles from those given in figure 22 and table 8 deg −	range of individual interstation coherences employed in angle estimates
1	76	3.04†	7.90‡	4	2	0.63–0.98
2	124	4.95	4.84	4	4	0.14–0.96
3	158	6.32	3.80	7	8	0.12–0.88
4	178	7.13	3.37	27	13	0.07–0.77
5	199	7.96	3.02	13	9	0.10–0.84
8§	257	10.28	2.34	13	11	0.13–0.91

† The modes were identified by peaks of spectral power coinciding with peaks of interstation coherence in all spectra from series A, B, C and D (table 6) combined. The particular spectral bands most often coinciding with the power and coherence peaks are listed in this table. The 'equivalent' frequencies and periods are the central values for those spectral bands.

‡ A more precise weighting, in the text and taking the power distribution in adjacent spectral bands into account, yields values of 3.05 c/d and 7.88 ± 0.02 h.

§ Identified as eighth mode by Rao & Schwab (see figure 32*b*).

Where interstation coherences were high, e.g. for the lower odd-numbered modes, variations between the estimates from the four spectral series, and also the variance within each series, were small – for example, $+4°$ to $-2°$ for the first mode. At lower coherences, e.g. for the higher and even-numbered modes, the variance of the estimates within and between the series increases; and large unresolvable discrepancies occasionally appear between estimates for particular stations, for example, MA and RO.

With the qualification that the station angle listed later in table 8 – at a recorder stilling well, in a harbour for example – may not exactly correspond to the phase angle at the nearest point on the main lake shore, the angle sets were used to estimate the 'observed' phase progressions of the first three modes in figure 22. The statistical confidence of these estimates is probably greater for the northern shore with four stations than for the southern shore with two; but it is clear that the phase patterns are amphidromic – otherwise the station phase angles, shown in boxes in figure 22, would everywhere have been either near 0° or 180° – and are consistent with a positive amphidrome, defined earlier in connexion with figure 13. The locations of the amphidromic points for all three modes are close to the nodal lines computed for the non-rotating basin by Rockwell (1966) and indicated by broad white arrows in figure 22.

It is also evident from those spectral comparisons which involve stations at the extremities of the basin – figure 18 for example – that the first mode is the most strongly excited of all.

PHILOSOPHICAL TRANSACTIONS OF THE ROYAL SOCIETY A MATHEMATICAL, PHYSICAL & ENGINEERING SCIENCES

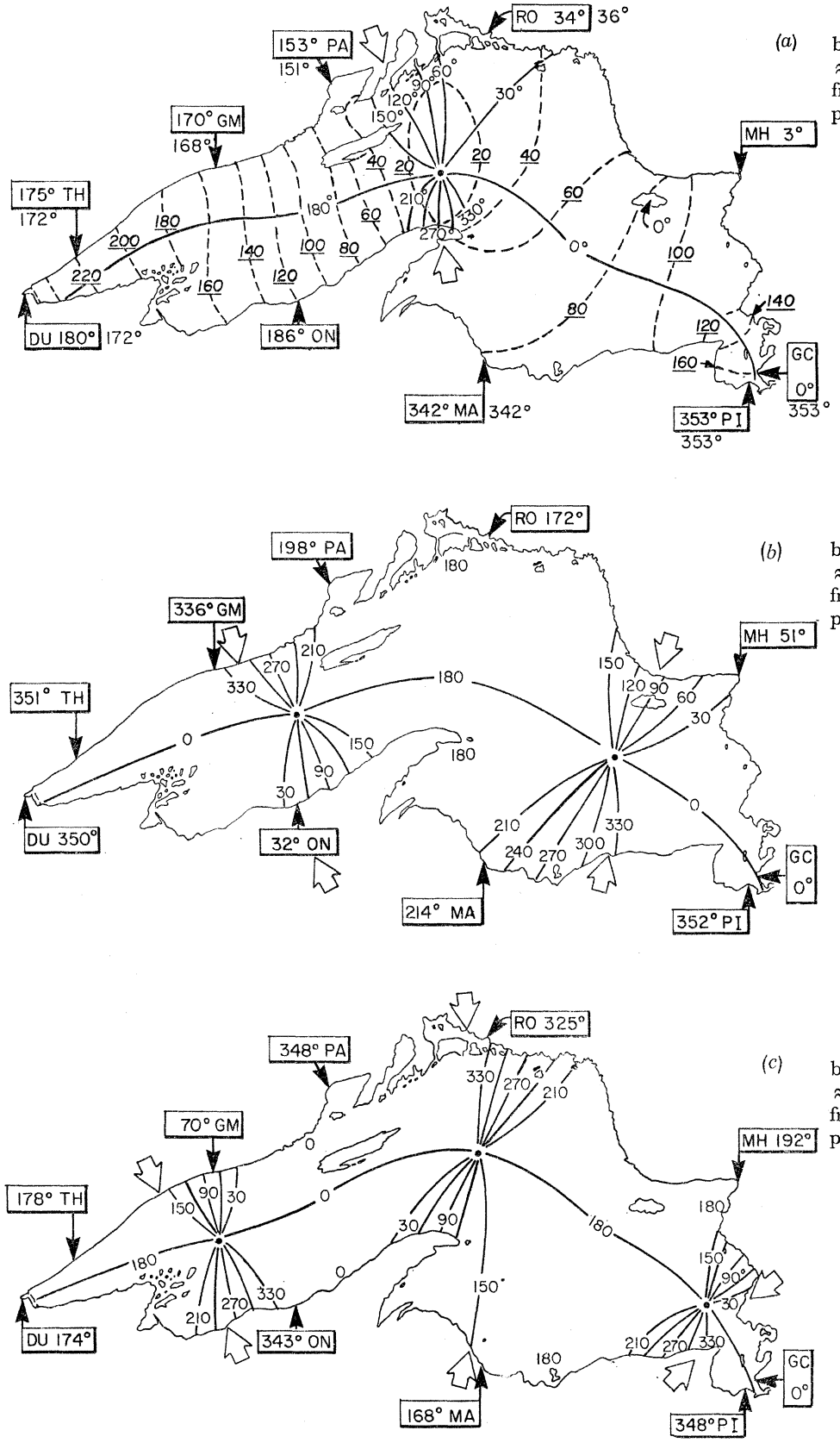

FIGURE 22. Lake Superior: station phase angles (boxed and relative to 0° at GC) for the first three surface seiche modes, based on 51 interstation comparisons (table 8, §3(*c*)). In section (*a*) the co-tidal and co-range lines are those illustrated in Platzman (1972); and, for comparison, Platzman's computed station phase angles are shown outside the boxes. In sections (*b*) and (*c*), the positions of co-tidal lines (at 30° intervals) and presumed amphidromic points are drawn to fit the station angles, but are otherwise guesswork, to be compared with the computed results of Rao & Schwab (1976). The large white arrows indicate the end of nodal lines computed by Rockwell (1966), ignoring rotation.

PHILOSOPHICAL TRANSACTIONS OF THE ROYAL SOCIETY A MATHEMATICAL, PHYSICAL & ENGINEERING SCIENCES

Next comes the third, which is much stronger than the second except at PI, the only station at which the second mode is the stronger of the two. For the first mode, none of the interstation coherences fall below 0.63, and the spread of the station angle estimates is only 6°. For the second and third modes the minimum coherences accepted were 0.14 and 0.12, respectively, and the spread of station angle estimates rose to 15° for the third mode.

The 'observed' periods and the station phase angles (shown boxed in figure 22) may now be compared in table 8 with values computed by the two dimensional procedures of Platzman (1972) for the first mode and most recently for modes 1–5 by Rao & Schwab (1976, the following paper) and for mode 8 in figure 32(*b*). Platzman's computed phase angles, relative to 0° at GC and assuming a PI/GC lead of 7°, are entered outside the boxes in figure 22*a*, which also reproduces his estimated cotidal lines and co-range (amplitude) lines, the latter normalized to r.m.s. 100. The observed and the (Platzman) computed periods are respectively

TABLE 8. LAKE SUPERIOR: COMPARISONS BETWEEN OBSERVED PERIODS OF THE FIRST FIVE AND THE EIGHTH MODES AND THOSE COMPUTED BY THE TWO-DIMENSIONAL PROCEDURE OF RAO & SCHWAB (1975). ALSO TABULATED ARE THE PHASE ANGLES OF INDIVIDUAL STATIONS, RELATIVE TO 0° AT GC AND WEIGHTED BY THE PROCEDURE DESCRIBED IN THE TEXT

	period/h		weighted estimates of station phase angles/deg (GC = 0) station:								
mode no.	observed	computed (Rao & Schwab)	MH	RO	PA	GM	TH	DU	ON	MA	PI
1	7.88	7.86†	3	34	153	170	175	180	186	342	353
2	4.84	4.45	51	172	198	336	351	353	32	214	352
3	3.80	3.76	192	325	348	70	179	174	343	168	348
4	3.37	3.17	176	61‡	—	118‡	342	333	173	116	345
5	3.02	2.94	177	71	155	301	111	115	300	319	350
8	2.34	2.32	174	170	352	268	166	155	170	350	348

† Platzman (1972) computed a period of 7.84 h.

‡ Based on the assumption that the estimates for RO and GM are correct, alhough interstation coherences were low: the RO estimate depends on two interstation comparisons both of low coherence (0.08 and 0.12); the GM estimates (series B and C) are based on one station pair (coherence 0.21) and five station pairs (coherence range 0.07–0.11), respectively.

7.88 ± 0.02 and 7.84 h, and at no station do the observed and computed phase angles differ by more than 8°. The period of the first mode computed by Rao & Schwab is 7.86 h and the computed minus observed station phase angles range from 19° at PA to −16° at RO, in each case less than the difference between neighbouring squares of their numerical grid at those locations. The average difference is 1.8°. The differences between the computed angles and our observed station phase angles for modes 1–5 are presented graphically, in terms of equivalent distance along the shoreline, in Rao & Schwab's figures 19 and 20.

Rao & Schwab's (1976) figures 11–13 estimate the (cotidal) phase and amplitude distributions for the first six gravitational modes. Amplitudes in each case are relative to 100 at the western end of the basin (DU). When Rao & Schwab's computed co-tidal lines are compared with those drawn from our observations in figure 22, the *computed* spread of the co-tidal lines along the shorelines near the amphidromic points is somewhat less than that '*observed*' in figure 22.

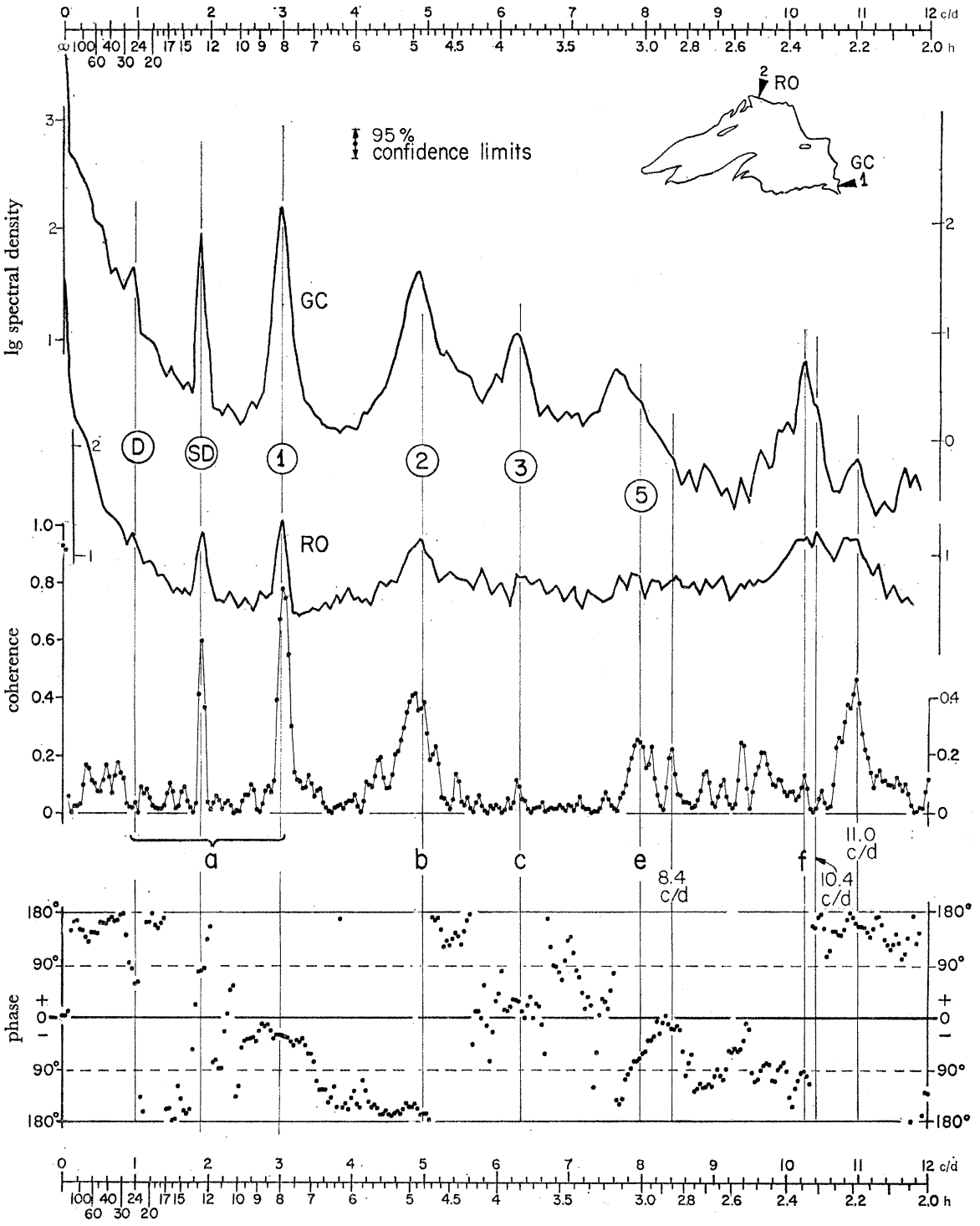

FIGURE 23. Lake Superior: power spectra of water level fluctuations at stations GC and RO (series A, table 6) and spectra of interstation coherence and phase difference. For further details see the last sentence of the description of figure 17.

PHILOSOPHICAL TRANSACTIONS OF THE ROYAL SOCIETY A MATHEMATICAL, PHYSICAL & ENGINEERING SCIENCES

The computed amplitude distributions are also generally in agreement with the relative amplitudes of peaks seen in our spectra. For example, figure 18 shows a somewhat larger first mode peak at TH than at PI, whereas the second mode peak is much higher at PI than at TH; it also appears as a large peak in the GC spectrum in figure 21. While interstation coherence for the second mode is low for most station pairs, it is high (as expected) for GC/PI and moderately high (0.4) with 180° phase difference for GC/RO (figure 23), consistent with the position of RO in the antinodal region (figure 22*b*).

The comparison between figures 21 and 23 is also instructive for other reasons. Although the RO spectrum appears to be severely contaminated by aliases or 'noise', the following conclusions can be drawn from it; (i) that the tidal and first mode peaks are lower for RO than for other stations, consistent with the 24° RO phase angle in figure 22*a*; and (ii) that the second mode peak, emerging above the aliasing contamination, is almost as high as the first. The amplitude of the third mode at RO must be low (cf. low GC/RO coherence at that frequency) which is in accord with the position of RO in figure 22*c* and with the low amplitude computed for that region by Rao & Schwab (1976, figure 12).

For all other station pairs, the third mode coherence is greater and often much greater (figures 20, 21) than that for the second mode. In figure 24 (MA/PA), for example, coherence (0.7) at the third mode is only exceeded by that at the first mode and only equalled by that at two other frequencies (SD and *f*), in spite of the fact that Rao & Schwab's computed amplitudes for those stations are only about one-tenth of that at DU. This is consistent with the MA and PA third mode phase angles in figure 22*c*, which differ by only 12° from 180° and 0°, respectively. Incidentally, the MA spectrum in figure 24 is that reproduced as MA (ii) in figure 16. The aliases (*l*), (*j*) and (*s*) are conspicuous; and (*s*) is associated with an interstation coherence of nearly 0.4, indicating that (*s*) must also be present in the PA spectrum. The highest peaks in that spectrum, at 8.4 and 10.5 c/d, are the subject of later discussion.

(*d*) *Speculations concerning the structure of the free modes in the frequency range* 7–12 c/d

Spectral peaks *d*–*l* in previous figures, i.e. those peaks which apparently represent oscillations of the whole or of large portions of the basin in the frequency range 7–24 c/d, are generally associated with much smaller interstation coherences than are the peaks of the first three modes. As frequency increases, interstation coherences become smaller and estimates of phase angle become less precise (table 7). This is a consequence of the limited resolution provided by only ten recording stations, irregularly spaced in a basin of complex shape. Although we examined all the spectral clues, our speculations on the structure of the modes higher than the third would have been of little value, were it not for the recent possibility of comparing them with the computed findings of Rao & Schwab (1976).

(i) *Peaks d* 7.13 c/d, (*j*) 7.6 c/d, *and e* 7.96 c/d

Peak *d* (at 7.13 c/d) is rarely excited strongly. An exception occurred with coherence 0.5 for the station pair TH/MH (series D, not illustrated). This peak which we have identified as the fourth mode appears, weakly excited, in figures 16, 18, 20, 24, 26, 27 and 29, but cannot be seen in figures 17, 21, 23, 25, 28 and 30. Its correct identification is therefore open to question. It cannot be ruled out that peak (*j*) near 7.6 c/d – tentatively identified in our diagrams as an alias of *j* and excited with moderate interstation coherence in figures 20, 26, 28, 29 and 30 –

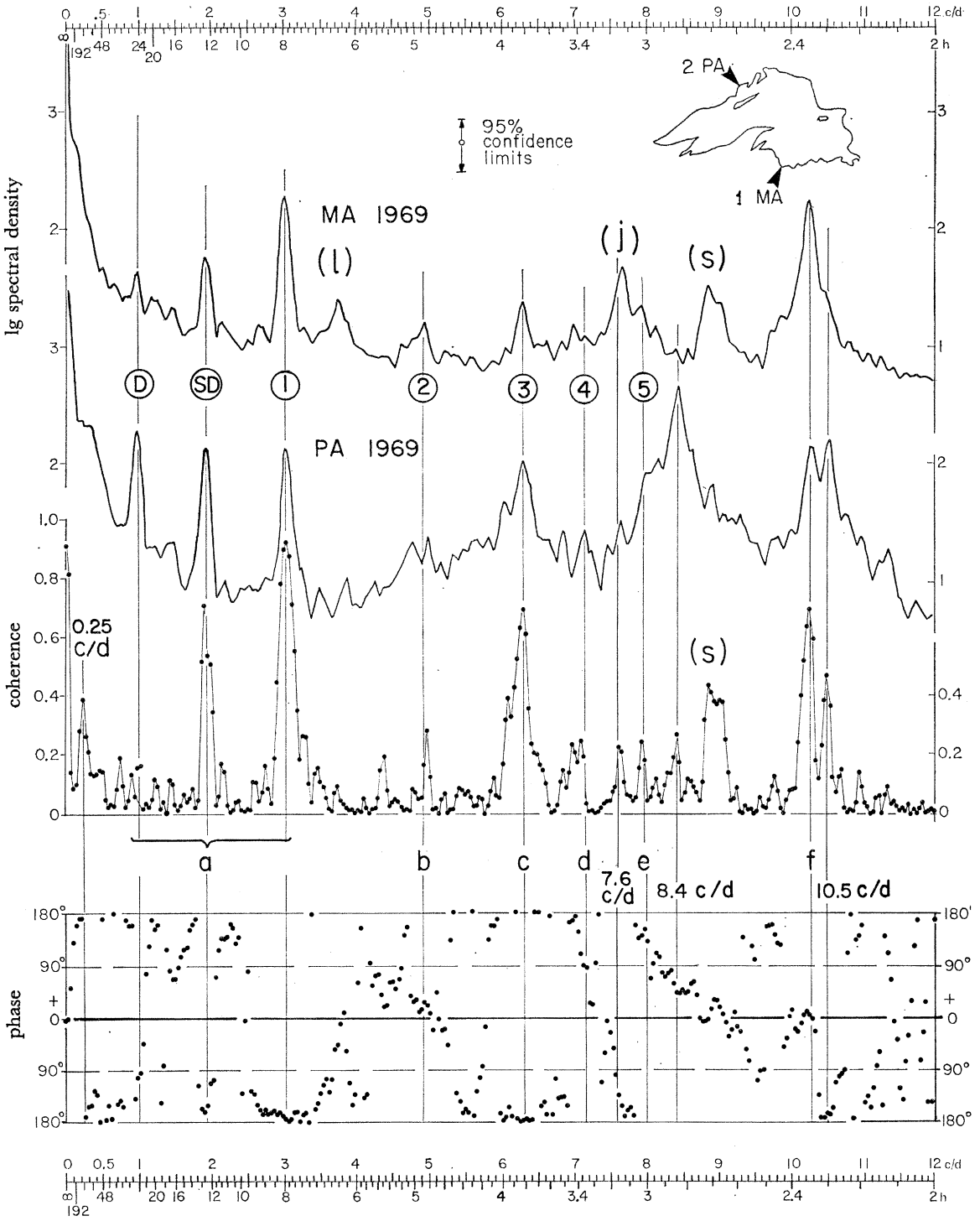

FIGURE 24. Lake Superior: power spectra of water level fluctuations at stations MA and PA (series D, table 6) and spectra of interstation coherence and phase difference. For further details see the last sentence of the description of figure 17.

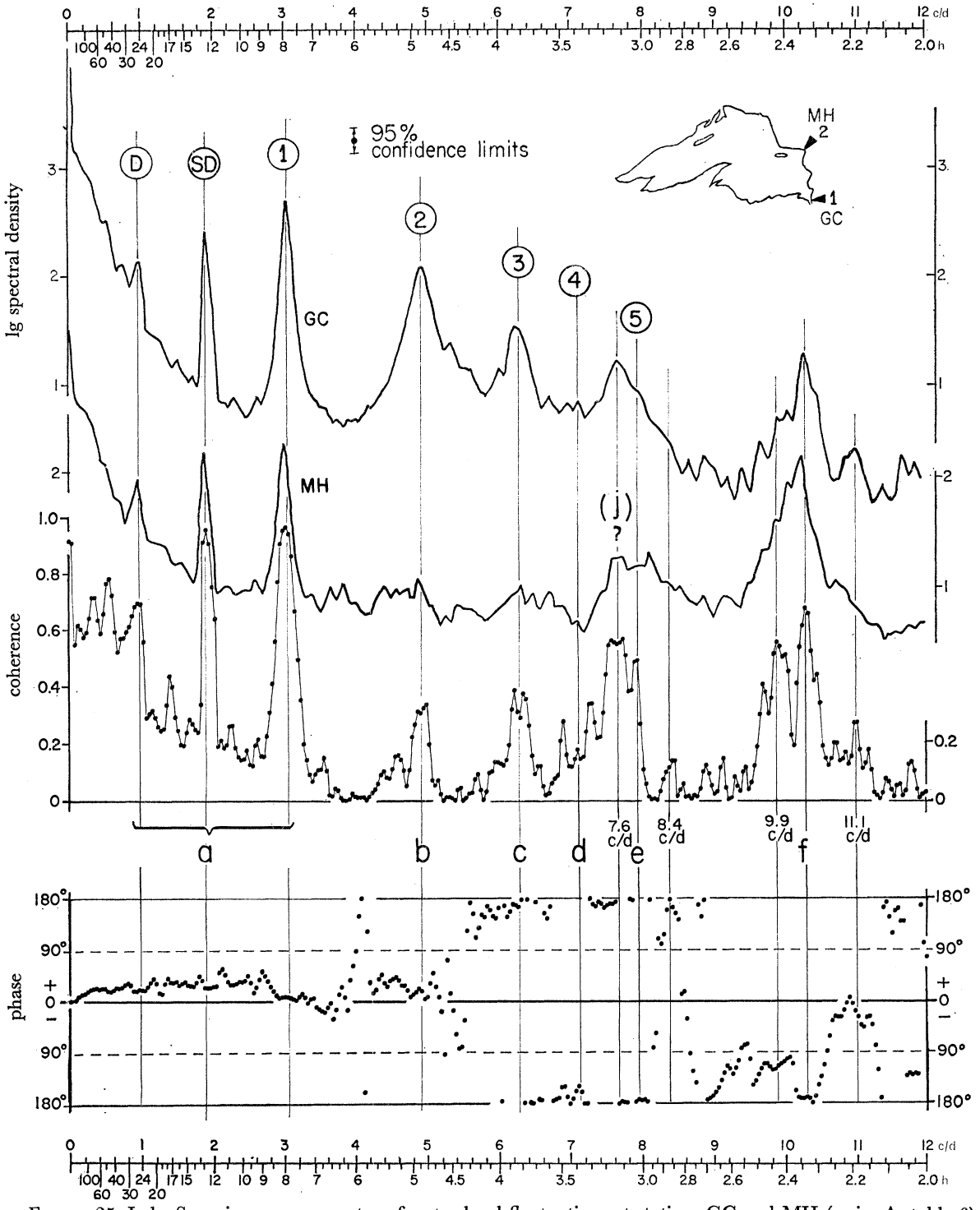

FIGURE 25. Lake Superior: power spectra of water level fluctuations at stations GC and MH (series A, table 6) and spectra of interstation coherence and phase difference. For further details see the last sentence of the description of figure 17.

PHILOSOPHICAL TRANSACTIONS OF THE ROYAL SOCIETY A MATHEMATICAL, PHYSICAL & ENGINEERING SCIENCES

may be the equivalent of Rao & Schwab's fourth mode, computed frequency 7.57 c/d. Their figure 12 shows relatively high amplitudes for the fourth mode near GC and in Keweenaw Bay, west of MA. It may be more than coincidental that the highest (*j*) peaks appear at GC (figure 21) and MA (figure 24), with an interstation coherence of more than 0.5 for GC/MH (figure 25). This result could also be produced by an alias of oscillation *j*, if that is strongly excited at both GC and MA. To settle this question requires further study, pending which the phase relations for peak *d* in figure 18 and comparable figures may be taken to support its tentative identification as the fourth mode.

Peak *e* (7.96 c/d) is more prominent in many spectra, frequently showing moderate interstation coherence (figures 18, 26, 27, 28 and 30). Rao & Schwab's amplitude distribution for their fifth mode (8.16 c/d) shows almost all the activity in the eastern half of the lake. The (*j*) peaks and the corresponding interstation coherences do, in fact, appear higher at eastern stations (for example GC/MH, figure 25); but because the nearby signal from (*j*) at 7.6 c/d is also strong at eastern stations, *e* appears as a 'shoulder' on a larger peak. However, the identification of *e* as the fifth mode appears well-founded.

(ii) *Local oscillation* 8.4 c/d *at PA and other peaks of restricted occurrence*

Although we are principally interested in whole-basin oscillations, other conspicuous responses which involve single stations or a particular pair of stations are also noteworthy, particularly in conjunction with the recently computed results of Rao & Schwab (1976).

Not identifiable with any prominent alias is the largest peak in the PA spectrum, which shows moderate interstation coherence at 8.4 c/d for GC/PA (figure 21) and also for PA/PI (coherence 0.6, series B, not illustrated). This 8.4 c/d peak is not found in spectra for other stations, although small interstation coherence maxima appear at this frequency for station pairs in the eastern part of the basin, figures 17, 23 and 24. The origin of the remarkable PA oscillation is obscure. It cannot be a mode of Thunder Bay alone, the fundamental period of which is much too short. Dr G. Godin (personal communication) has suggested that interaction between Thunder Bay and Black Bay is a possible explanation. Rao & Schwab's mode 6 (their figure 13) does show large amplitude in the Thunder Bay region, but its frequency (9.30 c/d) appears to rule it out as a candidate for the giant PA peak. That peak is, however, very broad; and the possibility of some resonance with the sixth mode cannot be excluded.

The isolated peak near 8.9 c/d in the MA spectra (figures 24, 29 and 30, with moderate interstation coherences for MA/PA and MA/MH) was previously identified as a possible alias of *s*. Its frequency is not far removed from 9.30 c/d calculated by Rao & Schwab for the sixth mode. Another nearby peak or 'shoulder' with moderate interstation coherence (GC/MH, figure 25, and MA/MH, figure 29) appears near 9.8 c/d and has not been identified as an alias. It seems unlikely that this peak is a signal of Rao & Schwab's seventh mode (10.0 c/d), the hitherto unpublished computed structure of which is illustrated in the supplementary figure 32*a*. That figure shows largest amplitudes at the western end, whereas the observed 9.8 c/d peak is strongest for eastern stations. Other relatively localized oscillations generate peaks at:

11.0 c/d, confined to the eastern region with highest coherences for station pairs including GC (figures 21, 23, 25), perhaps a signature of Rao & Schwab's ninth mode at 10.9 c/d (personal communication);

s (15.1 c/d) with moderate coherences confined to station pairs including MA (figures 16, 17 and 26);

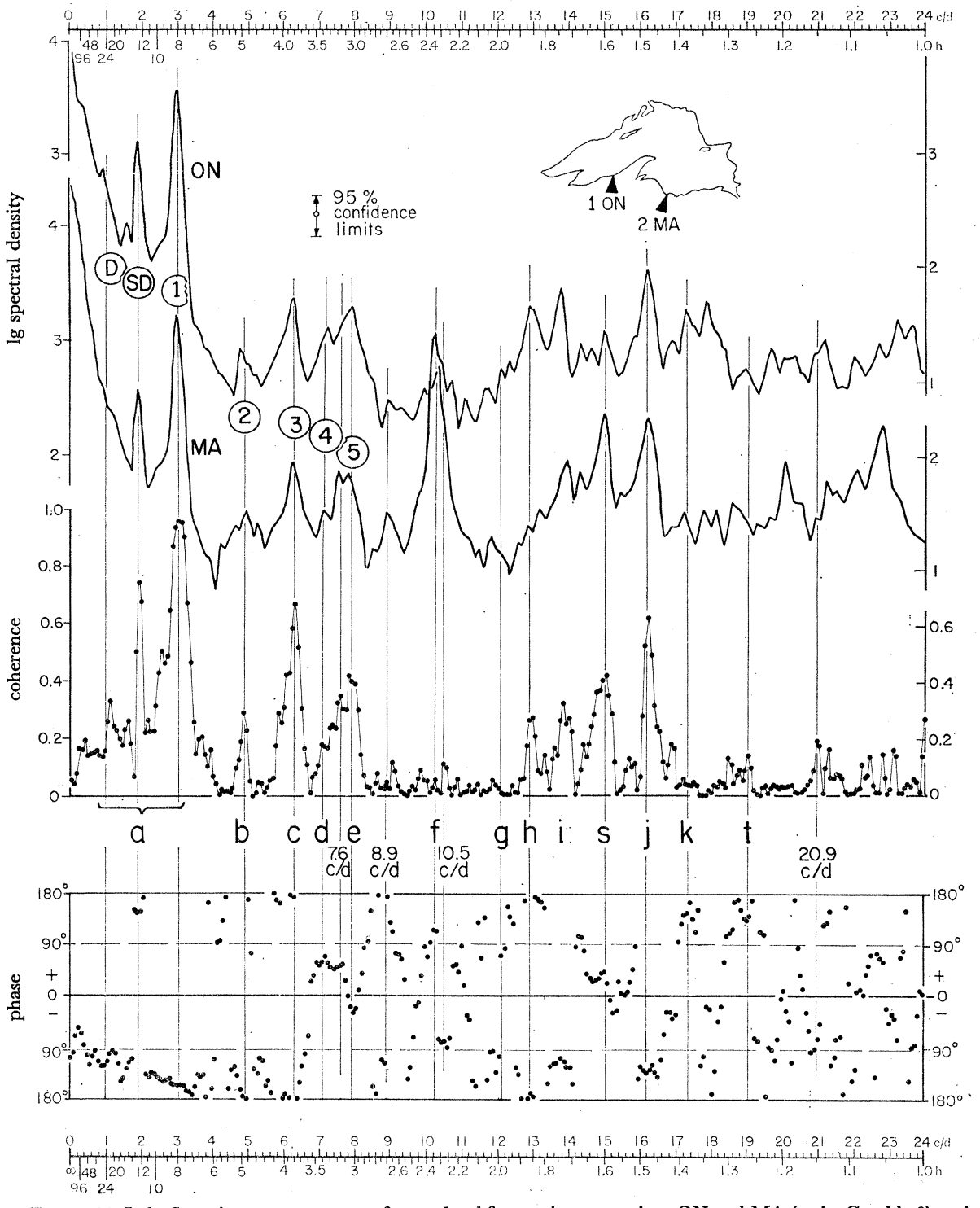

FIGURE 26. Lake Superior: power spectra of water level fluctuations at stations ON and MA (series C, table 6) and spectra of interstation coherence and phase difference. For further details see the last sentence of the description of figure 17.

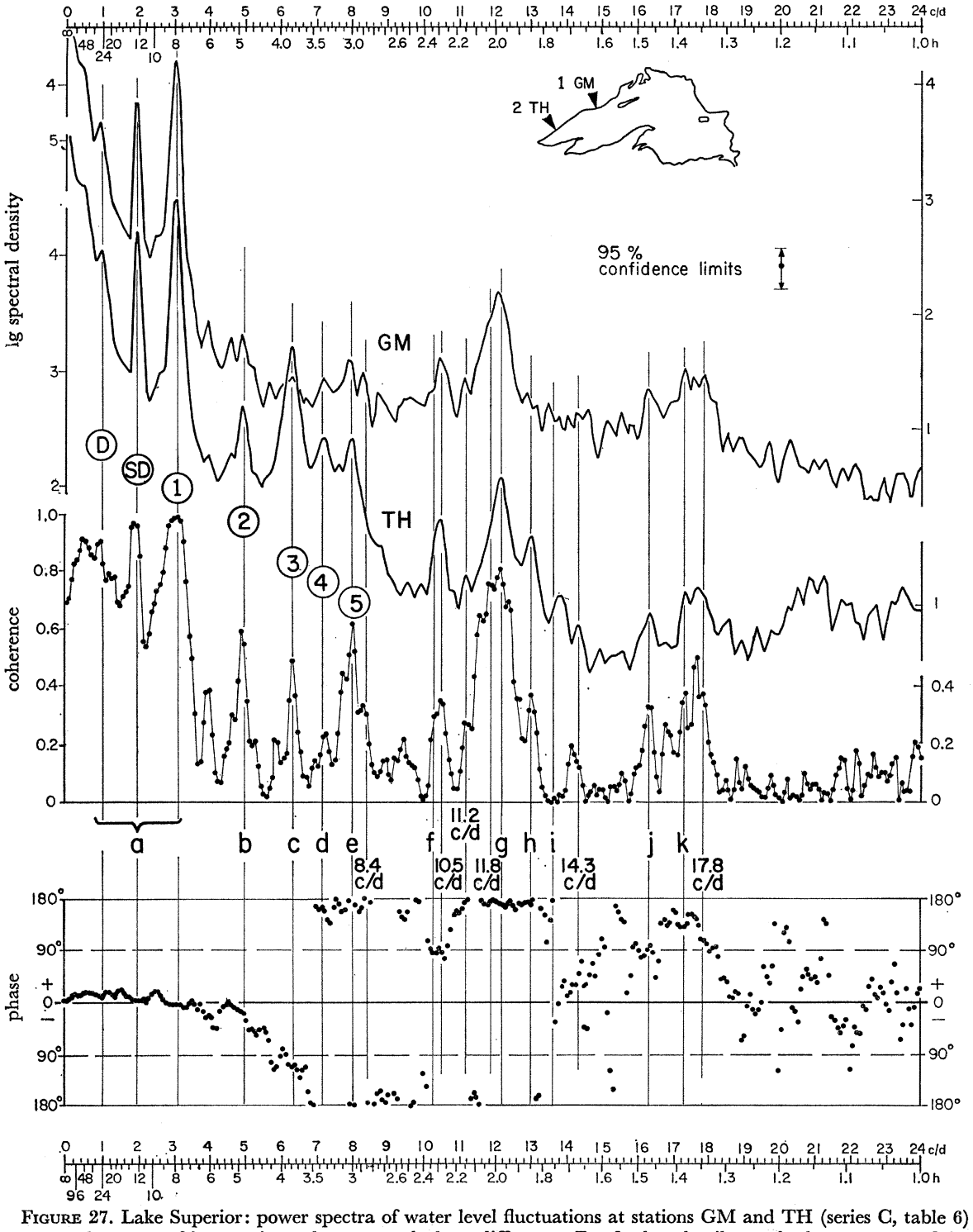

FIGURE 27. Lake Superior: power spectra of water level fluctuations at stations GM and TH (series C, table 6) and spectra of interstation coherence and phase difference. For further details see the last sentence of the description of figure 17.

PHILOSOPHICAL TRANSACTIONS OF THE ROYAL SOCIETY A MATHEMATICAL, PHYSICAL & ENGINEERING SCIENCES

17.8 c/d with moderate coherence for western station pairs GM/TH and GM/ON (figures 27 and 28) and ON/TH (not illustrated); and

l (20.3 c/d) represented by a distinct coherence peak only for TH/MA (figure 16) and perhaps as an alias with 0.3 coherence at 3.7 c/d in the 0–12 c/d MA/MH figure 29.

Less localized oscillations include the group *g* to *k* each of which, to judge from interstation coherences, occupies the greater part of the basin but is more strongly excited in one particular region than elsewhere. For example, *g* (12.0 c/d, often appearing with twin peaks at 11.8 and 12.2 c/d) yields strong coherence only for northwestern station pairs DU/GM (not illustrated), DU/TH, and GM/TH (figures 19 and 27). This may be the response of the western part of the lake, co-oscillating as a bay with the main basin to produce the '2 h seiche', which Housley (1962) found to occupy a greater proportion of the DU record than any other, except the first longitudinal '8 h seiche'. Other oscillations showing weak to moderate whole-basin coherences are:

h (12.9 c/d) with weak MA/PI coherence (figure 17) and moderate coherences for pairs including western stations (0.54 DU/PI figure 19, 0.52 ON/TH not illustrated, 0.34 GM/ON figure 28 with 180° phase difference – transverse oscillation in that case?);

i (13.8 c/d) with moderate or strong coherences for station pairs including MA (figures 16, 17 and 26), negligible coherences for station pairs including GM, and with small but distinct coherence peaks for other station pairs;

j (16.3 c/d) with high TH/MA coherence (0.6, figure 16) moderate to low for other station pairs (lowest 0.12 for GM/PI not illustrated) and apparently most strongly excited, possibly as a transverse oscillation in the RO/MA region; and

k (17.3 c/d) with moderate coherences between western station pairs (GM/TH, GM/ON, figures 27 and 28) and MA/PI (figure 17) and weak coherences for TH/MA and DU/PI (figures 16 and 18).

Moderate interstation coherence at 15.7 c/d for TH/MA (figure 16), MA/PI (figure 17), and GM/PI (not illustrated) may correspond to an alias of *y* (figure 15).

We can do no more than list these spectral peaks for future reference and study, based on a closer look at the structure of the higher modes, along lines pioneered by Rao & Schwab (1976).

Our failure to demonstrate a clear connection between any whole-basin oscillation in the frequency range 9–10 c/d and Rao & Schwab's computed sixth and seventh modes, suggests that these modes are not excited, at least not as widespread oscillations. This does not rule out the possibility of local bay resonances.

(iii) *Peak f* 10.3 c/d

This peak is among the most conspicuous in all spectra, except those at the western end of the basin, DU, TH and GM. At MA its summit is only slightly below that of the first mode. It therefore represents an oscillation strongly excited in the eastern half of the basin. Its frequency is close to 10.34 c/d, calculated for the eighth mode by Rao & Schwab (personal communication) using the method described in their 1976 paper. Its structure is illustrated in the supplementary figure 32*b*.

In some spectra peak *f* is accompanied by a separate, nearby peak at 10.4 or 10.5 c/d, for example at TH (figures 16, 20), PA (figures 20, 21 and 24), and RO (figure 23) in which it may be partially 'buried' by aliasing contamination. Other spectra show a main peak at about 10.3 c/d with a 'shoulder' at about 10.5 c/d, for example MA (figure 24) and GC (figure 21).

PHILOSOPHICAL TRANSACTIONS OF THE ROYAL SOCIETY A MATHEMATICAL, PHYSICAL & ENGINEERING SCIENCES

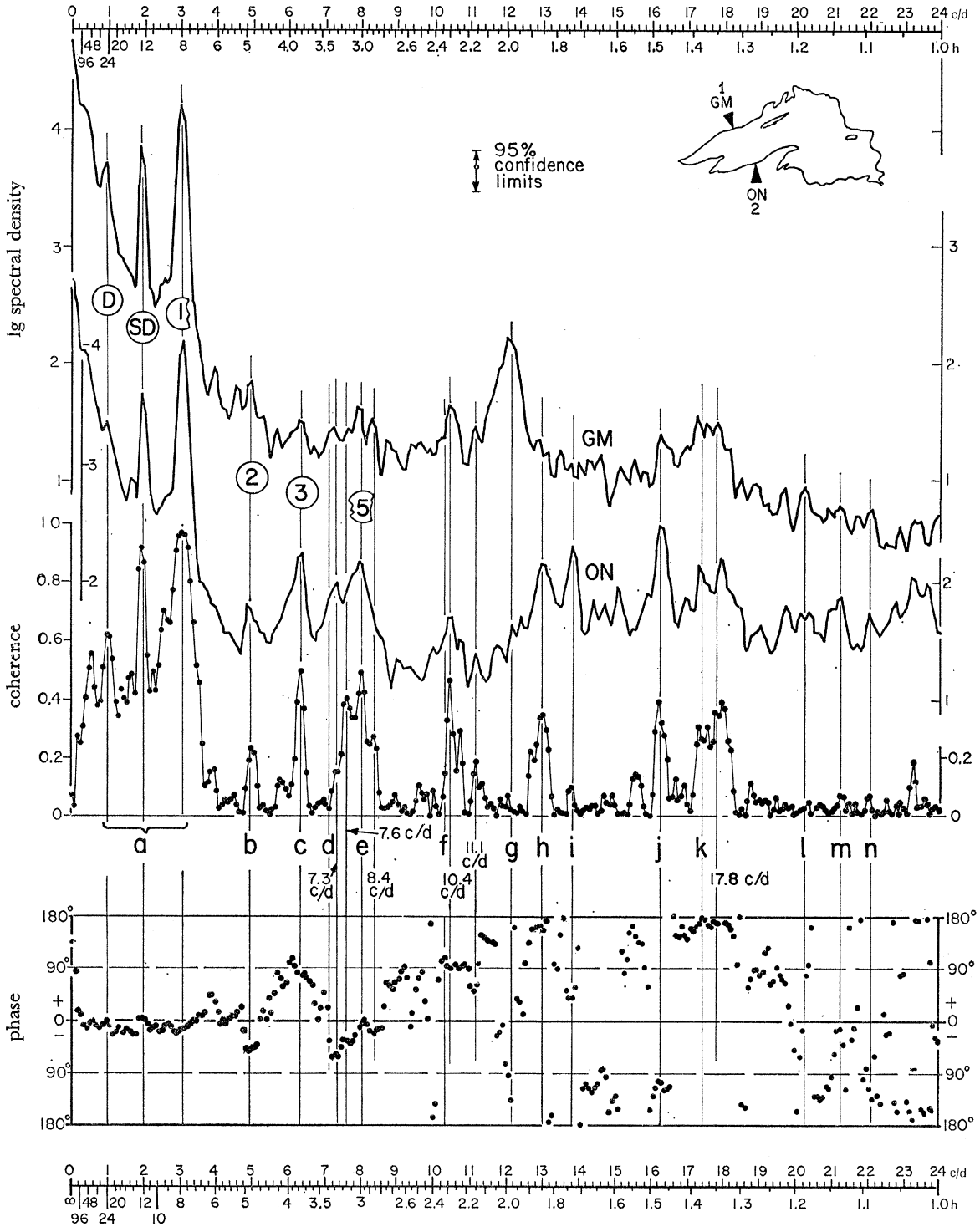

FIGURE 28. Lake Superior: power spectra of water level fluctuations at stations GM and ON (series C, table 6) and spectra of interstation coherence and phase difference. For further details see the last sentence of the description of figure 17.

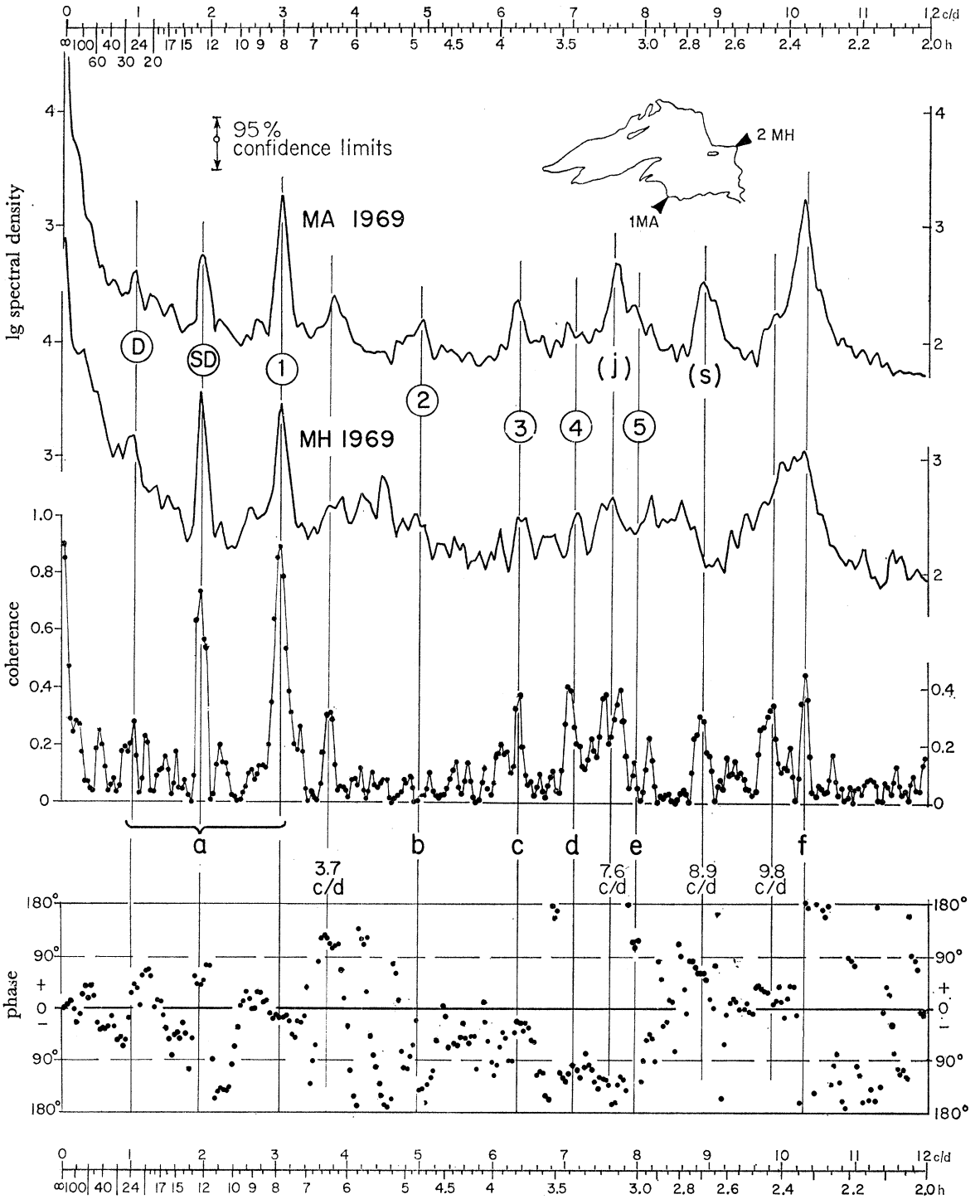

FIGURE 29. Lake Superior: power spectra of water level fluctuations at stations MA and MH (series B, table 6) and spectra of interstation coherence and phase difference. For further details see the last sentence of the description of figure 17.

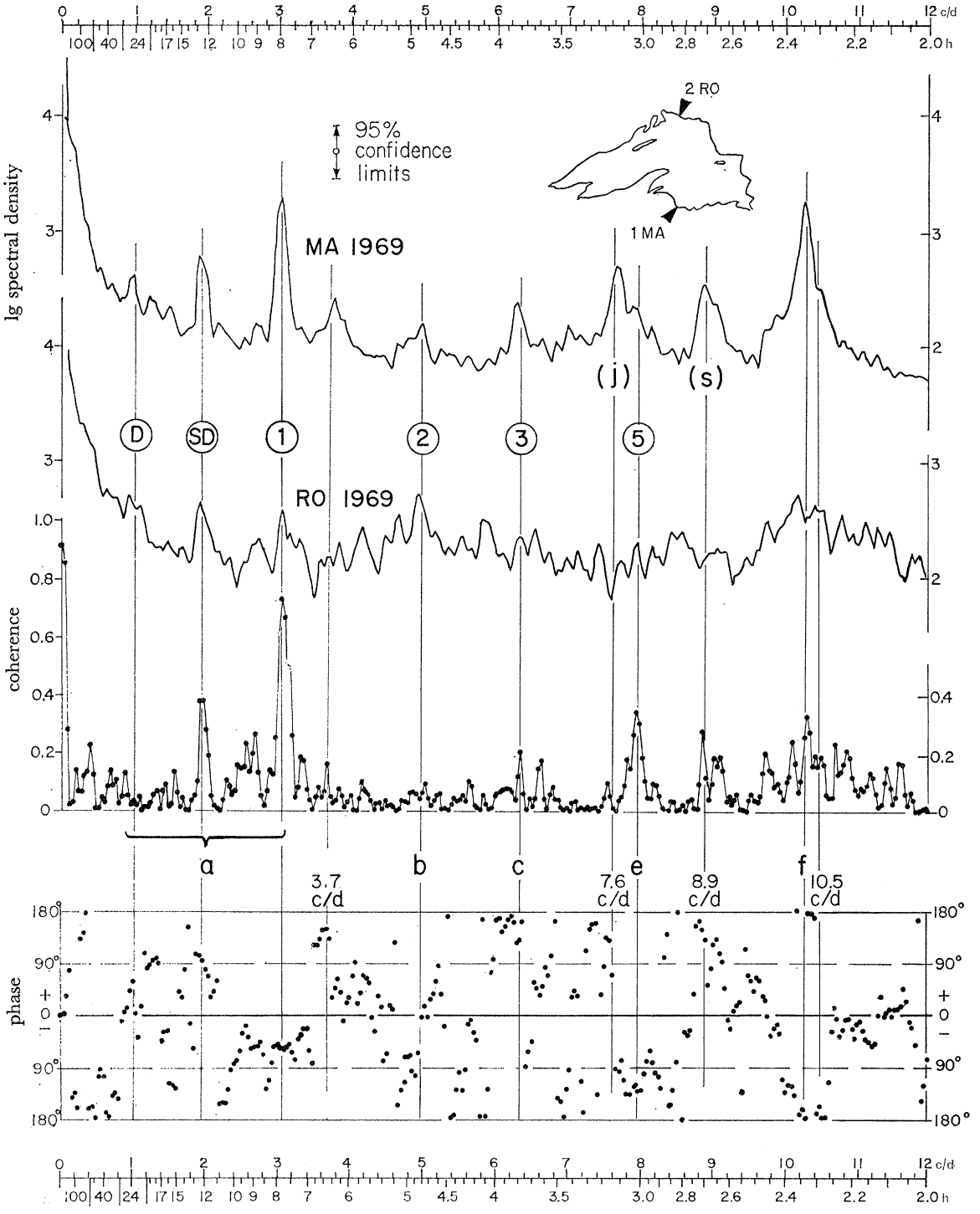

FIGURE 30. Lake Superior: power spectra of water level fluctuations at stations MA and RO (series B, table 6) and spectra of interstation coherence and phase difference. For further details see the last sentence of the description of figure 17.

Evidence for double maxima in interstation coherence in the 10.3 to 10.5 c/d region in some of these figures, and the absence of obvious aliases, suggests that we are observing spectral peak splitting resulting from amplitude variations (see Godin 1972, §1.10).

The principal feature of the computed eighth mode (figure 32*b*) is a strongly developed transverse seiche in the eastern basin, associated with a negative amphidrome, i.e. clockwise phase progression. This fits the approximately 180° phase differences between MA and MH (figure 29) and MA and RO (figure 30) and our rough estimate of 10.3 c/d for the uninodal transverse seiche along the RO-MA section, using Defant's (1918) one dimensional method. It is not surprising that a N-S oscillation of the eastern half should be a prominent component of Lake Superior's responses to storms. Strong northerly or southerly winds, and perhaps fast-moving barometric pressure changes are likely to set up transverse surges leading to seiches of large amplitude. Bajorunas (1960) refers to a 'surge' on 16 June 1939, reported on the southern shore in Munising Bay where the water 'rose as much as six feet above normal lake level and then receded the same distance below lake level, at about 30 min intervals.' A much earlier report (Mackenzie 1802, reprinted 1971) refers to a surge on the northern shore at Thunder Bay.

> 'The water withdrew with great precipitation, leaving the ground dry that had never been visible, the fall being equal to four perpendicular feet, and rushing back with great velocity above the common mark. It continued thus falling and rising for several hours, gradually decreasing till it stopped at its usual height. There is frequently an irregular influx and deflux, which does not exceed ten inches, and is attributed to the wind.'

Surges of this magnitude were most probably followed by large and persistent N-S seiches.

The computed distribution of amplitude in figure 32*b* shows large amplitudes in Keweenaw Bay, below the peninsula – therefore a good place to obtain records of this mode – but activity elsewhere, including the western end, marks this mode as a whole-basin oscillation. It is this mode which provides the driving force for the Chequamegon Bay seiche at 10.3 c/d, described by Ragotzkie, Ahrnsbrak & Synowiec (1969). The Bay must be in resonance with the eighth mode.

(*e*) *Low-frequency responses*

Of the fourteen Superior station-pair diagrams presented here, all but five (figures 16, 23, 26, 29 and 30) show more or less distinct coherence maxima ranging from 0.39–0.82 at or near 0.35 c/d. The highest coherences involve stations near the eastern or western ends of the basin, for example TH/PI (figure 18, nearly out of phase) and GM/TH (figure 27, nearly in phase). This low-frequency oscillation may represent the response of the basin to a prevalent forcing frequency of wind or barometric pressure; but the corresponding period of 60–70 h is less than that usually seen in spectra of meteorological variables and less than the average interval of storm passage.

For Lake Michigan–Huron we also noted, in §2 (*h*), a broad response near 0.35 c/d (figure 11) and postulated a response of the double basin in a fundamental free mode. No such explanation is possible for the Superior result. Therefore, we must consider the possibility that rotational modes, Ball (1965) associated with variable depth, may be involved in both basins. Rao & Schwab (1976) computed 79 h for the shortest-period rotational mode in Lake Superior. If this proves to be the correct explanation of the 0.35 c/d response, our Michigan–Huron postulate may have to be rejected or modified.

PHILOSOPHICAL TRANSACTIONS OF THE ROYAL SOCIETY A MATHEMATICAL, PHYSICAL & ENGINEERING SCIENCES

None of the Superior station-pair diagrams show distinct spectral or coherence peaks near 1.3 c/d, which could be interpreted as surface manifestations of internal waves of near-inertial frequency. In this respect also, the Superior and Michigan findings are in agreement.

4. The diurnal and semidiurnal tides in Lakes Michigan and Superior

The semidiurnal tide is represented by a conspicuous narrow peak centred at the spectral band number nearest 1.93 c/d and present in all Michigan and Superior spectra, with rare exceptions noted below. High interstation coherence also appears at this frequency. The phase progression in Lake Superior – for band 48, the nearest to 1.93 c/d – is illustrated in figure 31*a*, based on results obtained in the manner described in the second paragraph of §3*c*. The phase progression in Lake Michigan is shown in figure 31*b*. At station LA (Lake Huron) the semidiurnal tidal peak is also conspicuous (figure 7); LA lags 136° behind MC.

The phase estimates in figure 31 exhibit a remarkable internal consistency. For example, the estimates for the fourteen station pairs in Lake Superior series C (coherence range 0.78 to 0.95) differ from the illustrated values by 0° in seven cases, by $\pm 1°$ in three cases, and by $\pm 2°$ in four cases. Of the estimates for seventeen Lake Michigan pairs, eight differ by 0°, six by $\pm 1°$, two by $\pm 2°$, and one by $-3°$ from the values shown in figure 31*b*. The greatest variance was found for station pairs including LU (low coherence 0.17–0.27), at which the semidiurnal tidal amplitude is very low (figure 11). For all other station pairs (high coherence 0.76–0.91) the variance was not greater than $\pm 1°$.

The principal result, illustrated in figure 31, is that the semidiurnal tide conforms to a simple amphidromic pattern in both basins, but that the amphidrome is negative in Lake Superior and positive in Lake Michigan. In this respect Lake Superior conforms to the negative (clockwise) rotation of the semidiurnal equilibrium tide in the Northern hemisphere, while Lake Michigan does not. The explanation may be that the N-S elongation of the Michigan basin forces a canal-like Kelvin wave response. The Adriatic Sea, at the same latitude, behaves similarly to Lake Michigan, but in the Adriatic there is a co-oscillation with the Mediterranean tide. This question receives a theoretical treatment by Hamblin (1976) in a paper which follows.

In the Michigan and Superior basins the amplitude of the semidiurnal tide and corresponding interstation coherence is lower for stations near the amphidromic point, for example ST/LU (figure 3) or MA/RO (figure 30), than for those at the basin extremities, for example MC/CH (figure 7) or TH/PI (figure 18). In general, the coherence peaks for the semidiurnal tide are higher than those for the first longitudinal mode in Lake Michigan, while the reverse is true for Superior.

Small, distinct spectral peaks or interstation coherence maxima appear at 1.00 c/d in a few Lake Michigan examples (figures 5, 9) and, more frequently and conspicuously, in several Lake Superior station diagrams: TH/PA (figure 20); GC/MH (figure 25); TH/GM (figure 27); and GM/ON (figure 28). Except for station pairs MI/CH and CH/HO (coherences 0.33) the Lake Michigan interstation coherences at this frequency were also very low, with no reproducible phase pattern discernible, while much higher coherences were found between Superior station pairs, except for pairs including MA and, particularly, RO. Dr R. E. Cartwright (personal communication) points out that equilibrium theory may, partly at least, explain the smaller diurnal response in Lake Michigan. If ϕ is the latitude, the diurnal equilibrium tide is propor-

tional to sin 2ϕ and possesses no N–S gradient at 45°. Therefore Lake Michigan responds to it weakly, while Superior having large E–W extension responds to it more strongly.

However, diurnal winds probably play an important role (cf. Platzman 1966, and Simpson & Anderson 1967) and are the most probable explanation of the large variability of the response at the diurnal frequency, encountered between spectra for the same station prepared from different data sets. Compare, for example, the TH spectra in figures 16 and 17 (1969 and 1966–7) and also figures 9 and 10. Each of the latter figures shows a semidiurnal tide which is almost in phase between GB and the main basin stations MC and ST. The same should be true for a

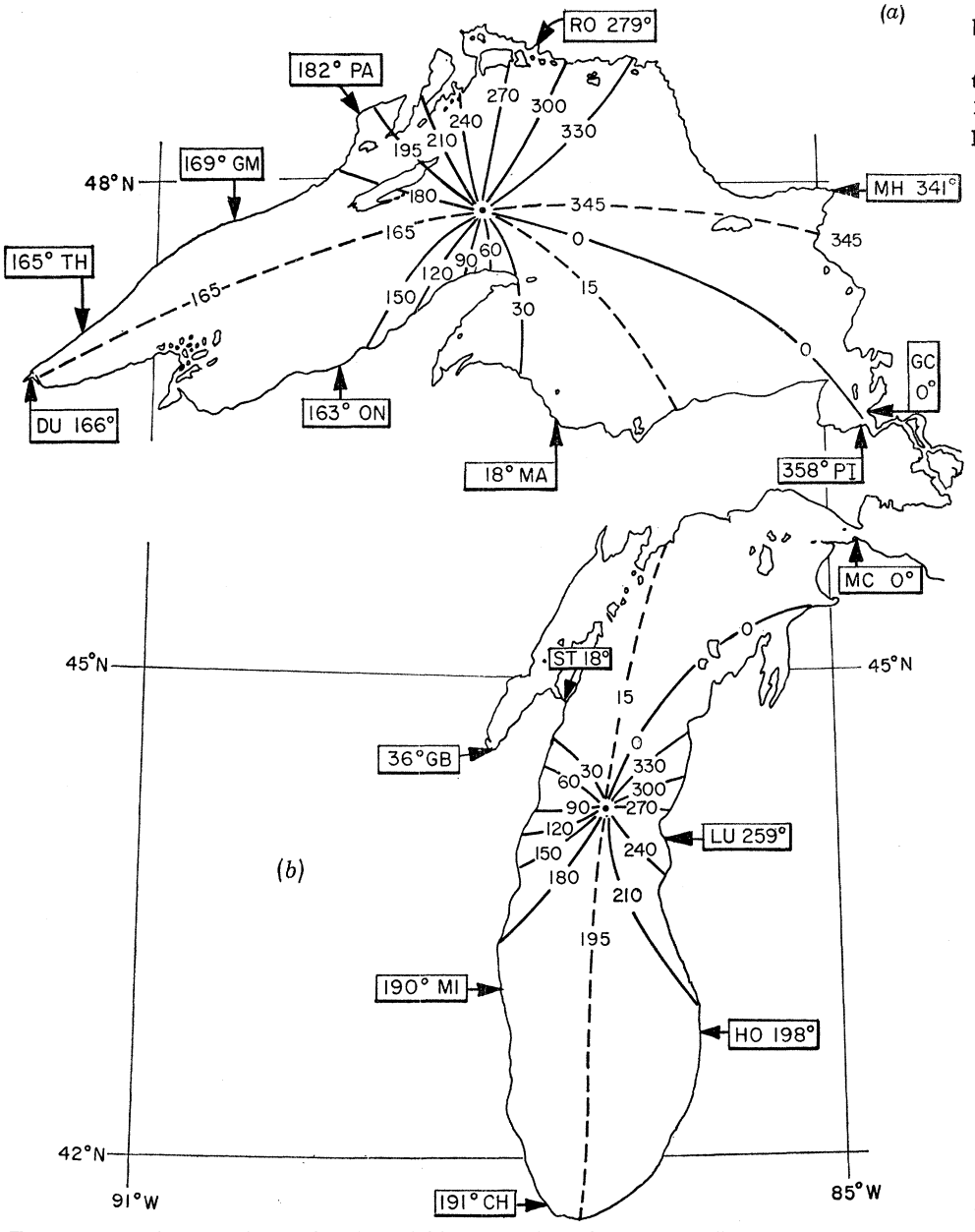

FIGURE 31. Lake Superior and Lake Michigan: station phase angles (boxed and relative to 0° at GC and MC, respectively) for the semidiurnal tide. The position of the co-tidal lines (at 30° intervals) and of presumed amphidromic points are drawn to fit the station angles, but are otherwise guesswork.

diurnal tide. But when the diurnal oscillations are compared, GB lags behind MC by 150° (coherence 0.14 in figure 9), while the corresponding lag and coherence in figure 10 is 90° and 0.02.

Examination of all station spectra suggests that stations on the northern Superior shore are more exposed to diurnal meteorological forcing – judging by the prominence of peak D and variation in the height ratio of the D and SD peaks – than are stations on the southern shore. Station PA is the most strongly affected, and this is the only case in which peak D is equal to (figure 21, series A) or higher than peak SD (figure 24, series D). The diurnal coherence displays a greater variability than the semidiurnal. It is 0.1 or less for MA/PA (figure 24) and for RO/PA (series A and D, not illustrated), but reaches 0.8 for TH/PA (figure 20).

The tides merit more detailed attention than we have been able to give them, and the phases in figure 1 should be related to the lunar passage. Further, the tidal and non-tidal responses could be resolved by correlating the data sets with the known time history of the equilibrium tide (Munk & Cartwright 1966) or by removing the tidal components from the input data, using methods described by Godin (1972). This would permit examination of the meteorologically-forced diurnal and other components and could perhaps also lead to an estimate of the local Earth tides, through comparison of the observed tidal components with the theoretical equilibrium tides.

We are greatly indebted to the following agencies for the generous supply of the input data – in the form of original charts, tables, data cards and tapes – which constitute the entire foundation for this analysis: Canadian Department of Energy, Mines, and Resources (now Environment, Canada), Marine Sciences Branch (Tides and Water Levels, Mr G. C. Dohler); and the United States Army Corps of Engineers (Lake Survey, now Lake Survey Center, National Oceanic and Atmospheric Administration, United States Department of Commerce, Mr E. Megerian). We are also grateful to Dr D. E. Cartwright, Dr G. Godin, Dr G. Platzman, and Dr N. S. Heaps for information and comment on specific points, and to Mr R. J. Ristić for his notable effort and skill in preparation of illustrations, of which only a small selection is presented here.

One of us (C.H.M.) is particularly pleased to acknowledge support from the Endowed Research Time Scheme of IBM, United Kingdom, Ltd, London (Share No. 1396).

5. A supplementary note and figure (added 7 March 1975) by C. H. Mortimer, D. B. Rao and D. J. Schwab

The computed periods and two dimensional structures of the first six barotropic, gravitational free modes of Lake Superior are presented by Rao & Schwab (1976) in the following paper. Additional results for the seventh and eighth modes are given in figure 32. The cotidal lines are computed relative to 0° at GC, to permit a direct comparison in figure 32*b* between the computed phase progression of the eighth mode and the observed station phase angles (table 8) corresponding to the strong oscillation *f* (10.3 c/d), §3 (*d*) (iii). The eighth mode pattern is made up of five amphidromes: two positive ones located at the basin ends; a positive amphidrome at the mouth of Keweenaw Bay associated with relatively very large amplitude at the head of the Bay; and two negative amphidromes centred respectively in the western and eastern halves of the basin. The western system generates moderate amplitude near the Apostle Islands and probably drives the resonant oscillation in Chequamegon Bay noted at the end of §3 (*d*) (iii).

The eastern negative amphidrome is very extensive, occupying the greater part of the basin

east of the Keweenaw Peninsula in the form of a transverse (N-S) seiche, attaining relatively large amplitudes at MH and MA. Except at ON and DU, the agreement between computed and observed phase angles is excellent. This agreement and that between the computed and observed frequencies identify peak *f* as the signature of a strongly excited eighth (first transverse) mode. It may be noted that the first transverse mode of Lake Michigan (T1, figure 6) is also strongly excited, probably also in the form of a negative amphidrome.

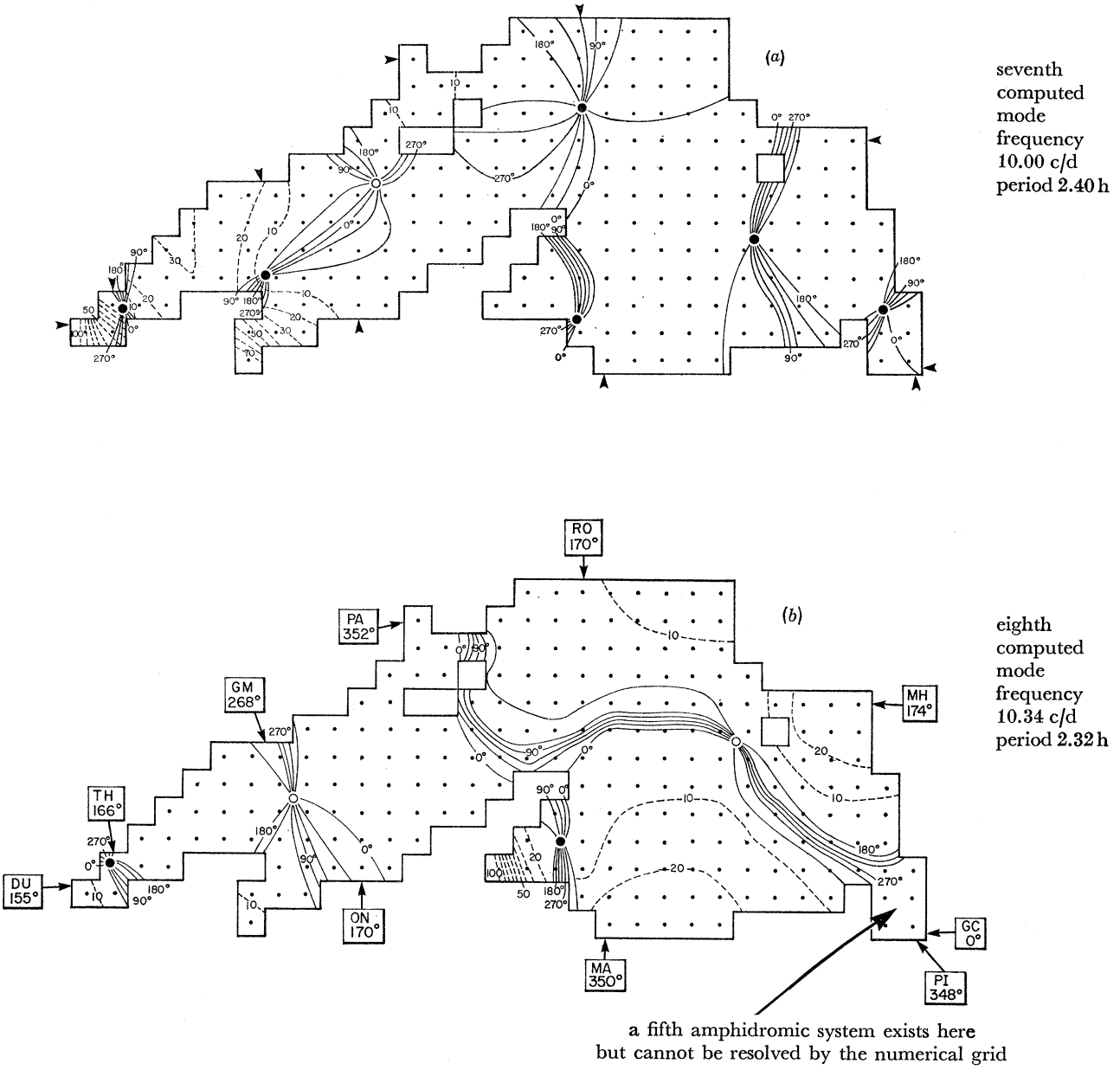

FIGURE 32. Lake Superior: the periods (frequencies), cotidal lines (unbroken and relative to 0° at GC) and co-range lines (broken and relative to 100) computed for (*a*) the seventh and (*b*) the eighth mode by D. B. Rao and D. J. Schwab (personal communication). The phase progression, so computed for the eighth mode, is compared with the observed station phase angles, shown boxed and determined from 51 interstation comparisons (table 8, §3 (*c*)). Solid and open circles indicate positive and negative amphidromes, respectively.

The computed pattern for the seventh Superior mode (figure 32*a*, 10.0 c/d, 1 negative and 6 positive amphidromes) shows large amplitudes only at the western end of the basin, near DU and near the Apostle Islands. No observed oscillation was found (§3(*d*) (ii)) to match that pattern and frequency. We therefore conclude that the seventh mode is not strongly excited.

References

Ball, F. K. 1965 The effect of rotation on the simpler modes of motion of a liquid in an elliptic paraboloid. *J. Fluid Mech.* **22**, 529–545.

Bajorunas, L. 1960 Water level disturbances in the Great Lakes and their effect on navigation. *Princeton Univ. Conf., Princeton, N.J.*, unnumbered rept., 39 pp.

Blackman, R. B. & Tukey, J. W. 1958 *The measurement of power spectra.* New York: Dover.

Cooley, J. W. & Tukey, J. W. 1965 An algorithm for the machine calculation of complex Fourier series. *Math. Computation* **19**, 297–301.

Defant, A. 1918 Neue Methode zur Ermittlung der Eigenschwingungen (Seiches) von abgeschlossenen Wassermassen (Seen, Buchten, usw). *Ann. Hydrogr. Berlin* **46**, 78–85. (This method is also described in next ref.)

Defant, A. 1961 *Physical oceanography*, vol. 2, p. 165. London: Pergamon.

Defant, F. 1953 Theorie der Seiches des Michigansees und ihre Abwandlung durch Wirkung der Corioliskraft. *Arch. Met. Geophys. Bioklimatol. Wien.* A **6**, 218–241.

Endrös, A. 1908 Vergleichende Zusammenstellung der Hauptseichesperioden der bis jetzt untersuchten Seen mit Anwendung auf verwandte Probleme. *Petermanns Mitt.* **54**, 39–47, 60–68, 86–88.

Fee, E. J. 1969 Digital computer programs for spectral analysis of time series. *Center for Great Lakes Studies, University of Wisconsin–Milwaukee, Spec. Rept.* No. 6, 35 pp.

Forrester, W. D. 1961 Tidal and meteorological influences on the current in Little Current Channel. *Can. Hydrogr. Serv., Dept. Mines Tech. Surv., Ottawa*, unnumbered rept. 55 pp.

Freeman, N. G. & Murty, T. S. 1972 A study of a storm surge on Lake Huron. *Proc. 15th Conf. Great Lakes Res., Int. Assoc. Great Lakes Res.* 565–582.

Godin, G. 1972 *The analysis of tides.* University Toronto Press.

Hamblin, P. F. 1968 The variation of the water level in the western end of Lake Ontario. *Proc. 11th Conf. Great Lakes Res., Int. Assoc. Great Lakes Res.*, 385–397.

Hamblin, P. F. 1976 A theory of short period tides in a rotating basin. *Phil. Trans. R. Soc. Lond.* A **281**, 97–111.

Housley, J. G. 1962 Seiches and currents in Duluth-Superior Harbor, June–November 1958. U.S. Army Waterways Exp. Sta., Vicksburg, Miss., *Misc. Pap. No.* 2–502, 34 pp., 12 pl.

Mackenzie, A. 1802 *Voyages from Montreal on the River St Lawrence through the continent of North America to the Frozen and Pacific Oceans in the years* 1789 *and* 1793, pp. 94–269. (Reprinted 1971.) New York: G. S. Hopkins.

Miles, M. W. & Ball, F. K. 1963 On free surface oscillations in a rotating paraboloid. *J. Fluid Mech.* **17**, 257–266.

Mortimer, C. H. 1963 Frontiers in physical limnology with particular reference to long waves in rotating basins. *Proc. 6th Conf. Great Lakes Res., Great Lakes Res. Div., University of Michigan, Publ.* No. **10**, 9–42.

Mortimer, C. H. 1965 Spectra of long surface waves and tides in Lake Michigan and at Green Bay, Wisconsin. *Proc. 8th Conf. Great Lakes Res., Great Lakes Res. Div., Univ. Michigan, Publ.* No. **13**, 304–325.

Mortimer, C. H. 1971 Large-scale oscillatory motions and seasonal temperature changes in Lake Michigan and Lake Ontario. *Center for Great Lakes Studies, Univ. Wisconsin–Milwaukee, Spec. Rept.* No. 12; Part I text, 111 pp; Part II illustrations, 106 pp.

Mortimer, C. H. 1974 Lake hydrodynamics. *Mitt. int. Ver. Limnol.*, **20**, 124–197.

Mortimer, C. H. 1975 Substantive corrections to SIL Communications (IVL Mitteilungen) Numbers 6 and 20. *Verhandl. int. Verh. Limnol.*, **19**, 60–72.

Munk, W. H. & Cartwright, D. E. 1966 Tidal spectroscopy and prediction. *Phil. Trans. R. Soc. Lond.* A **259**, 533–581.

Munk, W. H. & Macdonald, G. J. F. 1960 *The rotation of the earth: a geophysical discussion.* Cambridge Monogr. Mech. appl. Math., Cambridge Univ. Press, 296 pp.

Munk, W. H., Snodgrass, F. E. & Tucker, M. J. 1959 Spectra of low-frequency ocean waves. *Bull. Scripps Inst. Oceanogr.* **7**, 283–362.

Noye, B. J. 1968 The frequency response of a tide-well. *Proc. 3rd Austral. Conf. Hydraul. Fluid Mech., Sydney*, 65–71.

Noye, B. J. 1970 A study of tide-well systems, II. *Horace Lamb Centre Ocean. Res., Flinders Univ., S. Australia, Res. Pap.* No. 14, 75 pp.

Noye, B. J. 1972 On the differential equation for the conventional tide-well system. *Bull. Australian Math. Soc.*, **7**, 251–267.

Platzman, G. W. 1966 The daily variation in water level in Lake Erie. *J. geophys. Res.* **71**, 2471–2483.

Platzman, G. W. 1972 Two-dimensional free oscillations in natural basins. *J. phys. Oceanogr.* **2**, 117–138.

PHILOSOPHICAL TRANSACTIONS OF THE ROYAL SOCIETY A MATHEMATICAL, PHYSICAL & ENGINEERING SCIENCES

Platzman, G. W. & Rao, D. B. 1964*a* The free oscillations of Lake Erie. In *Studies on oceanography* (Hidaka volume, ed. K. Yoshida), pp. 359–382. Tokyo University Press, 568 pp.

Platzman, G. W. & Rao, D. B. 1964*b* Spectra of Lake Erie water levels. *J. geophys. Res.* **69**, 2525–2535.

Ragotzkie, R. A., Ahrnsbrak, W. F. & Synowiec, A. 1969 Summer thermal structure and circulation of Chequamegon Bay, Lake Superior – a fluctuating system. *Proc. 12th Conf. Great Lakes Res., Int. Assoc. Great Lakes Res.*, 686–704.

Rao, D. B. & Schwab, D. J. 1976 Two dimensional normal modes in arbitrary enclosed basins on a rotating earth: application to Lakes Ontario and Superior. *Phil. Trans. R. Soc. Lond.* A **281**, 63–96.

Rockwell, D. C. 1966 Theoretical free oscillations of the Great Lakes. *Proc. 9th Conf. Great Lakes Res., Great Lakes Res. Div., University of Michigan, Publ.* No. 15, 352–368.

Saylor, J. H. 1964 Survey of Lake Michigan harbor currents. *Proc. 7th Conf. Great Lakes Res., Great Lakes Res. Div., University of Michigan, Publ.* No. 11, 362–368.

Simpson, R. B. & Anderson, D. V. 1964 The periods of the longitudinal surface seiche of Lake Ontario. *Proc. 7th Conf. Great Lakes Res., University of Michigan, Great Lakes Res. Div., Publ.* No. 11, 369–381.

Simpson, R. B. & Anderson, D. V. 1967 The surface tides of Lake Ontario. *Dept. Lands, Forests, Ontario, Res. Rep.* No. 76, 42 pp.

U.S. Department of the Interior 1967 Water quality investigation, Lake Michigan basin: Lake currents. *Fed. Water Pollution Control Admin., Great Lakes Region, Chicago, Rep.*, 364 pp.

Young, R. K. 1929 Tides and seiches on Lake Huron. *J. R. astronom. Soc., Canada*, **23**, 445–455.

Yuen, K. B. 1969 A numerical study of large-scale motions in a two-layer rectangular basin. *Dept. Energy, Mines, and Resources, Ottawa, Canada: Marine Sciences Branch, Manuscript Report Series*, No. 14, 119 pp.

PHILOSOPHICAL TRANSACTIONS OF THE ROYAL SOCIETY A MATHEMATICAL, PHYSICAL & ENGINEERING SCIENCES